

ABSTRACT OF THESIS

Name of Candidate William Graeme M^CNaught
Address 8 Hamilton Terrace, Edinburgh 15
Degree Ph.D. Date 1 October 1970
Title of Thesis An Investigation of Reactions Relevant to an Understanding
..... of the Mechanism of Catalytic Steam Reforming.

SUMMARY

This thesis is primarily intended to investigate an industrial chemical process in an academic environment. The catalytic steam reforming of hydrocarbons is an extremely successful commercial process but the chemistry of it is still not completely understood. Using a static system and a simple metal catalyst an attempt has been made to study some reactions relevant to steam reforming in the hope that the data obtained may be related to the full scale industrial process.

The first reaction studied was the hydrogen/heavy water exchange over evaporated films of nickel, rhodium, palladium and platinum which revealed a trend of activities of the order Pt>Rh>Pd>Ni. The next series of reactions investigated showed that for the exchange reaction between propylene and heavy water the activities were of the order Pd>Ni>Rh with platinum initially the most active metal but poisoning to become least active. In an attempt to relate the work more closely to industrial conditions the chemical reactions between propylene and water and between propane and water were studied over films of nickel and rhodium and over catalysts of these metals supported on α -alumina. In all cases the reaction products were carbon monoxide, carbon dioxide, methane, and hydrogen. No intermediates, either oxygenated species or C₂ hydrocarbons, were detected.

An Investigation of Reactions
Relevant to an Understanding of the Mechanism
of Catalytic Steam Reforming.

William Graeme McNaught, B.Sc.

University of Edinburgh,
1970.



Acknowledgements

The research described in this thesis was carried out in the Department of Chemistry, University of Edinburgh between October 1967 and September 1970.

I am very grateful to my supervisors, Professor C. Kemball, F.R.S. and Dr. H.F. Leach who were always ready to advise, discuss, and generally encourage me in my work.

I am also indebted to I.C.I. for their hospitality during the three months I worked with them, and for the interest shown in my research. In particular I should like to thank Professor D.A. Powden, Mr. G.W. Bridger, Mr. G.C. Chinchin, and Dr. D.R. Ashmead, all of whom ensured that my liason with I.C.I. was both interesting and useful.

My thanks are also due to the technical staff at Edinburgh and to Miss P. Stirling for typing this thesis.

I acknowledge the award of an S.R.C. grant and the Cooperative Award for Postgraduate Study scheme which I found most enjoyable.

W. Graeme McNaught.

PART I

<u>CHAPTER 1.</u>	<u>Introduction to Catalysis</u>	<u>Page</u>
1.1	Historical Background.	1
1.2	Heterogeneous Catalysis.	2
1.3	Adsorption.	3
1.4	Kinetics and Mechanism.	5
1.5	Exchange Reactions.	6
1.6	Catalytic Activity.	7
1.7	The I.C.I. Steam Reforming Process	10
1.8	The Objectives of This Thesis.	11
<u>CHAPTER 2.</u>	<u>Experimental Apparatus</u>	
2.1	Introduction.	15
2.2	The Gas Handling System.	15
2.3	The Reaction Vessel and Capillary Leak.	16
2.4	Volume Calibrations.	17
2.5	The Mass Spectrometer.	18
2.6	Mass Spectrometric Analysis.	20
2.7	Analysis of the Reforming Reaction.	23
2.8	Preparation and Properties of Evaporated Metal Films.	24
<u>CHAPTER 3.</u>	<u>Exchange Reactions</u>	
3.1	General Aspects of Exchange Reactions.	26
3.2	The Final Equilibrium of an Exchange Reaction.	27
3.3	The Determination of Rate Constants.	28
3.4	Arrhenius Plots.	29
3.5	Kinetics.	29
3.6	Classification and Possible Mechanisms of Exchange Reactions.	30
<u>CHAPTER 4.</u>	<u>The Preparation of some Supported Metal Catalysts and the Measurement of their Surface Areas.</u>	
4.1	The Support.	32
4.2/		

	<u>Page</u>
4.2 Catalyst Preparation.	33
4.3 Surface Area Measurements of Nickel and Rhodium on α -alumina.	35
4.4 The Experimental Determination of Catalyst Surface Areas by CO Adsorption.	36

PART 2

CHAPTER 1. The Exchange Reaction Between Hydrogen and Heavy Water over Nickel, Rhodium, Platinum and Palladium Films.

1.1 Introduction.	40
1.2 Experimental.	40
1.3 Results.	43
1.4 Discussion.	45

CHAPTER 2. The Exchange Reaction Between Propylene and Heavy Water over Nickel, Platinum, Palladium and Rhodium Catalysts.

2.1 Introduction.	47
2.2 Experimental.	49
2.3 Results.	50
2.4 C_3H_6/D_2O Exchange over Palladium and Rhodium Films.	51
2.5 C_3H_6/D_2O Exchange over Platinum.	54
2.6 C_3H_6/D_2O Exchange over Nickel.	58
2.7 Discussion.	61

CHAPTER 3. The Chemical Reaction Between Propylene and Light Water and between Propane and Light Water over Nickel and Rhodium Catalysts.

3.1 Introduction.	65
3.2 Experimental.	65
3.3/	

	<u>Page</u>
3.3 The Propylene/Steam and Propane/Steam Reactions over Nickel.	66
3.4 The Propylene/Steam and Propane/Steam Reactions over Rhodium.	72
3.5 Discussion.	76
Conclusion,	82
Appendix I.	85
Appendix II.	87
Appendix III.	92
Appendix IV.	93
References	94

SUMMARY

This thesis is primarily intended to investigate an industrial chemical process in an academic environment. The catalytic steam reforming of hydrocarbons is an extremely successful commercial process but the chemistry of it is still not completely understood. Using a static system and a simple metal catalyst an attempt has been made to study some reactions relevant to steam reforming in the hope that the data obtained may be related to the full scale industrial process.

The first reaction studied was the hydrogen/heavy water exchange over evaporated films of nickel, rhodium, palladium and platinum which revealed a trend of activities of the order $\text{Pt} > \text{Rh} > \text{Pd} > \text{Ni}$. The next series of reactions investigated showed that for the exchange reaction between propylene and heavy water the activities were of the order $\text{Pd} > \text{Ni} > \text{Rh}$ with platinum initially the most active metal but poisoning to become least active. In an attempt to relate the work more closely to industrial conditions the chemical reactions between propylene and water and between propane and water were studied over films of nickel and rhodium and over catalysts of these metals supported on α -alumina. In all cases the reaction products were carbon monoxide, carbon dioxide, methane, and hydrogen. No intermediates, either oxygenated species or C_2 hydrocarbons, were detected.



PART 1

UNIVERSITY
OF
EDINBURGH



UNIVERSITY

CHAPTER I

Introduction to Catalysis.

1.1 Historical Background.

The word "catalysis" is very much in vogue at present, being used in both a scientific and a non-scientific context to describe an object which, when introduced into a slowly changing environment will accelerate this rate of change while itself remaining unaltered. An excellent example of a catalyst is a book such as "The Bible" or "Das Kapital" which may influence the thinking of people already inherently sympathetic to the general content to accept a philosophy more rapidly than if they were to formulate it themselves. In everyday use the crucial phrase "without itself being altered" is often conveniently forgotten, indeed the word catalyst is often synonymous with "dynamic change".

From the viewpoint of chemistry the first glimmerings of an understanding of catalysis came in 1812 when Kirchoff⁽¹⁾ demonstrated that mineral acids in hot water solution changed starch into dextrose and sugar without themselves being altered. A further advance was made by de Saussure⁽²⁾ who introduced the concept of acceleration in 1818 while Davy⁽³⁾ & Dobereiner⁽⁴⁾ were looking at surface catalysis in the phenomenon of glowing metals in mixtures of air and combustible gases. A few years later in 1836 Berzelius⁽⁵⁾ realised that a number of apparently unrelated chemical reactions had as a common factor that in the presence of a catalyst more reaction occurred. In fact yield is not affected by the presence of a catalyst as the equilibrium remains the same/

same only being achieved more rapidly in a catalysed reaction. The qualitative description of Berzelius was put in quantitative form by Ostwald⁽⁶⁾ who defined a catalyst as "any substance which alters the velocity of a chemical reaction without appearing in the end products". The increase in rate of a catalysed reaction may be accounted for by postulating an alternative reaction route via intermediates formed by reaction with the catalyst which later yield products while the catalyst itself is regenerated. Catalytic reactions may, for convenience, be divided into two major classes.

1. Heterogeneous catalytic reaction involving reaction at an interfacial layer between distinct phases;
2. Homogeneous catalytic reaction where both catalyst and reactants are in the same phase. This thesis is concerned with the former class.

1.2 Heterogeneous Catalysis.

Heterogeneous catalysis involving gas reactants and solid catalyst is a rate enhancing process occurring at the gas-solid interface. A study of various catalytic reactions convinced Faraday⁽⁷⁾ that films of gas known to be absorbed by the solid, are the seat of chemical reactions but he mistakenly concluded that the resulting increase in rate could be attributed to the increased concentration of reactants on the surface. This concept was subsequently labelled "contact action" by Mitscherlich⁽⁸⁾ but the theory does not account for the specific character of some catalysts. For example ethanol over copper at 300°C. gives acetaldehyde and hydrogen but over alumina at the same temperature the products are ethylene and water. Langmuir/

Langmuir⁽⁹⁾ attempted to explain this discrepancy by proposing that short-range attractions between surface and adsorbate gave rise to bonding, essentially chemical in nature, which was limited by the number of "sites" available for bonding in the surface. Further investigation of the phenomena of adsorption has established that there are two main ways in which a molecule may be held to a catalyst surface. These are referred to as Physical Adsorption and Chemisorption.

1.3 Adsorption.

Physical Adsorption

Physical adsorption refers to the formation of a film of gas, similar in many respects to a liquid film, held by relatively weak van der Waals forces. Low heats of adsorption, rapid interchange between gas phase and surface film, mobility of adsorbed molecules and multilayer formation characterise physical adsorption. Generally the weakness of the forces makes this of minor importance in catalysis with a few exceptions⁽¹⁰⁾.

Measurements by physical adsorption, however, are invaluable in surface area determinations by the Braunaur, Emmett, Teller⁽¹¹⁾ method and in determining the pore size in capillaries in catalysts⁽¹²⁾ and pore volume distribution curves⁽¹³⁾.

Chemisorption

Chemisorption refers to the formation of a chemical bond between a gaseous molecule and a catalyst surface caused by the changes occurring in the electron distribution of the adsorbate⁽¹⁴⁾ which may be attached to the surface by covalent or ionic bonds or may/

may be dissociated into similarly bound atoms or radicals^(15, 16). High heats of adsorption (80-400 kJ mole⁻¹) are implicit, chemisorption usually being an activated process proceeding at a finite rate which increases with temperature. Surface coverage by chemisorbed species will not exceed a monolayer.

A relationship between pressure of gas and the amount adsorbed on the surface was derived by Langmuir⁽¹⁷⁾ who formulated a theory based on an equilibrium being established between molecules in the gas phase and on the surface. On the assumptions that the heat of chemisorption was independent of the extent of chemisorption and that the surface was energetically homogeneous he derived the equation

$$\theta = \frac{ap}{1 + ap}$$

where θ is the fraction of surface covered by adsorbed molecules, p is the gas pressure and a is a constant. Although more sophisticated theories have since been derived the Langmuir isotherm's simplicity has prolonged its usefulness in catalysis.

Heats of chemisorption at small surface coverage and the amounts adsorbed at saturation increase on proceeding to the left in each long period and the more reactive gases are more strongly and extensively held⁽¹⁸⁾. From isotope exchange it has been found that the chemisorption of all molecules is accompanied by some degree of bond weakening or fission so that metals have the prerequisites to function as catalysts for many reactions.

1.4 Kinetics and Mechanism.

A catalytic reaction may normally be broken down into five distinct steps:-

1. Diffusion of the reactants to the catalyst surface;
2. Chemisorption of at least one reactant species on the catalyst surface which may involve dissociation;
3. Reaction of these adsorbed species either among themselves, with physically adsorbed species, or with other molecules colliding with the surface.
4. Desorption of the products;
5. Diffusion of the products away from the surface.

In an analysis of a catalytic reaction it is essential to know which step is rate-controlling. The processes of diffusion are not normally rate-controlling in gas-solid systems and are generally characterised by rates of reaction which are not closely related to temperature.

Study of the mechanism of a surface reaction is made difficult since the nature of the various chemical species cannot easily be determined. Advances in E.S.R., microwave and other types of spectroscopy are giving an improved picture of the surface and surface species but to date the most useful studies have used isotopes as tracers⁽¹⁹⁾.

The thermodynamic data for a complex catalytic reaction comprising several different steps may be summarised⁽¹⁸⁾ as:

- (a) in practice reversible or irreversible under the operating conditions, i.e. - ΔG small or large respectively;
- (b) giving the desired substances either as end-products or/

or intermediates, i.e. according to whether or not the derived products are formed by the reaction with the largest free energy change;

(c) endothermal (positive ΔH) or exothermal (negative ΔH) thus having larger equilibrium constants at higher and lower temperatures respectively, or

(d) composed of coupled reactions where an expendable product of an endothermal reaction is itself combined with a suitable reactant making the overall process exothermal and thus allowing the reaction to proceed at lower temperatures.

1.5 Exchange Reactions.

The study of exchange reactions provides information on the ability of a catalyst to make and break particular bonds in a reactant molecule. Since deuterium became available for catalytic studies in 1933 it has been the most commonly used element for examining exchange reactions, especially since the adoption of the mass spectrometer as an analytical tool.

In the early work the exchange of hydrogen with deuterium was measured using a thermal conductivity technique to measure the dilution of hydrogen with deuterium and one of the first points to arise from these studies was that the exchange of ethane and propane with deuterium occurs at temperatures substantially lower than those required for carbon-carbon bond cleavage although the C - H bond is substantially stronger than the C - C bond in a gas phase molecule. Inadequate techniques meant that a precise mechanism could not be established.

More/

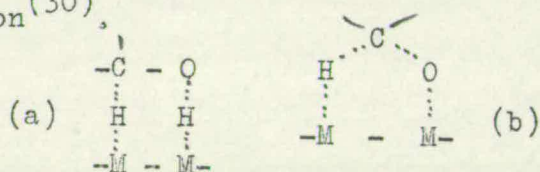
More recently it has been possible to determine how the deuterium is distributed in the hydrocarbon using gas chromatography as a supplement to mass spectrometry. Deuteration, cis-trans isomerisation and double bond migration may also be studied. From research of this nature data on the catalytic activity of the metal for the making and breaking of different kinds of C - H bonds and information on the nature of the adsorbed hydrocarbon may be obtained.

1.6 Catalytic Activity.

The main essentials of a good catalyst are an accessible surface on which reaction may occur and some specific property which determines the adsorption of the activated complex with a corresponding decrease in activation energy. Although it is possible that some reactions, e.g. the H_2/D_2 exchange, proceed over the entire surface of the catalyst the experimental evidence available now suggests that in general catalytic activity is confined to limited areas of the catalyst surface. This non-uniformity of surface was evidenced by study of the inhibiting effect of carbon monoxide on the reaction between ethylene and hydrogen on copper⁽²⁰⁾ and from the carbon dioxide and hydrogen reaction on platinum⁽²¹⁾. An explanation lies in the catalyst surface which is not perfectly smooth but contains the well defined facets of metal crystals in which the different planes have different lattice spacings. The energy of adsorption of any atom will therefore depend on its position in the metal and its relationship to other atoms. Thus not only will the edges and corners of crystallites differ in free energy as well as the different planes but spiral growth produces screw dislocations and consequently steps and other surface/

surface imperfections including atomic vacancies will be present. H.S. Taylor⁽²²⁾ proposed that these active patches were determined by the reaction catalysed and these reactions ranged from use of the entire surface^(23, 24, 25) to a more selective use of particular patches^(26, 27) in, for example, the decomposition of ammonia on a monocrystal of copper where the (111) plane was found to be twelve times more active than the (100) plane.

The relationship between catalytic activity and surface geometry provides a simple explanation for some reactions. This requires a reactant molecule to "fit" onto the catalyst surface and necessitates suitable atomic spacing of the substrate metal atoms for reaction to proceed. Burk⁽²⁸⁾ and Balandin⁽²⁹⁾ developed this idea introducing the concept of multiple adsorption which supposes that a molecule is only activated when it is adsorbed at two or more active centres producing a direct strain in a particular bond or bonds, and accounts for the catalytic specificity in the alternative decomposition reactions of alcohols where the products depend on the spacing of active centres and other surface properties, e.g. case (a) favours dehydrogenation and (b) favours dehydration⁽³⁰⁾.



Sherman and Eyring⁽³¹⁾ provided a theoretical basis for the link between chemisorption and surface geometry showing the activation energy for the chemisorption of hydrogen on carbon to be dependant on the inter atomic spacing of the relevant carbon atoms.

A study of the adsorption on ethylene on nickel by two point contact involving opening of the double bond led Twigg and Rideal⁽³²⁾ to predict that different crystal planes of the same metal could differ in catalytic power due to the different spacing of the atoms contained in them. This prediction was justified/

justified by Beeck⁽³³⁾ whose later work^(34, 35) confirmed that surface interatomic distances, with respect to a particular reactant molecule, were vital in determining the catalytic activity for that reaction.

Balandin summarised this work noting that the attractive forces between different parts of the reactant molecule and surface atoms, being short range, meant that their interaction would be dependant only on the relative spacing of surface and reactant atoms. Thus it is possible to predict catalytic activity for certain systems, e.g. benzene hydrogenation occurs only on face-centred cubic structures of nickel/iron alloys where it is possible to get a π -adsorbed benzene complex on a hexagonal lattice.

A wide variety of techniques are being employed to gain a better understanding of the "geometric factor" in catalysis. These include the use of electron diffraction measurements on the spacing of chemisorbed atoms,⁽³⁶⁾ investigations of chemisorption and catalysis on different faces of single crystals,⁽³⁷⁾ and the field emission technique to observe preferential coverage of certain planes during chemisorption⁽³⁸⁾.

Along with the geometric factor there is an electronic factor both of which are involved to a greater or lesser extent in any catalytic reaction. The catalysts considered in this work are transition metals characterised by a narrow d-band with many levels overlapped by a broad s-band and both these bands only partly filled with electrons. There is good evidence that the chemisorption of hydrogen and hydrocarbons on metals of the transition series involves covalent bonding between the adsorbate and the vacant d-orbitals of the metals⁽³⁹⁾. Beeck⁽³⁵⁾ and Trapnell⁽⁴⁰⁾ explained the apparent anomalies of adsorption of ethylene over transition metals relating/

relating them to Pauling's percentage d-character of the metals which in turn is closely related to inter-atomic spacings in the crystal lattice. Other workers⁽⁴²⁻⁴⁹⁾ provided further evidence of the link between electronic configuration and the catalytic activity, and it appears that a reasonable correlation holds between percentage d-character of transition metals and their catalytic activity⁽⁵⁰⁾.

The activation energy of the exchange of ammonia with deuterium on evaporated metal films was shown by Kemball⁽⁵¹⁾ to exhibit a linear relationship with the work function of the clean metal suggesting that the highly ionic character of the bonding involved entry of electrons into the d-band of the metals thus forming an ammonium ion. A study of the exchange of cyclo-alkanes with deuterium led Rooney, Gault and Kemball⁽⁵²⁾ to propose that some heterogeneous catalytic reactions proceed through a π -bonded intermediate.

In an attempt to relate catalytic activity of transition metals for various reactions to the thermodynamic stability of reaction intermediates, Balandin^(53, 54) demonstrated that a continuous change in any parameter related to the strength of the reactant metal bond should give rise to increased catalytic activity which would reach a maximum and then decrease resulting in a "volcano shaped" curve. The concept of a chemical factor has since been improved on by Balandin⁽⁵⁵⁾ and other authors^(56, 57).

1.7 The I.C.I. Steam Reforming Process.

The catalytic reaction of light hydrocarbons with steam, known as the Steam Reforming Process is of great importance in the production of synthesis and town gas. Figure 1.1 shows a simplified flow sheet of an I.C.I. typical/

A simplified flow sheet of an ICI typical steam-naphtha plant

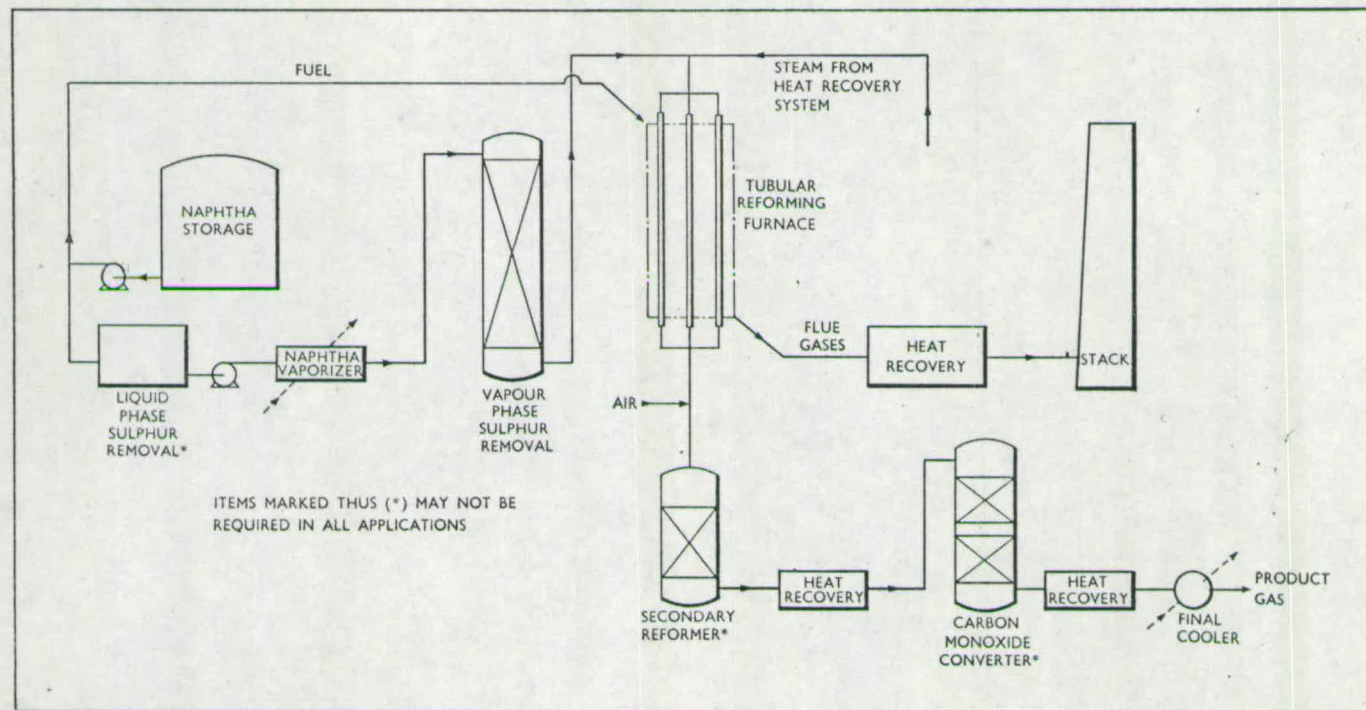


FIGURE 1-1

typical steam-naptha plant. Naptha is a convenient and economic feedstock which is first desulphurised by converting the sulphur to hydrogen sulphide over a combination of catalysts at $350 - 450^{\circ}\text{C}$ and absorbing this in zinc oxide. The sulphur free naptha vapour is then reformed over a selective I.C.I. catalyst in a tubular furnace with a tube outlet temperature of $700 - 830^{\circ}\text{C}$. The higher temperatures are needed only when producing nitrogen free hydrogen for methanol synthesis or hydrogenation. For other purposes, such as production of town gas and ammonia synthesis gas, the temperature is low.

Where ammonia synthesis gas is to be produced a secondary reforming step, which is in effect a catalytic partial oxidation process using air added to the mixture leaving the primary reformer and burning with it raising its temperature to about $1,200^{\circ}\text{C}$. The heated mixture then flows over a single bed of nickel catalyst in a refractory-lined mild steel vessel where the methane present reacts with the excess steam. The endothermic nature of this reaction results in a drop in temperature to about 900°C and the methane content falls to 0.2%. The amount of air added is exactly that required to introduce the amount of nitrogen required for ammonia synthesis. A final step uses a CO converter to reduce the level of CO to less than 0.5%.

1.9 The Objectives of this Thesis.

Although catalytic steam reforming is a well established industrial reaction the fundamental chemistry of the process is still not fully understood. This/

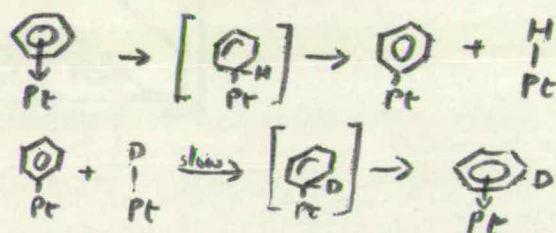
This thesis sets out to investigate some reactions which might give a better understanding of the overall process. As the bulk of the work has been carried out in an academic environment the techniques employed in the investigation differ markedly from those used in an industrial context, the primary difference being the use of a static system with low pressures and relatively low temperatures as opposed to the high temperature and pressure flow systems used industrially. The catalysts used are either in the form of a metal film or a simply supported metal on α -alumina type rather than the more complex commercial catalyst such as I.C.I. No. 46-1 which is of nickel metal supported on a mixture of refractory oxides containing alkali.

Three main types of bond cleavage are possible with a hydrocarbon/steam mixture, namely the O-H bond in water and the C-H and C-C bonds in the hydrocarbon. Each case has been studied, the first two over nickel, platinum, palladium, and rhodium and the last over nickel and rhodium. The hydroxyl bond in water and the C-H bond in the hydrocarbon were studied by using deuterium exchange. Isotope exchange reactions generally are extremely useful in obtaining information on catalytic reactions and have the advantage over other techniques of products which may be regarded as identical to the reactants in almost all respects.

To determine the relative strength of a hydroxyl bond over various metals a series of exchange reactions were performed between D_2O and H_2 . The C-H bond was investigated using a propylene/heavy water mixture, propylene being chosen as previous work at I.C.I. had suggested that an olefin was a likely reactive intermediate in steam reforming while heavy water served the dual purpose of avoiding the possibility of deuteration occurring simultaneously with exchange and/

and emphasising the relationship of the experiments to the steam reforming process. Analysis was carried out using a mass spectrometer enabling measurement of each isotopic species formed and initial reaction rates to be made.

A study of the propylene/heavy water system has also been made by Hirota^(58,59) using a microwave spectroscopic technique to investigate the deuterium exchanged positions of the monodeuterated propylenes produced over Cu, Pd, Pt, Rh, and Ni. Early work with D₂O/ethylene and D₂O/benzene mixtures was performed by Horiuti and Polanyi⁽⁶⁰⁾ who suggested that unsaturated compounds adsorbed through an associative process involving opening of the double bond. Later studies by Garnett et al⁽⁶¹⁻⁶³⁾ rejected this in favour of a π -complex followed by a dissociative mechanism for exchange as shown below:



Several subsidiary experiments, including a study of the CH₄/D₂O exchange, the C₃H₈/D₂O exchange, and the C₂H₄/D₂O exchange, all over nickel catalysts, were performed and are described more fully in context.

The final part of this thesis is designed to link this work more closely to the industrial process by chemically reacting a hydrocarbon and water at elevated temperatures (300 - 420°C). Propylene/H₂O and propane/H₂O mixtures were used as feedstocks and the reaction was again performed in the same static system/

system and analysed with the mass spectrometer

Other workers who have studied similar systems include Schnell⁽⁶⁴⁾, Phillips et al⁽⁶⁵⁾, and Bhatta and Dixon⁽⁶⁶⁾ whilst the related methanation reaction has been investigated by Bousquet and Teichner⁽⁶⁷⁾.

From the work in this thesis it is hoped that the steam reforming reaction may be better understood as the behaviour of water and hydrocarbons over different metals is investigated. The exchange reactions give some indication of the reactivities of the O-H and C-H bonds over the different metal catalysts. The chemical reactions demonstrate the differing build up of the major products over nickel and rhodium catalysts from which possible reaction pathways may be inferred.

CHAPTER 2

Experimental Apparatus

2.1 Introduction

The apparatus described below was designed to study exchange reactions of hydrocarbons and heavy water over evaporated metal films and consists essentially of three parts:

- (a) A high vacuum gas handling system enabling mixtures of pure gases and liquid vapours of definite composition and pressure to be used.
- (b) A reaction vessel coupled to a capillary leak.
- (c) A mass spectrometer.

The capillary leak between reaction vessel and mass spectrometer allows the reaction mixture to be continuously analysed.

2.2 The Gas Handling System.

The apparatus used is shown diagrammatically in Figure 2.1 and is constructed of "Pyrex" glass with ground glass taps and joints lubricated with "Apiezon N" vacuum grease. The gas handling system could be evacuated with a mercury diffusion pump backed by a "Speedivac" rotary pump to a pressure of 10^{-6} mm Hg measured by the McLeod Gauge.

Hydrogen and deuterium gas were purified by diffusion through a heated palladium thimble and liquids or condensible gases were purified by trap to trap distillation.

Mixtures/

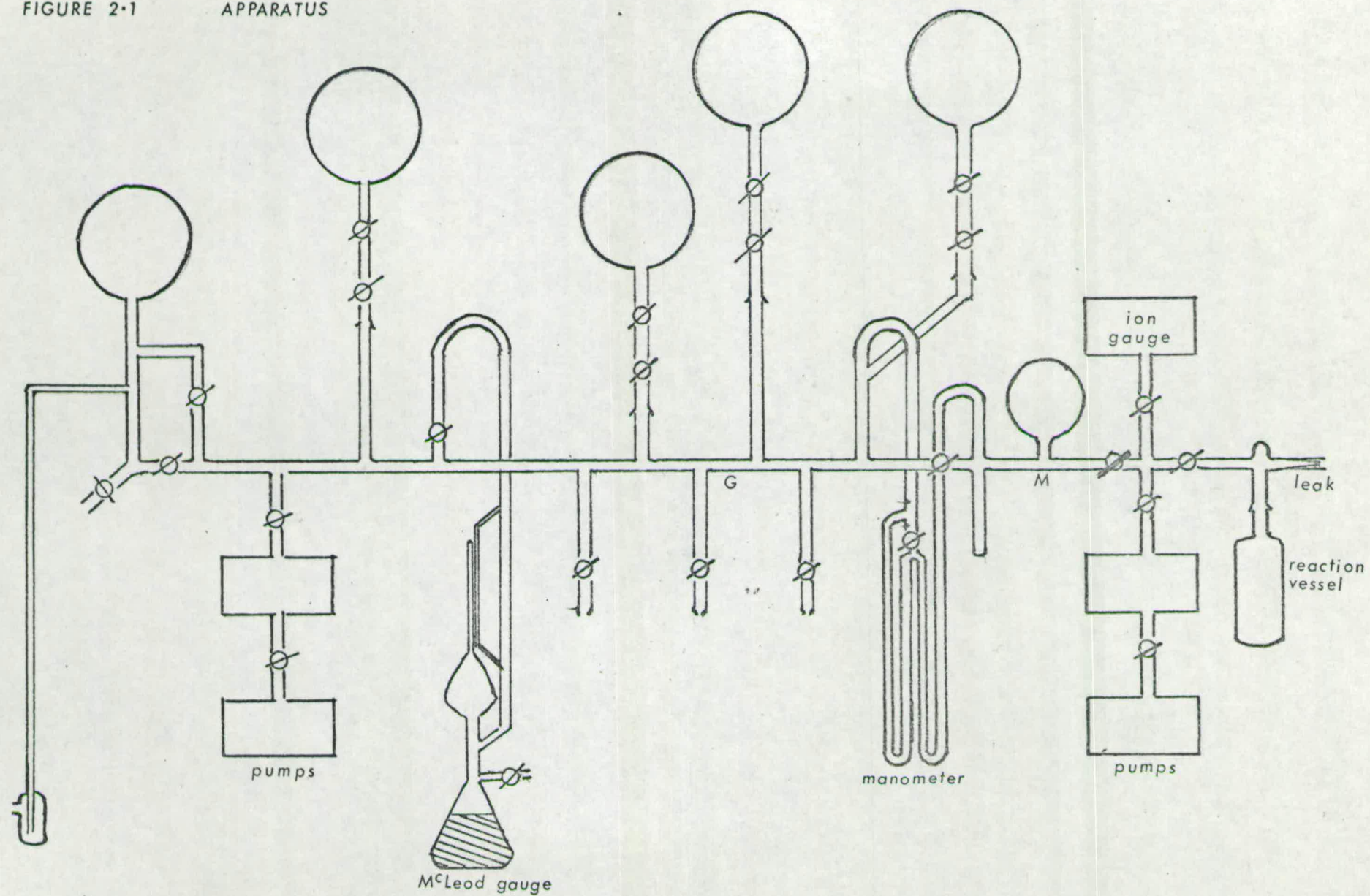


FIGURE 2.1 Apparatus

Mixtures of condensible gases and heavy water were prepared by admitting the required pressure (p_1) of one component into the mixing volume (M) then filling the gas line (G) with a calculated pressure of gas (p_2) required to give the requisite pressure when frozen into the mixing volume. Measurement of the total pressure in the mixing volume provides a check on the accuracy of the mixture preparation. In the case of heavy water and a non-condensable gas, the heavy water was frozen into the mixing volume then the gas line filled with a higher pressure of the non-condensable gas (p_3) and expanded through to the mixing volume. Mixtures were generally allowed to stand overnight to improve their homogeneity before being expanded into the reaction vessel.

2.3 The Reaction Vessel and Capillary Leak.

The reaction vessel, shown in Figure 2.2, is of pyrex glass or silica glass for high temperature work and is joined to the apparatus by means of a B 24 ground glass joint into a "pyrex" water cooled socket. A close fitting furnace could be placed round the reaction vessel and temperature measured by a thermocouple wire held to the reaction vessel with aluminium foil.

Analysis of the gas mixture was effected by means of a fine tapering capillary leak attached to the reaction vessel enabling a small continuous gas stream to be drawn into the mass spectrometer. The capillary leak was constructed from "pyrex" glass by partially collapsing a section of 8 mm bore tube and drawing it out to a fine capillary whose length was then adjusted to give a leak rate of 20 mm air into a volume of 20 mls in 20 minutes with a pressure difference of one atmosphere. The capillary length, similar to that used by/

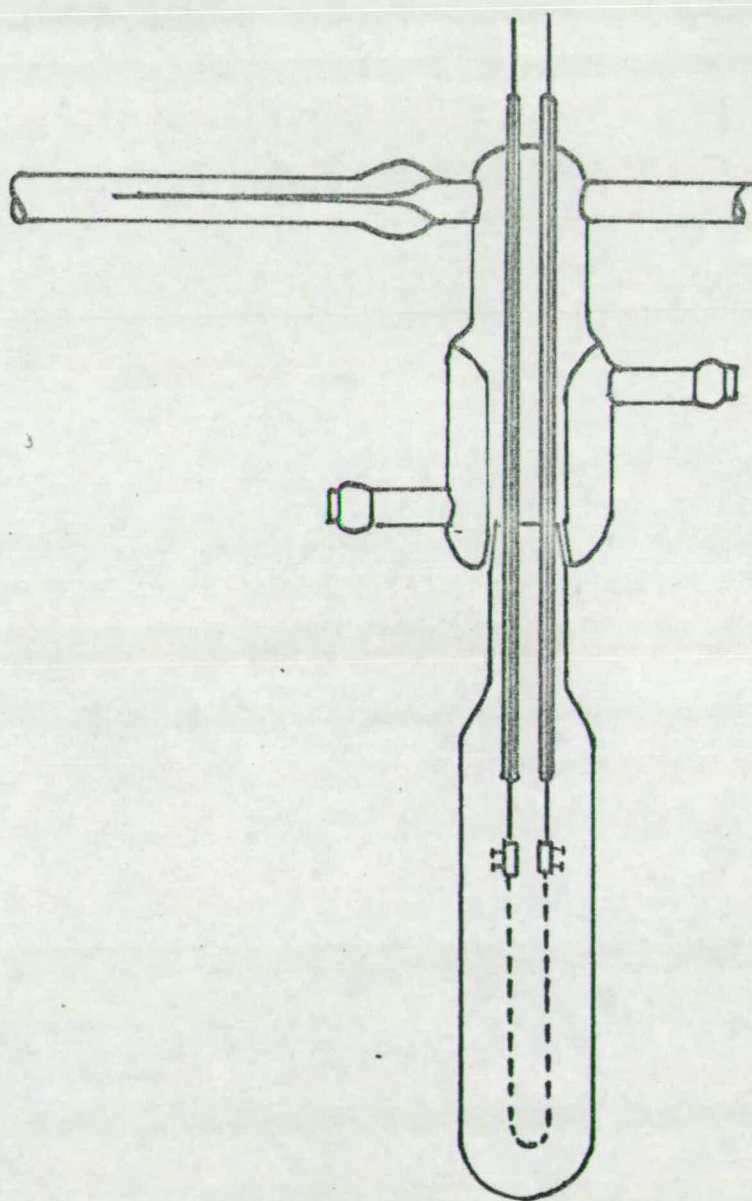


FIGURE 2-2

REACTION VESSEL

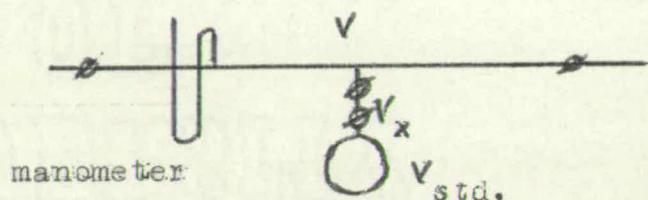
by Nier⁽⁶⁸⁾ was normally about 15 cm long and was found to provide an adequate sample for mass spectral analysis over a period of 12 hours without any appreciable depletion of gas in the reaction vessel.

Capillary leak design has been studied by several authors⁽⁶⁹⁻⁷¹⁾ and the conclusions reached suggest that gas flow through a capillary leak may occur either by viscous flow or by molecular flow. If the former is the case the gas entering the mass spectrometer will have the same composition as that in the reaction vessel but molecular flow discriminates against the higher mass elements in the mixture. A satisfactory leak should, therefore, permit only viscous flow.

In the study of exchange reactions it is assumed that a true cross-section of the species in the reaction vessel is leaked through for analysis and any error in this assumption is usually small as the masses of the isotopic species are similar and molecular flow offers only a small contribution. Where gases analysed differ markedly in size, as with hydrogen and deuterium, contributions from molecular flow should be taken into account in analysis of results.

2.4 Volume Calibrations.

Volumes of different parts of the apparatus were measured by expanding air from a standard bulb attached to the line into the volumes to be calibrated any applying Boyle's Law. Calibration with water showed the volume of the standard bulb "Vstd" to be 143,31 mls at 20°C and the volume of the connection " V_x " between "Vstd" and "V", the volume to be calculated, was measured by expanding a known pressure of gas from "Vstd" into the evacuated volume " $V + V_x$ ".



A second expansion was carried out from the volume "V" into the previously evacuated volumes " V_x " + " V_{std} "

$$P_3 V = P_4 (V_x + V_{std})$$

Knowing P_1 , P_2 , P_3 , P_4 , measured by the manometer and knowing " V_{std} ", then " V " and " V_x " may be calculated.

Other apparent volumes calculated are given below:

Reaction vessel at 23°C	192.5 ml.
Mixing Volume at 23°C	361.4 ml.
Dosing volume at 23°C	16.1 ml.

Using these figures pressures of gases expanded into the reaction vessel may be calculated and using Avogadro's Number, the number of gas molecules in the reaction vessel may also be determined.

2.5 The Mass Spectrometer.

An A.E.I. model M.S. 10 mass spectrometer was employed throughout and Figure 2.3 is a diagrammatic representation of this instrument. An orifice plate "O" restricted the removal of gas entering the tube from the reaction vessel and a plate giving a pumping speed of 1 l sec^{-1} provided adequate spectra. The pumping system included a cold trap filled with liquid nitrogen separating the tube unit from the diffusion and backing pumps. The diffusion pump was a "Metrovac" type O330 pump operated with Apiezon B.W. oil and the backing/

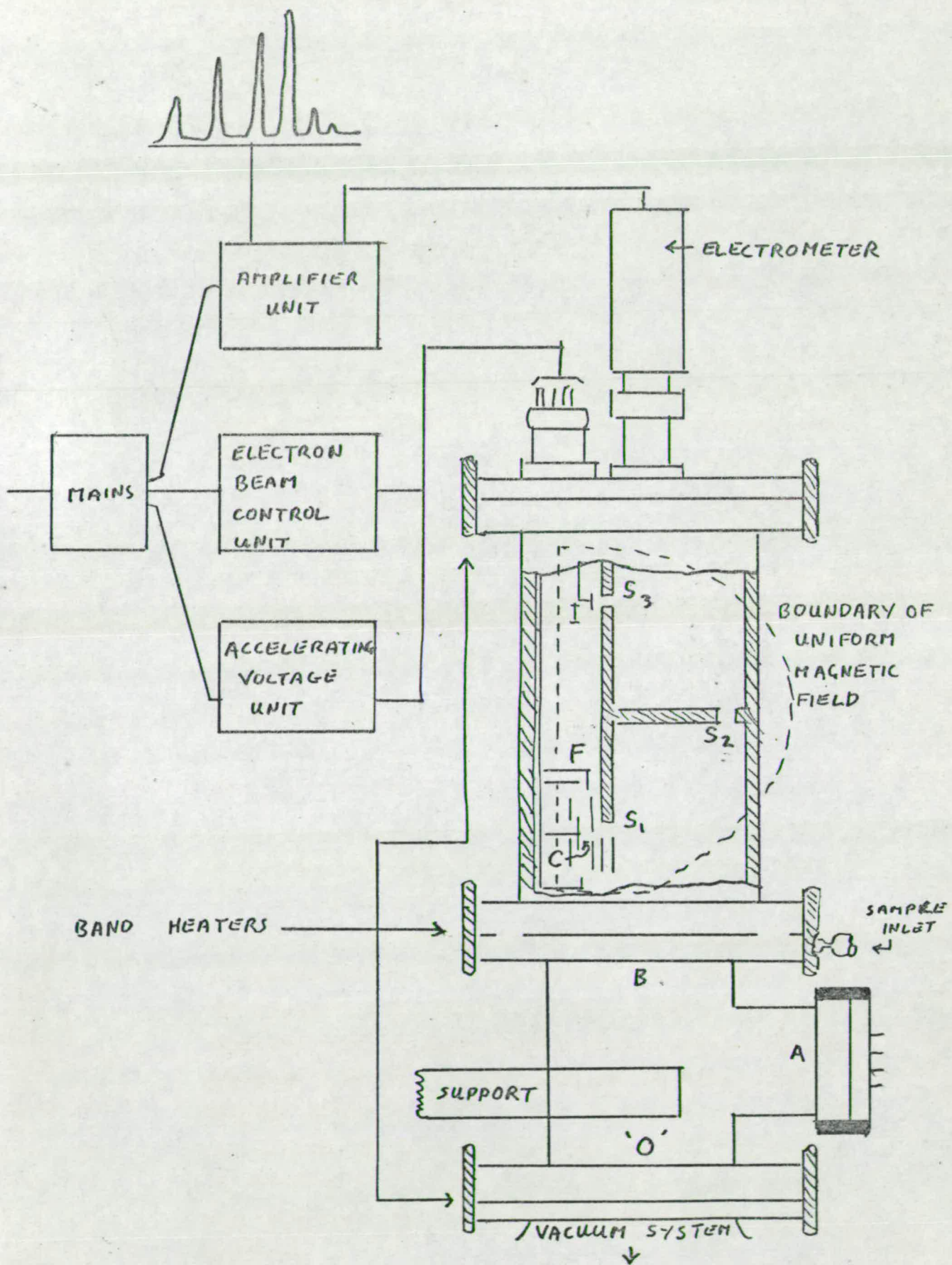


FIGURE 2.3 M.S. 10 MASS SPECTROMETER.

backing pump a "Metrovac" type GDRI two stage rotary pump equipped with a P_2O_5 trap and discharge tube. The part of the system above the cold trap could be baked out to $300^\circ C$. using band heaters and a radiation shield. Pressure in the mass spectrometer was measured by an insertion ionisation gauge at "A" also acting as a trip circuit for vacuum failure in the mass spectrometer. The diffusion pump was also protected by a water switch. For analysis gas enters the analyser tube where the constituent molecules are ionized within the source cage "C" by bombardment with a controlled electron beam originating from a hot wire filament, "F" made of 0.178 mm diameter rhenium wire. The ions produced are accelerated by an accelerating voltage applied to the cage and describe circular orbits under the influence of the uniform magnetic field from the magnet. The orbital radius varies with the ratio of the ion, (m = mass, e = charge), with accelerating voltage "V" and the applied magnetic field "H" according to the relationship.

$$R = \left(\frac{m}{e} \times \frac{2V}{H^2} \right)^{\frac{1}{2}}$$

Where R = orbital radius of ion in magnetic field. At constant "V" and "H" the ion beam is separated into beams of one particular $\frac{m}{e}$ ratio with an orbit characteristic of that ratio. Variation of "V" or "H" thus varies the orbit of the ions and individual beams may be successively brought into focus on the collector I by passing through the slits " S_1 ", " S_2 " and " S_3 " named the resolving, defining and collector slits respectively. Instrument resolution and sensitivity was largely determined by the size of the slits S_2 and S_3 .

A permanent magnet of approximately 1830 gauss supplied the magnetic field and variation of the accelerating voltage allowed masses 2, 3, 4, and 12 to

85/

85 to be resolved accurately, the voltage required to focus any particular mass being approximately $\frac{400}{\text{mass number}}$ (assuming singly charged species). Spectra were displayed on a "Servoscribe" recorder.

2.6 Mass Spectrometric Analysis.

To study exchange reactions the catalyst, after being suitably activated, was brought into contact with the reaction mixture and the temperature then raised until a change in the relative peak heights corresponding to the parent molecule and those at higher masses indicated that a reaction was taking place. The temperature was then stabilised and scans of the mass spectrum in the region of the parent molecule were recorded, a time scale being derived from the measurement of the recorder chart speed. Once sufficient reaction had taken place to allow an accurate measurement of the rate of change of peak height the temperature was raised and the process repeated.

A plot of peak height of the various isotopes and fragments against time permitted smooth curves to be drawn and a measure of the relative amounts of each particular mass at specific times could be measured. These "raw peak heights" could then be subjected to further treatment to determine the percentage of each isotopic species present at that time.

Isotope Corrections

Carbon and hydrogen contain small amounts of heavy isotopes, ^{13}C and D, thus their mass spectra contain peaks at mass numbers higher than those of the parent molecules. Contributions from these isotopes must be taken into account before any accurate data can be obtained and may be measured experimentally or calculated/

calculated theoretically since it is known that the ratios $100^{13}\text{C}/^{12}\text{C}$ and $100^{\text{D}}/\text{H}$ are constant throughout the range of naturally occurring hydrocarbons. These ratios are 1.082 and 0.016 respectively and thus for any hydrocarbon C_nH_m of mass M the peak heights 'P' at mass $M + 1$, $M + 2$, etc. may be calculated using the above factors. For C_nH_m

$$100 \frac{P_{M+1}}{P_M} = \left[n \left(\frac{1.081}{98.919} \right) + m \left(\frac{0.016}{99.984} \right) \right] 100$$

$$\text{and } 100 \frac{P_{M+2}}{P_M} = \left[\frac{n}{2} (n-1) \left(\frac{1.081}{98.919} \right)^2 + \frac{m}{2} (m-1) \left(\frac{0.016}{99.984} \right)^2 \right] 100$$

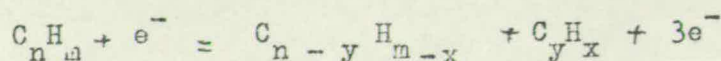
The derived values will vary with the isotopic content of the molecules since replacement of H by D diminishes the contributions of naturally occurring D. For the species $\text{C}_n\text{H}_{m-x}\text{D}_x$ the values of $\frac{P_{M+1}}{P_M}$ and

$\frac{P_{M+2}}{P_M}$ are obtained by substituting $m-x$ for m in

the above equations. The isotopic contribution of ^{13}C is not affected by the exchange process. Corrections are carried out from low masses to high masses.

Fragmentation Corrections

Molecules entering the source region of the mass spectrometer are subjected to impact by electrons from the filament. If the electron transfers sufficient energy to the molecule to exceed its ionization potential then positive ions may be produced in accordance with the Franck-Condon Principle, i.e. for a hydrocarbon C_nH_m we have $\text{C}_n\text{H}_m + e^- = \text{C}_n\text{H}_m + 2e^-$. Other processes may also occur giving smaller positive ions, e.g. $\text{C}_n\text{H}_m + e^- = \text{C}_n\text{H}_{m-x} + x\text{H} + 2e^-$



A hydrocarbon molecule of mass M will therefore exhibit peaks at $M - 1$, $M - 2$, $M - 3$, etc. and so to determine the isotopic content of partially exchanged hydrocarbons the contributions of one isotope to lower mass numbers caused by this fragmentation process must be taken into account. The corrections were minimised by use of low electron energies. The choice of electron voltage is critical as too low a voltage markedly decreases sensitivity and for most hydrocarbons values of between 10 and 20 eV were most satisfactory.

Fragmentation was measured for the undeuterated hydrocarbon and it was assumed that for the fragmentation of the deuterated species the ease of loss of H and D were identical making it possible to carry out fragmentation corrections statistically from this assumption. Generally hydrocarbons lose H more readily than D and for more accurate analysis this should be included. There is also a possibility of preferential loss of H or D at a particular position in the molecule and the fragmentation pattern will depend on whether an H or D atom occupies this position. For the work in this thesis it was found that a simple statistical picture gave satisfactory results.

The fragmentation corrections carried out from high to low masses give a measure of the relative abundance of the different species present.

Computer Analysis

A computer programme was devised to calculate isotopic distributions from raw peak heights and is shown in Figure 2.4 as a flow diagram. A copy of the actual programme is contained in Appendix 1.

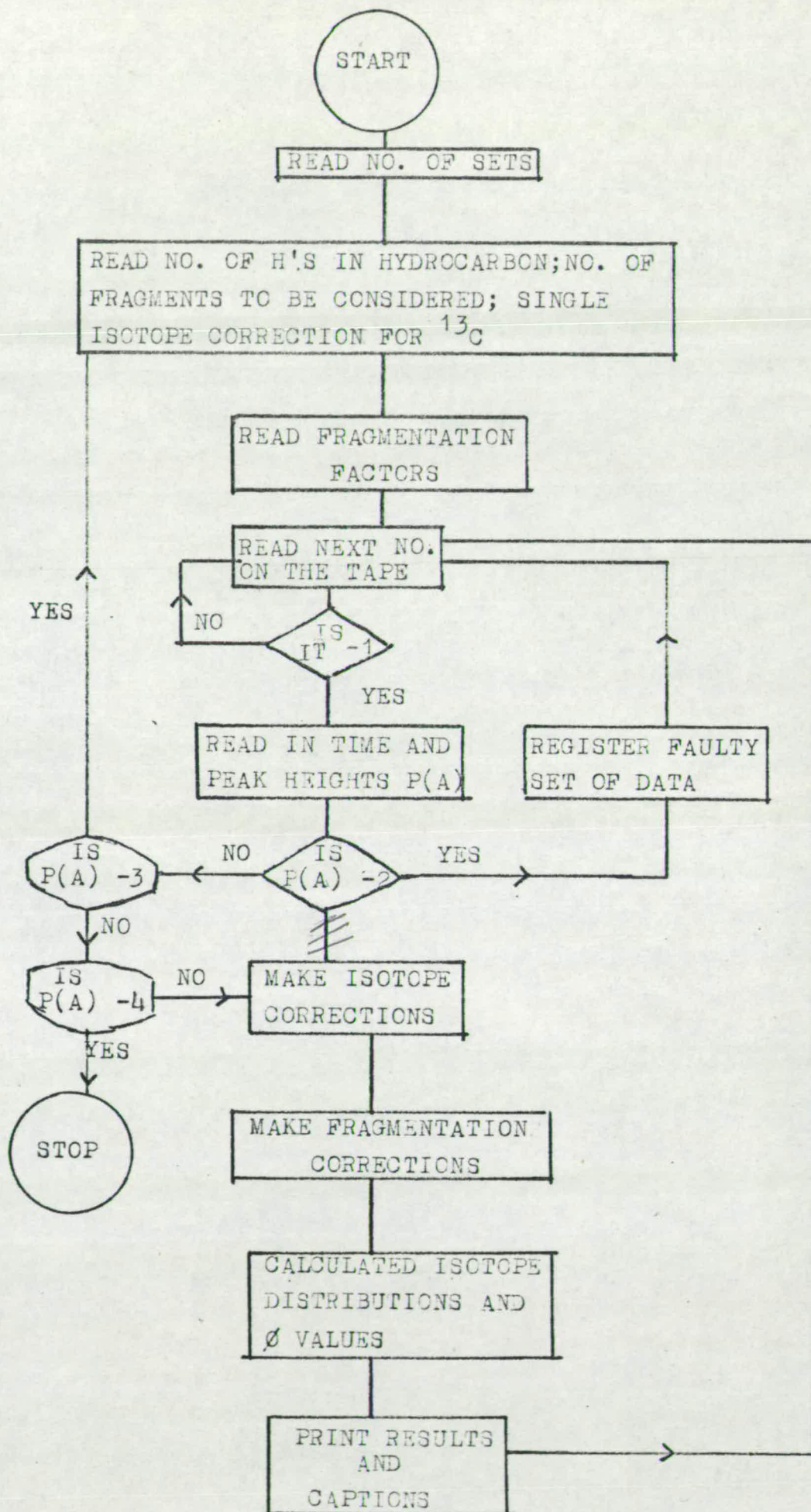


FIGURE 2.4

Flow Chart for Atlas Autocode Program.

2.7 Analysis of the Reforming Reaction.

The reaction between hydrocarbons and steam was investigated over nickel and rhodium catalysts. Using a propylene/water feedstock it was necessary to be able to analyse for propane, ethane, ethylene, methane, carbon dioxide, carbon monoxide, hydrogen and any hydrocarbons present with more than three carbon atoms. This was done using the apparatus described previously together with the MS 10 mass spectrometer which proved adequate for a semi-quantitative analysis of reaction products. The method of analysis is summarised below.

Using a low electron voltage, 10 eV reading on dial, 15 eV true, to minimise fragmentation and so simplify calculation, mass spectral data over the entire range of possible products, with the exception of hydrogen which required a higher electron voltage, were obtained and corrected firstly for background and secondly for naturally occurring isotopes. The accuracy of the isotope correction for ^{13}C will be slightly impaired as peaks 28 and 44 may include contributions from molecules with different numbers of carbon atoms present, i.e. CO and C_2H_4 , CO_2 and C_3H_8 . Using previously measured fragmentation patterns for the individual gases, fragmentation corrections must be made working down from the compound with the highest m/e value. Assuming no molecules with $m/e > 44$ have been detected corrections must firstly be made for propane. As the propane peak coincides with the CO_2 peak an isolated fragment peak must be substituted for one compound, in this case peak 43 is used as a base for propane and the propane contribution removed from all other peaks. Similarly any propylene contributions must be subtracted. There being no significant CO_2 fragmentation to CO at such low voltages, the process is now completed by removing/

removing the contributions from C_2H_6 , C_2H_4 , and CO if they are present using $m/e = 26$ as a base for C_2H_4 to avoid any clash with CO. All that should now remain are peaks 44, 43, 42, 30, 28, 26, 16 and 2 corresponding to CO_2 , C_3H_8 , C_3H_6 , C_2H_6 , CO, C_2H_4 , CH_4 and H_2 respectively.

This qualitative picture may now be put in quantitative form by relating peak heights to gas pressures in the reaction vessel from previously drawn graphs showing the relative sensitivities of the different molecules, Figure 2.5. At low pressures the graphs approximate to straight lines but day to day fluctuations in the sensitivity of the mass spectrometer result in error although relative sensitivities remain fairly constant. A further source of error lies in the use of pressures of pure gases plotted against peak height whereas in practice a wide variety of reactants are being continuously analysed. However results obtained by this method are fairly consistent and it may be regarded as giving a good semi-quantitative analysis of the reaction.

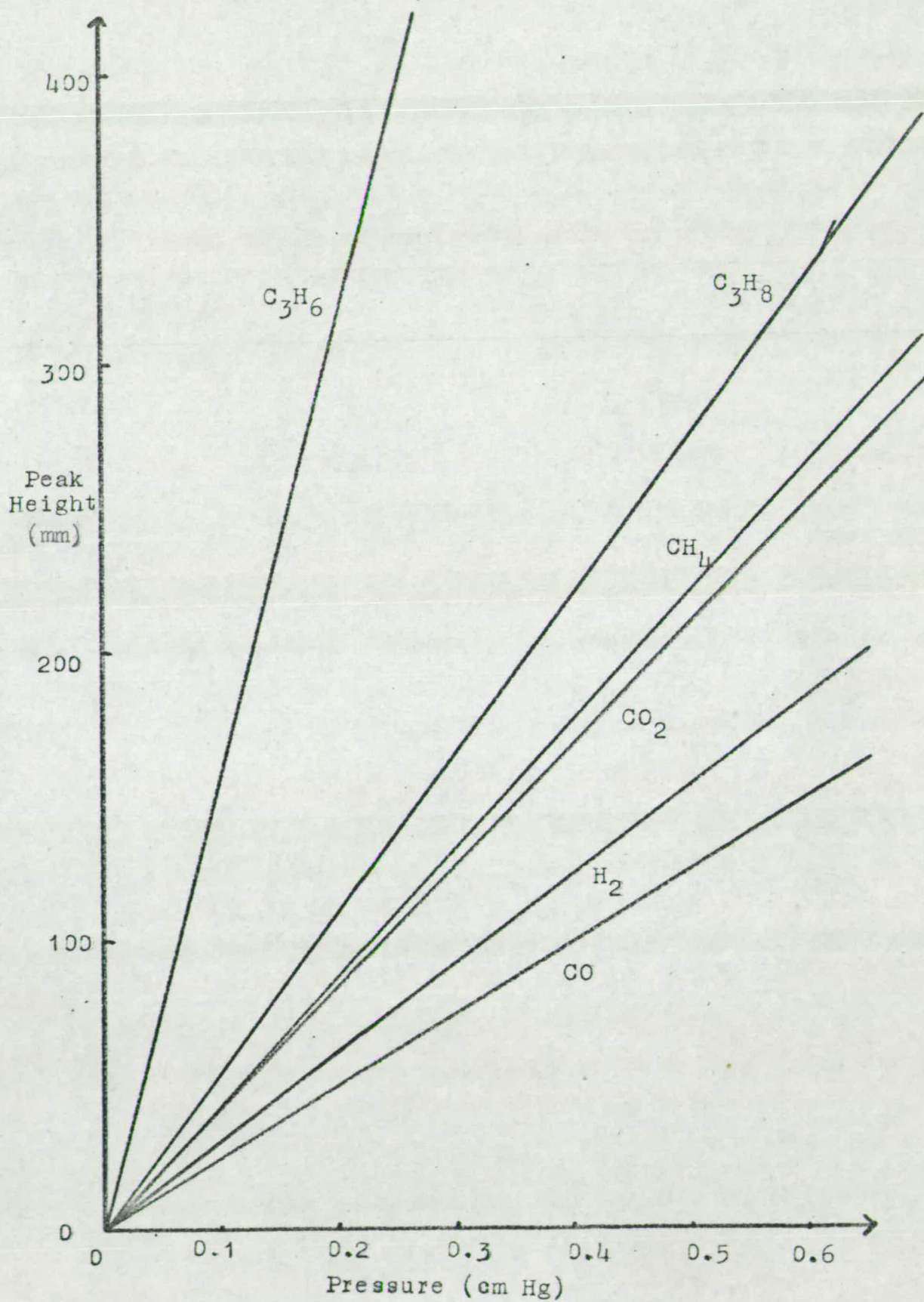
2.8 Preparation and Properties of Evaporated Metal Films.

The preparation of evaporated metal films followed the procedure used by Kemball⁽⁷²⁾ based on that of Beeck, Smith and Wheeler⁽³³⁾. Preparative procedures were standardised to try to ensure the production of clean films with reproducible surface areas and activity.

Evaporation of the films was effected by the passage of a current through a loop of wire of the pure metal in the cases of rhodium and nickel. This method was impracticable for metals which melted before a vapour pressure suitable for film deposition was/

FIGURE 2.5

Peak Height from Mass Spectrometer vs
Pressure of Gas in Reaction Vessel.



was obtained as with platinum and palladium. In these cases wire of the pure metal was wound round a loop of tungsten wire of suitable thickness and heated indirectly, tungsten being used as a support because of its relatively much higher evaporation temperature. Mild steel connectors attached the filament to the tungsten leads in the upper part of the reaction vessel.

Outgassing of the wires was carried out before evaporation and in the case of rhodium at a temperature just below that at which evaporation occurred. It was not possible to outgas the other metals as thoroughly due to their lower evaporation temperatures. In these cases the first film thrown was discarded, subsequent films being more active and reproducible. In all cases films were thrown with the walls of the reaction vessel at 0°C . Preparative details are given in Table 2.1. Palladium and nickel wires could be used repeatedly, reducing the current by 0.1A each time to ensure reproducibility in film weight, but platinum would not give reproducible films after an outgassing film and one other had been thrown. Only one film could be obtained from a rhodium wire as evaporation continued until breakage of the wire.

Table 2.1
Preparation of Evaporated Metal Films.

Metal	Source and Quality	Evaporation Method	Outgassing Current	Evaporation Current	Time for 10 mg film (min)
Pd	Johnson, Matthey & Company, Ltd. "Spectroscopically Tested"	30 cm 0.2 mm Pd wire wound round 15 cm 0.3 mm pure Tungsten.	4.8 amps	6.5 amps	10
Pt	"	30 cm 0.2 mm Pt wire wound round 15 cm 0.3 mm pure Tungsten.	6.5 amps	7.7 amps	20
Ni	"	15 cm 0.5 mm Ni wire.	4.9 amps	6.6 amps	10
Rh	"	3 cm 0.5 mm Rh wire spot welded to two 0.5 cm 0.5 mm pure tungsten leads.	9.0 amps	13.3 amps	Burns out after approx. 5 mg film

CHAPTER 3

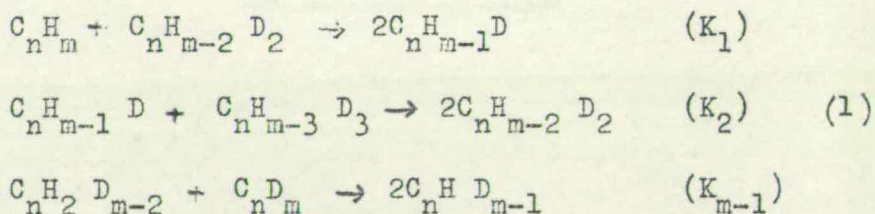
Exchange Reactions

3.1 General Aspects of Exchange Reactions.

Exchange reactions have a number of features in common and it is helpful to consider these briefly before describing the method of treatment of experimental results.

3.2 The Final Equilibrium of an Exchange Reaction.

In the exchange reaction between a hydrocarbon $C_n H_m$ and D_2 or D_2O two kinds of equilibria will be established. These are firstly an equilibrium distribution between the total amount of deuterium in the "hydrocarbon" and the total amount of deuterium in the "hydrogen" and secondly an equilibrium between the relative amounts of the different isotopic species of hydrocarbon present. These equilibria may be represented as shown below.



The values obtained for equilibrium constants of this type for a random or classical distribution of the hydrogen or deuterium atoms between the various isotopic species of the hydrocarbon approximate to the experimentally obtained values. The distribution of the deuterium between the "hydrocarbon" and the "hydrogen" is usually found to differ slightly from the value expected in terms of a random distribution.

The/

The values from the equilibrium constants for the reactions shown in Equation (1) may be calculated from a combination of terms in the appropriate binomial expansion and may be expressed in general terms as

$$K_i = \frac{\binom{i}{m}^2}{(i-1)(i+1)} \quad (2)$$

where $\binom{i}{m}$ represents the number of ways of selecting i objects from a group of m identical objects. A comparison of the calculated interconversion equilibrium constants with experimental results shows good agreement.

3.3 The Determination of Rate Constants.

Two methods of calculation of the rate of an exchange reaction are available and depend on either measurement of the rate of incorporation of deuterium into the hydrocarbon or measurement of the rate of disappearance of the parent hydrocarbon. In the former case the rate is determined from the parameter ϕ defined by

$$\phi = \sum i d_i \quad (3)$$

where d_i is the percentage of isotopic species containing i deuterium atoms at time t . Provided all the hydrogen atoms in the molecule are equally susceptible to exchange and that the influence of isotopes on the rate of reaction is ignored, the course of the exchange reaction will be given by the first-order equation:

$$\frac{d\phi}{dt} = k_\phi \left(1 - \frac{\phi}{\phi_\infty}\right) = \frac{k_\phi}{\phi_\infty} (\phi_\infty - \phi) \quad (4)$$

where k_ϕ is the rate constant equivalent to the number of deuterium atoms entering 100 molecules of the hydrocarbon in unit time at the start of the reaction and ϕ_∞

ϕ_{∞} is the equilibrium value of ϕ .

Integration of equation (4) gives

$$\int \frac{d\phi}{(\phi_{\infty} - \phi)} = \int \frac{k\phi}{\phi_{\infty}} dt$$

$$-\ln (\phi_{\infty} - \phi) = \frac{k\phi}{\phi_{\infty}} t + C$$

When $t = 0$ $\phi = \phi_0$ $[\phi_0 = \text{initial value of } \phi]$

$$C = -\ln (\phi_{\infty} - \phi_0)$$

$$-\log_{10} (\phi_{\infty} - \phi) = \frac{k\phi t}{2.303 \phi_{\infty}} - \log_{10} (\phi_{\infty} - \phi_0) \quad (5)$$

Equations (4) and (5) are only approximations as it has been assumed that all isotopic species react at the same rate, however, they are found to be obeyed in a wide variety of exchange reactions. A reaction which does not obey equation (5) may indicate differences in reactivity between the different hydrogen atoms in the hydrocarbons or poisoning of the catalyst.

A second rate constant k_0 representing the initial rate of disappearance of the light hydrocarbon C_nH_m in percentage per unit time may be calculated using the empirical first order equation.

$$-\log (d_0 - d_{\infty}) = \frac{k_0 t}{2.303 (100 - d_{\infty})} - \log (100 - d_{\infty}) \quad (6)$$

where d_0 is the percentage of C_nH_m at time t and 100 and d_{∞} are the initial and final percentages of this species.

The ratio of the two rate constants, known as the "M value" is defined as

$$M = \frac{k\phi}{k_0} \quad (7)$$

and represents the mean number of hydrogen atoms replaced/

replaced by deuterium atoms in each molecule of the hydrocarbon undergoing exchange in the initial stages of the reaction.

3.4 Arrhenius Plots.

Calculation of isotopic distributions at particular times and temperatures supplies the necessary data to plot $\log (\phi_{oo} - \phi)$ and $\log (d_o - d_{ooo})$ against time according to equations (5) and (6). The resultant lines should be straight for an unpoisoned or non-accelerating reactions and initial reaction rates may be obtained and the M value of the reaction calculated.

The Arrhenius Equation

$$k = Ae^{-\frac{E_a}{RT}}$$

(where k = rate constant, A = frequency factor, E_a = apparent activation energy in kJ mole^{-1} , R = gas constant in $\text{kJ deg.}^{-1} \text{ mole}^{-1}$ and T = temperature in $^{\circ}\text{K}$) may be expressed as

$$\log_{10} k = \log_{10} A - \frac{E_a}{2.303 RT}$$

and values of E_a and $\log A$ may be estimated from plots of $\log_{10} k$ vs. $\frac{1}{T^{\circ}\text{K}}$. In $\log_{10} A$, A is expressed in $\text{mol sec}^{-1} \text{ m}^{-2}$ and calculated from the number of molecules of reactant in the reaction vessel and the catalyst surface area.

3.5 Kinetics.

The rate constants defined above differ from those of an ordinary chemical reaction being constant only for/

for the course of an exchange reaction with a single mixture of reacting gases. They are pressure dependent and assume different values for different initial pressures of the reactants so the true kinetics of an exchange reaction may only be determined by performing a series of experiments with different reactant mixtures as the course of a reaction with a single mixture follows the apparent first order equation (5). That an exchange reaction is apparently first order, irrespective of the true kinetics, may be seen from consideration of the processes occurring during reaction. When a reaction mixture is admitted to a catalyst there is a build up of the surface concentrations of adsorbed species to their equilibrium values after which they remain constant, and there is the exchange reaction leading to equilibrium between all the species in the system, including molecules in the gas phase and adsorbed surface species. The former process is normally rapid but the latter requires all the gas phase molecules to go through adsorption and desorption before it is complete. Throughout most of the time required for the exchange reaction there will be an equilibrium concentration of the adsorbed species. The only factor which reduces the rate of the exchange from the initial value is the approach of the isotopic content of the "hydrogen" and "hydrocarbon" to their equilibrium values and this factor causes the apparent first order behaviour.

3.6 Classification and Possible Mechanisms of Exchange Reactions.

The exchange reactions of hydrocarbons with deuterium may be separated into two main categories namely those in which hydrogen is replaced by deuterium in a simple or stepwise fashion and those involving/

involving multiple exchange.

A simple exchange reaction is characterised by an "M value" of unity, initial production of the mono deuterated species only, and the satisfaction of the interconversion equilibria provided that the isotopic species of the hydrocarbon used as reactant are in equilibrium and provided that all hydrogen atoms in the molecule are equally susceptible to exchange⁽⁷³⁾.

Simple exchange implies an adsorbed intermediate, either associative C_nH_{m+1} or dissociative C_nH_{m-1} , as a comparatively stable entity on the catalyst surface. There must be little chance of the species undergoing further reaction on the surface as this would produce multiple exchanged products.

The existence of multiple exchange is recognised in three ways analogous to those for simple exchange. Firstly "M" will be greater than unity and will give a measure of the mean number of deuterium atoms entering each hydrocarbon molecule in the initial stages of the reaction. Secondly the initial stages of the products will contain molecules having more than one deuterium atom, and finally the isotopic distribution will be richer in more highly deuterated species than would be expected from the calculated distributions based on Equation (2).

Product distribution must be measured at low conversions to exclude species formed by successive interactions with the catalyst if the second criterion is used and the effect of approaching equilibrium from the third criterion since equilibrium is independent of the method of reaching it.

Other aspects of exchange reactions and the results obtained with some hydrocarbons have been reviewed by Kemball^(74,75).

CHAPTER 4

The Preparation of Some Supported Metal Catalysts and the Measurement of Their Surface Areas.

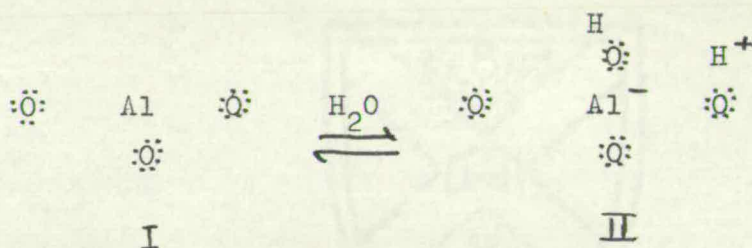
4.1 The Support.

Since catalytic reactions depend on the available surface any extension of the surface by the impregnation of the catalyst on a support material is obviously desirable. Such a support may also enhance the usefulness of the catalyst by simple improvement of its mechanical strength, imposition of restraint on the rate of crystallisation and grain growth, improvement of packing characteristics, and, in addition, affecting the life as well as exerting some promoter effects on the catalyst itself. The promoter effects may be due to epitactic alteration of the atomic spacing of the catalyst or to modification of the 'valency' due to incorporation in the crystal field, while other physical factors such as the porosity of the support must also be considered.

The supported catalysts employed in the present work use α -alumina as a support for either nickel or rhodium. Alumina itself is regarded as an acid type catalyst and Pines and Haas⁽⁷⁸⁾ have shown that these acidic properties are a basis for an explanation of the role of alumina in a number of catalytic reactions. Although there is general agreement as to the acidic nature of alumina surfaces an exact chemical description has not been forthcoming although some advances have been made by Peri⁽⁷⁹⁾. There are two general classes of aluminas which are of catalytic interest, the highly porous aluminas and the low/

low surface area 'alpha' alumina or corundum, and it is the latter class which is of interest here.

The acid sites on a partially hydrated alumina are thought to comprise of both Bronsted and Lewis sites although as water is removed from the surface Bronsted sites are probably converted to Lewis sites. These sites arise from the existence of incompletely coordinated aluminium atoms at the surface. An aluminium atom has an unoccupied p-orbital which may accept an electron pair to form a Lewis acid site, (I). The presence of a water molecule at this site converts it to a Bronsted acid site, (II).

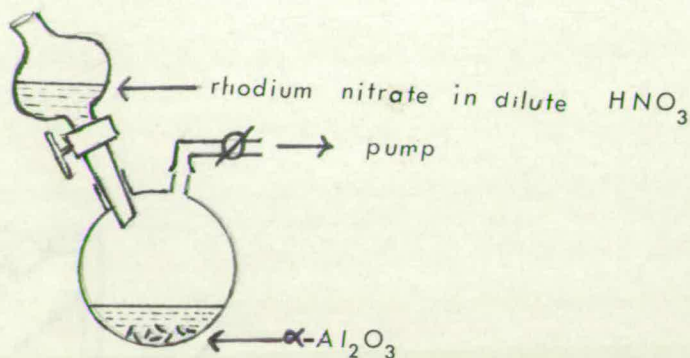


4.2 Catalyst Preparation

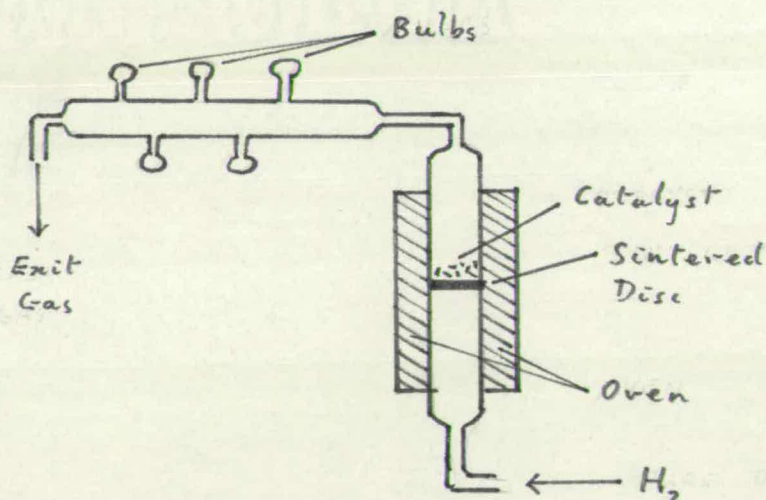
Rhodium on α -Alumina.

To prepare a catalyst containing between 0.5% and 1.0% rhodium on α -alumina a solution of rhodium nitrate should be absorbed on $\frac{3}{8}$ " pellets of α -alumina in the presence of 10% nitric acid.

The porosity of the α -alumina was first calculated by immersion of the pellets in water and measurement of the water loss. To provide the necessary quantity of rhodium a solution of rhodium nitrate containing 4.1g rhodium in 100 ml solution was prepared and introduced to the experimental system shown diagrammatically below.



30g of dried α -alumina pellets were placed in the 250 ml 2 necked flask and the flask evacuated. 25 ml of the rhodium nitrate solution was then added and the pellets left to soak for 3 hours then dried in an oven at 200°C . Finally they were placed in a muffle at 500°C where the nitrate decomposed. The catalyst was then powdered and placed in a reduction apparatus (shown below) where it was reduced in hydrogen at 500°C for 3 hours.



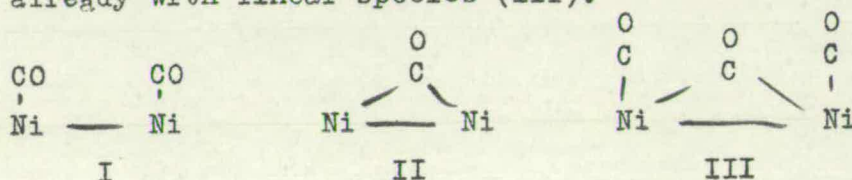
Two samples of rhodium catalyst were prepared containing 0.81% and 0.59% rhodium. The preparation of a nickel on α -alumina catalyst was essentially the same, α -alumina pellets soaked in nickel nitrate giving 6.3% nickel metal content after loss at 500°C.

4.3 Surface area measurements of nickel and rhodium on α -alumina.

When considering the surface area of a supported catalyst a gas selectively adsorbed by the catalyst and not the support is required. Carbon monoxide is chemisorbed on nickel and rhodium and as chemisorption requires the sharing of electrons between a gas phase molecule and the surface it follows that only a monolayer of gas may be formed on the metal surface. A considerable amount of work has been devoted to the attachment of chemisorbed carbon monoxide molecules on to surface metal atoms⁽⁸⁰⁾. Beeck et al⁽³³⁾ concluded that chemisorption of CO on nickel occurred through a single site mechanism but later work showed that two site attachment was also possible. Lanyon and Trapnell⁽⁸¹⁾ comparing the chemisorption of CO and H₂ over a number of metal films found that over molybdenum and rhodium both gases exhibited similar chemisorption suggesting that since hydrogen was known to dissociate over these metals each carbon monoxide molecule must be attached to two metal atoms.

Yates and Garland⁽⁸²⁾ have proposed that several different types of bonding are possible for carbon/

carbon monoxide chemisorbed on nickel supported on α -alumina, the exact type depending on both the nickel content and the fractional coverage of CO. On 'crystalline' nickel, found mainly in catalysts with a high content ($>10\%$ Ni) an infra-red technique showed both a bridged (II) and a linear (I) form present, while at higher pressures of CO a third form appears with a bridged form between two nickel atoms already with linear species (III).



Catalysts with a low nickel content ($\sim 1.5\%$ Ni) have less strongly bonded CO with linear bonding, these 'dispersed' nickel catalysts being of an imperfect crystalline form. A value of 1.4 nickel sites per molecule of CO has been used in calculating the metal surface areas.

4.4. The Experimental Determination of Catalyst Surface Areas by CO Adsorption.

An apparatus of the type shown in Figure 4.1 was used to determine the surface areas of nickel and of rhodium supported catalysts. This may be used to find the point at which a monolayer of gas is formed on the metal and hence the surface area as described below.

A simplified version of Figure 4.1 is shown below.

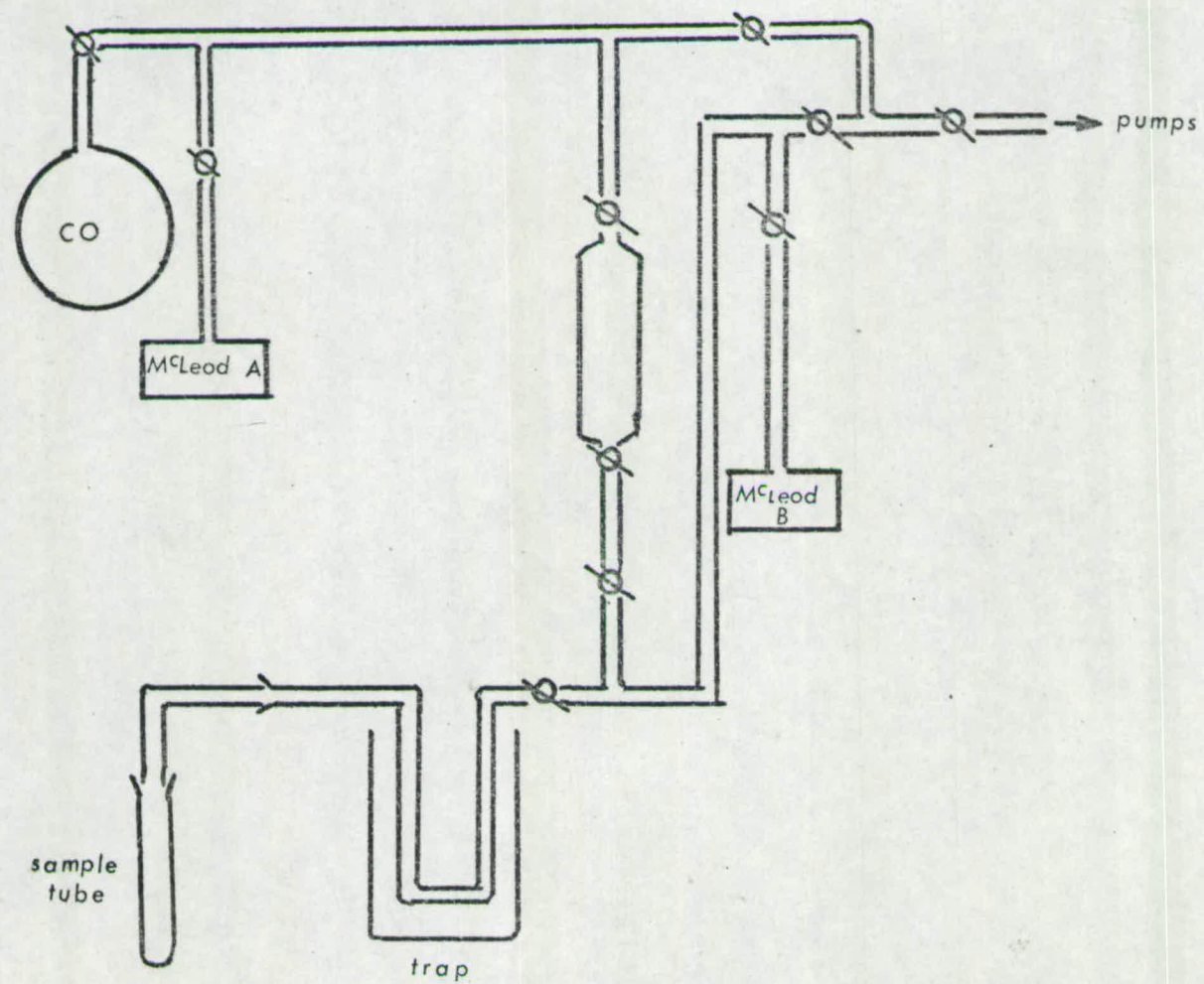
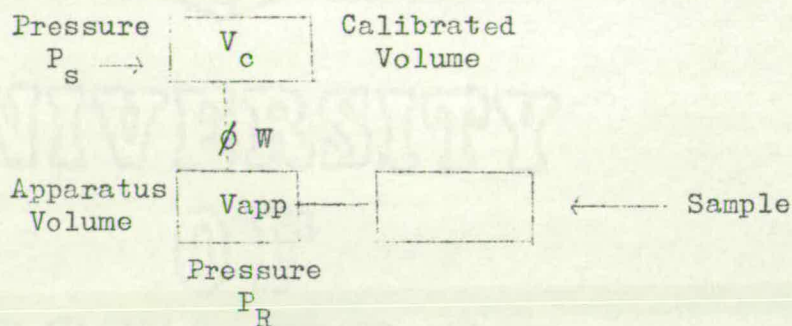


FIGURE 4-1 CO ADSORPTION APPARATUS



By admitting successive known gas pressures into the sample volume and noting the resultant pressure loss due to adsorption of gas by the sample an adsorption isotherm may be drawn as in Figure 4.2 where V_{ads} is the volume of gas adsorbed at 20.5°C , P_R is the pressure of gas in the sample volume at the same temperature, and V_{CO} is the critical volume of gas required for monolayer formation. The calculations are shown in Appendix II together with a sample computer programme.

Results of Surface Area Measurements.

(1) Nickel on α -alumina.

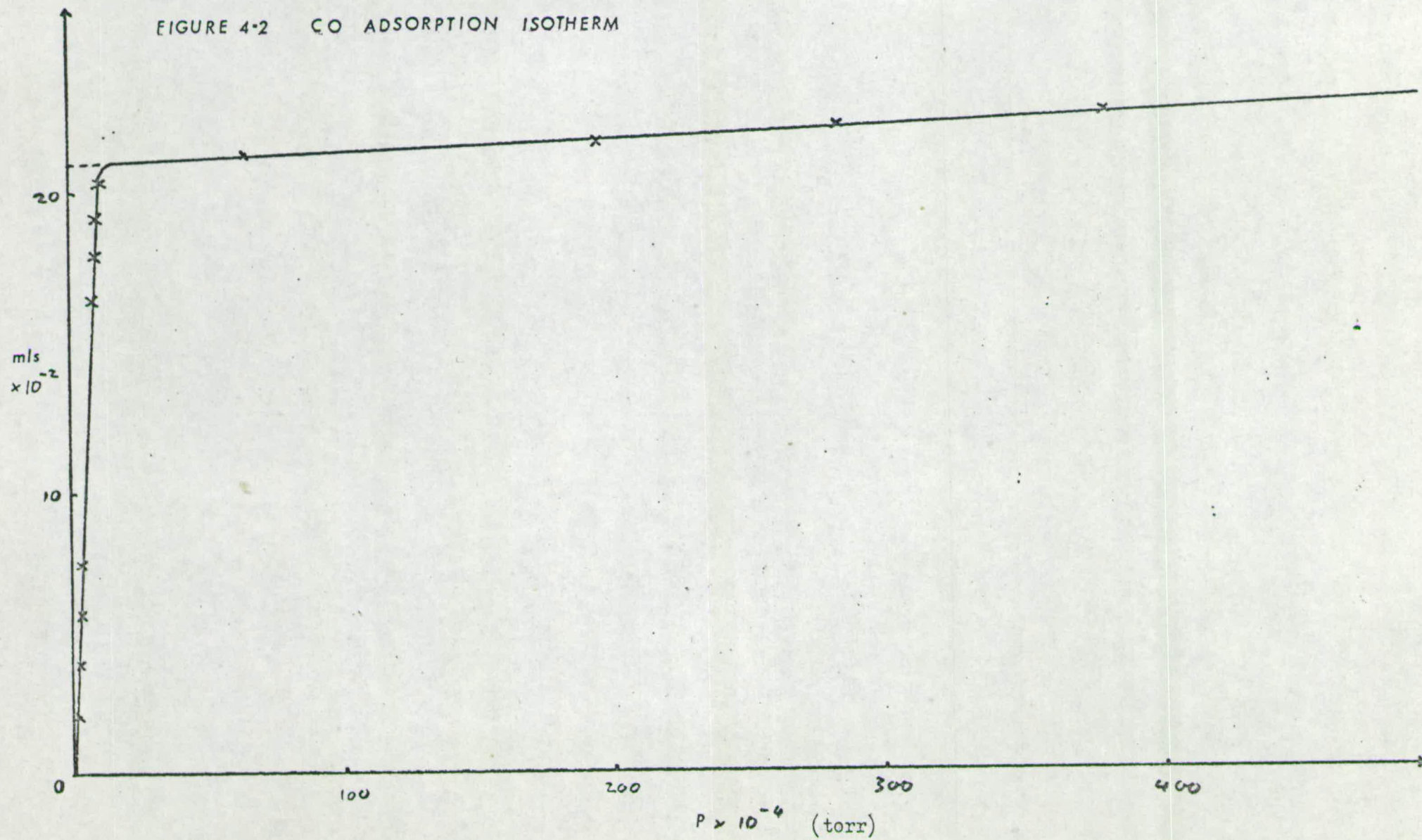
6.3% nickel on α -alumina, reduced at 500°C in dry hydrogen for 26 hours and sealed under hydrogen for testing with CO adsorption and x-ray diffraction techniques.

<u>Sample</u>	<u>S.A. m^2g^{-1} catalyst</u>	<u>S.A. m^2g^{-1} nickel</u>
CO adsorption	1.1	17.5
CO adsorption	1.03	16.3
X-ray diffraction	1.25	19.8

These results were obtained from I.C.I. along with a batch of the catalyst used in this work. Further surface areas of similar batches were obtained using the same technique by the author but as these have no relevance to this work the results are not included.

(2)/

FIGURE 4-2 CO ADSORPTION ISOTHERM



(2) Rhodium on α -Alumina.

The surface areas of the two samples of 0.81% rhodium and 0.59% rhodium on α -alumina reduced in dry H_2 at $500^\circ C$ for 3 hours and sealed under hydrogen were measured by CO adsorption.

<u>Sample</u>	<u>S.A. $m^2 g^{-1}$ catalyst</u>	<u>S.A. $m^2 g^{-1}$ rhodium</u>
(%Rh)	1.00	123.4
0.81	0.98	121.0
	1.03	127.5
	0.68	115.0
0.59	0.69	116.5

PART 2



UNIVERSITY
OF
EDINBURGH



CHAPTER I

The Exchange Reaction Between Hydrogen and Heavy Water over Nickel, Rhodium, Platinum, and Palladium Films.

1.1. Introduction

To understand the mechanism of catalytic steam reforming it is necessary to know how the individual molecules behave. In the course of a steam reforming reaction all three main bonds in the reactant molecules are broken, namely the O-H bond in water, and the C-H and C-C bonds in the hydrocarbon. This chapter deals with the simplest case of the hydroxyl bond in water studied by the exchange of deuterium in heavy water with hydrogen gas over a temperature range of 0-90°C. The relatively low temperature range makes a direct comparison with reactions at the much higher temperatures involved in steam reforming difficult but still valuable.

1.2. Experimental.

The experimental apparatus and the methods of preparation of the evaporated metal film catalysts have been described previously (Part 1 Chapter 2). Hydrogen (99.9%) was obtained from the Matheson Company and was purified before use by diffusion through a palladium thimble, and deuterium oxide (99.7%) was obtained in 25 gm containers from Imperial Chemical Industries Limited and degassed by vacuum distillation before use. A 1:1 mixture of hydrogen and heavy water was prepared in the mixing volume and allowed/

allowed to stand overnight to improve the homogeneity of the sample which could then be expanded into the reaction vessel giving a total pressure of approximately 200.1 mm^{-2} . After throwing the metal film the temperature of the reaction vessel was adjusted to that required for reaction and the gas mixture then admitted for the ensuing exchange reaction to be monitored by the mass spectrometer. An ionizing beam of 70 eV gave ample sensitivity for measurement of the hydrogen isotopes.

The M.S.10. proved inadequate for analysis of the 'water' species as it took several hours for a given pressure of water in the reaction vessel to reach its optimum peak height on the mass spectrometer due to adsorption on the walls of the spectrometer. A further complication was the 'memory effect' whereby adsorbed water on the mass spectrometer walls exchanged with the isotopic water species admitted from the reaction vessel, the admission of D_2O into the spectrometer after saturation with H_2O , requiring several days to remove all traces of light water. It would be possible to overcome this problem by running the spectrometer at a higher temperature but this was not necessary as the results from study of the 'hydrogen' species proved adequate.

Analysis of the data required corrections for naturally occurring isotopes, correction for the contribution of fragmented deuterium to the hydrogen peak, and consideration of the relevant sensitivities of the different hydrogen species obtained by experiment. Using these corrections the distributions of the various isotopic 'hydrogens' at known times and temperatures were calculated and the equation:

$$- \log_{10}(\phi_{\infty} - \phi) = \frac{k \phi t}{2.303 \phi_{\infty}} - \log_{10} \phi_{\infty}$$

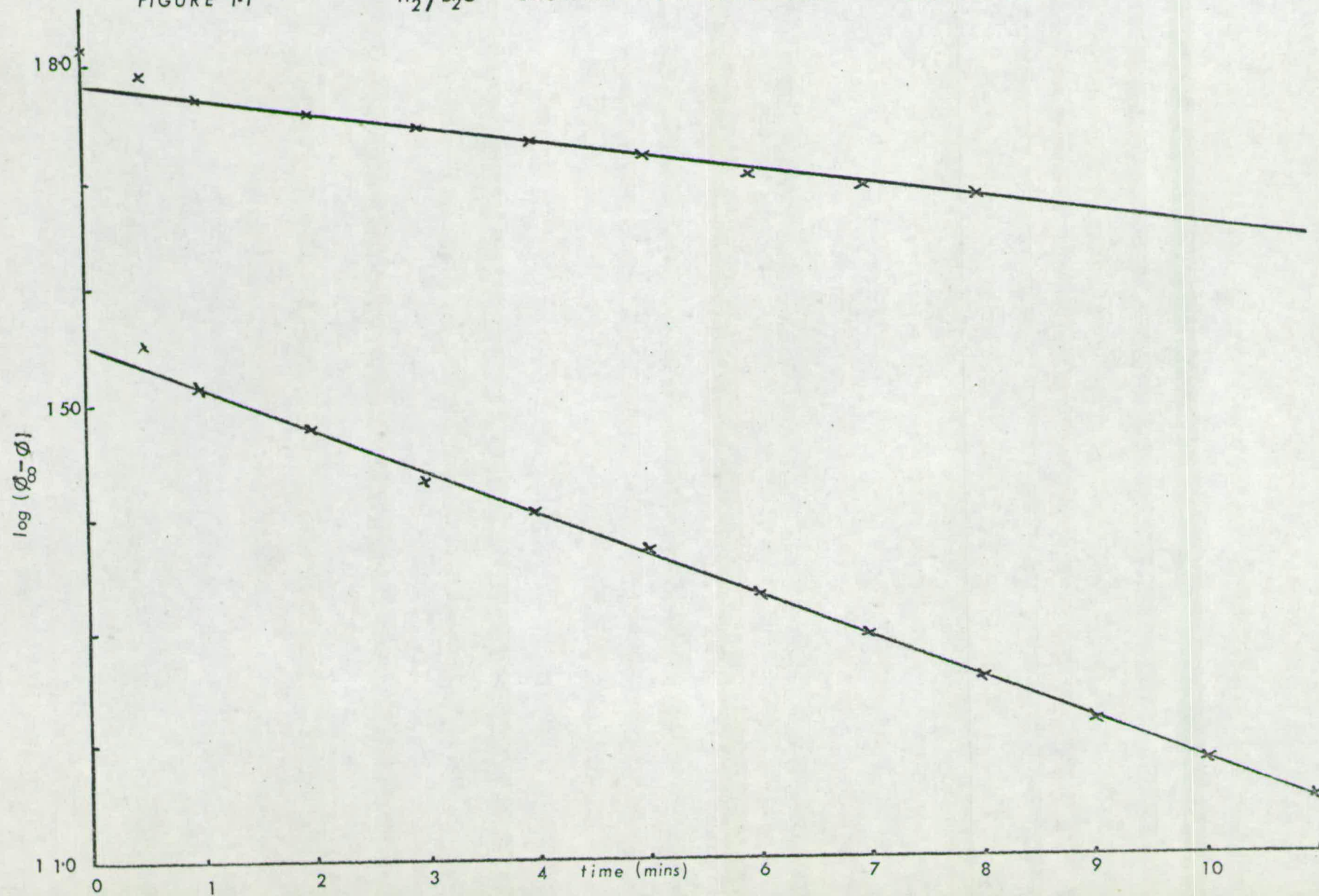
derived in Part I, Chapter 3.3 used to calculate the initial/

initial rate of entry of deuterium atoms into 100 molecules of hydrogen. A typical rate plot is shown in Figure 1.1. The equilibrium value ϕ_{∞} may be calculated from knowledge of the ratio of H:D in the reactant mixture and the equilibrium constants for the relevant equations⁽⁴¹⁾, or it may be measured experimentally.

To improve the correlation between the kinetic data obtained for reactions over various metal films, the observed rate at any given temperature on a film was converted to a rate per unit weight of film. This assumption that the catalytic activity of a metal film is proportional to the film weight has been verified for a range of reactions. Beeck, et. al.⁽³³⁾ showed the rate of hydrogenation of ethylene at 0°C over unoriented films of nickel evaporated in high vacuum at room temperature, increased linearly with film weight below about 20 mg, while above this value increased orientation of the film slightly impairs this relationship. The films in the present work were of 5 - 12 mg. Kemball⁽⁷⁶⁾ showed the initial rate of exchange of methane with deuterium on nickel films was proportional to film weight within an error of about 5% and in various other work reaction rates reduced to unit weight of film satisfactorily obey the Arrhenius equation.

Reaction rates over films of nickel, rhodium and platinum were all reduced to rates per unit weight of film while over palladium films the surface area of the catalyst was taken to be its geometric surface area after the method of Gault and Kemball.⁽⁷⁷⁾ The results for H_2/D_2O exchange were also calculated in terms of rate per unit weight of palladium and the temperature required for a rate of $1\% \text{ min}^{-1} (10\text{mg})^{-1}$ shown in Table 1.1.

FIGURE 1-1

 H_2/D_2O EXCHANGE ON PALLADIUM $0^\circ C$ & $18.5^\circ C$ 

1.3 Results.

Where no catalyst is present in the glass reaction vessel a slow exchange reaction occurs between hydrogen and heavy water at temperatures between 19°C and 142°C. A slight decrease in rate is evidenced between $1.8 \times 10^{-1} \% \text{ min}^{-1}$ at 19°C and $4.4 \times 10^{-2} \% \text{ min}^{-1}$ at 142°C, a possible contributing factor being dilution of the heavy water by light water adsorbed on the glass walls. The reaction on an evaporated nickel film occurred at a comparable rate to that on glass, increasing slightly with temperature, and with an activation energy of approximately $15.1 \text{ kJ mole}^{-1}$. On platinum the rate at 0°C is too fast to be accurately determined using the available apparatus, being at least $20\text{--}30 \% \text{ min}^{-1}$. The exchange rates on palladium and rhodium catalysts fall between these two extremes, measurable rates being obtained at room temperature. The activation energy for the reaction on palladium is $40.0 \text{ kJ mole}^{-1}$ but difficulties in obtaining accurately known metal surface areas using a rhodium catalyst due to the problem of throwing films using a high current (12.5 amps) without breaking the wire resulted in a certain irreproducibility in the kinetic results. However sufficient data was obtained to place it slightly above palladium as a catalyst for the exchange of hydrogen and heavy water. Table 1.1 summarises the Arrhenius data for the $\text{H}_2/\text{D}_2\text{O}$ exchange reaction.

1.4/

Table 1.1.

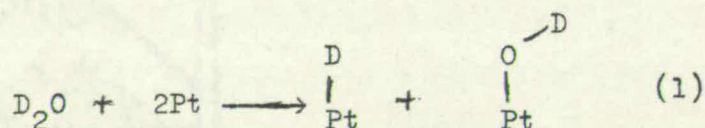
Arrhenius Parameters for H_2/D_2O Exchange on Evaporated
Metal Films.

Catalyst	Temp. Range °C	E_A kJ mole ⁻¹	$\log_{10} A$ (A in mol sec ⁻¹ m ⁻²)	Temp. for
				$k = 1\% \text{ min}^{-1}$ (10m) °C
Nickel	0-52	15.1	18.9	144
Palladium (Apparent areas)	0-20	40.0	20.6	37
Rhodium	0-20	75	32	0
Platinum	0	Reaction too fast to analyse (20-30% min ⁻¹)		

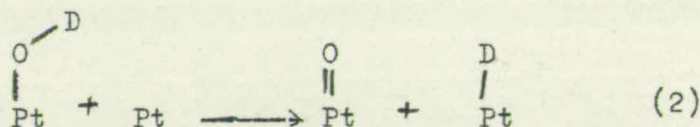
1.4 Discussion.

The exchange reaction between hydrogen and heavy water over evaporated films of platinum, rhodium, palladium, and nickel shows a trend of activities of the order $\text{Pt} > \text{Rh} > \text{Pd} > \text{Ni}$, the rates over rhodium and palladium being similar at 0°C . It is of interest to note that the various forms of alumina are inert for this reaction although Olariu and Marginean have noted an increase in activity using alumina promoted nickel⁽⁸³⁾.

All four metals rapidly catalyse the hydrogen/deuterium exchange reaction which is generally agreed to follow a dissociative mechanism, however the mechanism by which water exchanges is less well established. Garnett⁽⁸⁴⁾ has proposed that on a platinum catalyst heavy water dissociates as shown:

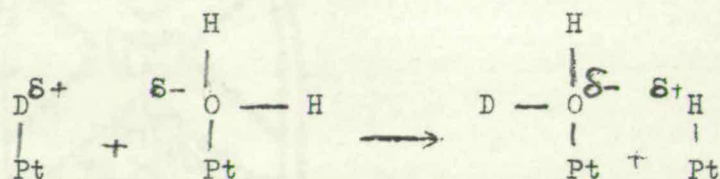


There is little chance of the further thermodynamically unfavourable step



occurring as free hydrogen has a very strong affinity for chemisorbed oxygen. The main evidence for the dissociative chemisorption of water (1) originates from the rapid equilibration of the water/deuterium gas mixtures^{(85), (86)} but the evidence is less conclusive than in the case of hydrogen/deuterium mixtures/

mixtures since rapid exchange is also possible by a proton transfer mechanism:



There is now general agreement that water exists dissociatively on the surface of platinum and also palladium, rhodium and nickel although the non-dissociative adsorption of water is also possible on some parts of the metal surface⁽⁸⁷⁾.

In conclusion it would appear that the order of adsorption and dissociation of water in the presence of hydrogen is $\text{Pt} > \text{Rh} > \text{Pd} > \text{Ni}$, nickel being most inactive allowing for the possibility of the dissociation of water being an important step in steam reforming. This order of activities is in agreement with that found by Anderson and Kemball⁽⁸⁸⁾ for the exchange of the hydroxyl hydrogens of some aliphatic alcohols with deuterium and these authors suggest that some relationship may exist between catalytic efficiency and work function as in the case of ammonia exchange.

CHAPTER 2

The Exchange Reaction Between Propylene and Heavy Water over Nickel, Platinum, Palladium and Rhodium Catalysts.

2.1 Introduction

The second stage in the examination of the catalytic steam reforming reaction was a study of the behaviour of the carbon-hydrogen bond in the reactant hydrocarbons with different catalysts. Heavy water was used as a source of deuterium in an exchange reaction with propylene providing a demonstration of the carbon-hydrogen bond reactivity. The choice of heavy water as a reactant not only emphasised the relevance of the experiment to steam reforming but was convenient for use in exchange with an unsaturated hydrocarbon as no hydrogenated products would normally be formed. An olefin was preferred to a paraffin for exchange as previous research at I.C.I. had suggested that olefins were likely to act as reactive intermediates in the steam reforming reaction and propylene provided a simple olefin which would readily exchange with heavy water. This was doubly convenient as the paraffins are much less reactive for exchange, propane reacting chemically with heavy water over nickel above 300°C before exchange could occur. Methane proved equally reluctant to exchange with heavy water over nickel although experiments were carried out with varying mixtures of methane and D_2O at temperatures in excess of 400°C . To examine the methane/ D_2O system it was necessary first to include a nitrogen cold trap between the capillary leak and the mass spectrometer to remove all traces of 'water'.

'water' species which would otherwise have interfered with the methane peaks as both appear in the same mass range, (m/e values 16 \rightarrow 20). Secondly a ~~pyrex~~^{silica} glass reaction vessel was constructed as little reaction occurs with a methane/water mixture below 420°C at which point a ~~silica~~^{pyrex} glass vessel shows signs of melting. Methane too reacts chemically with water at temperatures in excess of 400°C before exchange occurs. The products from a $\text{CH}_4/\text{D}_2\text{O}$ mixture over nickel are CO , CO_2 , 'hydrogen', 'methane' and 'water' species. To investigate this reaction it would be necessary to simplify the mixture to $\text{CH}_4/\text{H}_2\text{O}$ and analyse the products using gas chromatography as the cold trap, essential for removing water, will also remove CO_2 rendering the analysis valueless. The exchange reaction between ethylene and heavy water over nickel was also investigated and turned out to be more complex than expected. In the first place the distribution of isomers turned out to be very different from the binomial distribution as shown in Table 2.1.

Table 2.1

Distribution of Isomers for $\text{C}_2\text{H}_4/\text{D}_2\text{O}$ Exchange over a Nickel Film at 200°C.

<u>Catalyst</u>	<u>ϕ</u>	<u>Distributions</u>				
		<u>d_0</u>	<u>d_1</u>	<u>d_2</u>	<u>d_3</u>	<u>d_4</u>
Nickel film	100	38	31	24	7	1
Binomial	100	32	42	21	5	0

Secondly, as the reaction approached equilibrium readings from the mass spectrometer corresponding to m/e values of 33 to 36 indicated that a complete range of deuterated ethylenes and ethanes were being formed. Such a mixture of products could not be analysed with the available apparatus and a fuller investigation of this system would require a system of gas chromatographic separation/

separation of olefins and paraffins followed by a mass spectrometric analysis of the products.

A subsidiary experiment involving a C_2H_4/H_2O mixture over nickel showed ethane formation occurring in increasing amounts at temperatures between $27^\circ C$ and $300^\circ C$. The ethylene/ D_2O system was studied within the temperature range $100 - 300^\circ C$ and the Arrhenius parameters corresponding to the rate of disappearance of C_2H_4 , either to deuterated ethylenes or to ethanes, are

$$r_o = 10^{16.0} e^{-\frac{40}{RT}}$$

where r_o is the absolute rate in $\text{mol sec}^{-1} \text{ m}^{-2}$ and the activation energy is in kJ mole^{-1} .

2.2 Experimental.

The apparatus and method of film preparation has been described previously. Reactions were carried out in a pyrex glass reaction vessel at temperatures between $0^\circ C$ and $220^\circ C$ with a reaction mixture of three parts heavy water to one part propylene, the propylene pressure being 33.3 Nm^{-2} , i.e. 1.7×10^{19} molecules at room temperature. The mixture of reactants was admitted to the reaction vessel by expansion from the mixing volume at room temperature and the temperature of the reaction vessel then raised to the required level. The M.S.10 mass spectrometer was used to monitor the peaks with m/e values 36 to 48, using a low (15eV) electron voltage, and the data processed as described in Part I, Chapter 2. Initial rates k_ϕ and k_o were measured and where poisoning of the reaction occurred both initial and final values of the rate of reaction k_ϕ were calculated.

The exchange was followed over four metal catalysts, namely nickel, palladium, platinum, and rhodium, /

rhodium, and also over a nickel supported catalyst. The supported nickel catalyst was of 6.3% nickel impregnated on α -alumina and prepared by reduction in dry hydrogen for 24 hours at 500°C, the nickel surface area being about 1 m² per gram of catalyst. The reduction was performed at I.C.I. Billingham and the catalyst supplied in glass bulbs and could be exposed by breaking the bulb in situ with a magnet sealed in glass. I.C.I. kindly supplied the prepared nickel catalysts used in this work.

2.3 Results.

The hydrogen atoms of propylene and the deuterium atoms of heavy water are readily exchangeable over evaporated films of nickel, platinum, palladium, and rhodium at temperatures under 200°C. Two metals, rhodium and palladium, were found to catalyse the reaction in a straightforward manner with no evidence of poisoning of the catalyst or of any side reactions while both platinum and nickel catalysts introduced complications into the exchange. Thus it is convenient to describe the results of the reaction over palladium and rhodium together and over platinum and nickel separately.

Control experiments proved the pyrex glass reaction vessel to be catalytically inert for the propylene/heavy water exchange reaction up to 400°C, the point at which the reaction vessel began to show signs of melting.

C₃H₆/D₂ Exchange/

C₃H₆/D₂O Exchange over Rhodium and Palladium Films.

The 'hydrogen' exchange between propylene and heavy water proceeds at conveniently measurable rates over the temperature range 0-130°C on palladium and 100-280°C on rhodium. A general characteristic of the exchange reaction is an initial period of settling lasting a few minutes followed by a steady reaction, probably due to super-active sites on the reaction vessel or the fresh unsintered catalyst.

Figure 2.1 displays the percentage distribution of isomers plotted against time for the propylene/heavy water exchange reaction over a rhodium catalyst at 184°C. The distribution clearly shows the formation of all six possible deuterated propylenes building up in sequence, the higher deuterated species only appearing late in the reaction. This suggests a simple or stepwise mechanism for the replacement of hydrogen by deuterium over rhodium and a very similar distribution is obtained over palladium. Further confirmation of this mechanism is supplied by a comparison of the distributions of the deuterated species with those from a binomial expansion, (Appendix III), shown in Table 2.2 for exchange over both palladium and rhodium catalysts.

Figures 2.2 and 2.3 are typical examples of rate plots for propylene/heavy water exchange over rhodium in terms of k_{ϕ} and k_0 respectively, similar plots being obtained over palladium. Table 2.3 summarises the reaction rates at different temperatures over rhodium and includes the 'M' values from the ratio k_{ϕ}/k_0 . Figure 2.4 is a graphical representation of the rates in the form of an Arrhenius plot from which the equation

$$r_0 = 10^{21.1} e^{-41.8/RT}$$

(where r_0 is the absolute rate in mol sec⁻¹ m⁻² and the activation energy is given in kJ mole⁻¹) may be derived./



FIGURE 2-1 DISTRIBUTION OF ISOMERS FOR C_3H_6/D_2O EXCHANGE ON RHODIUM AT $184^\circ C$

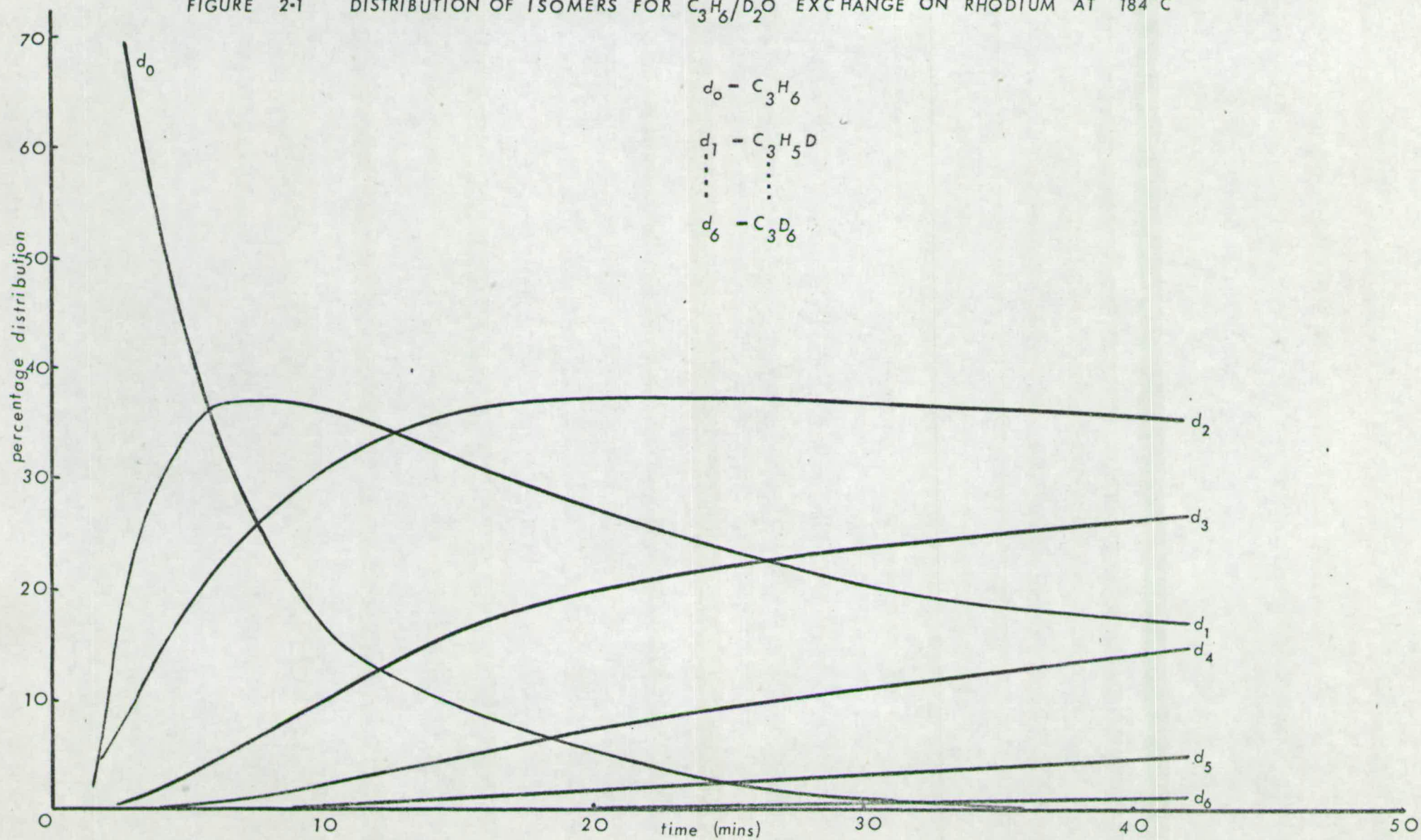
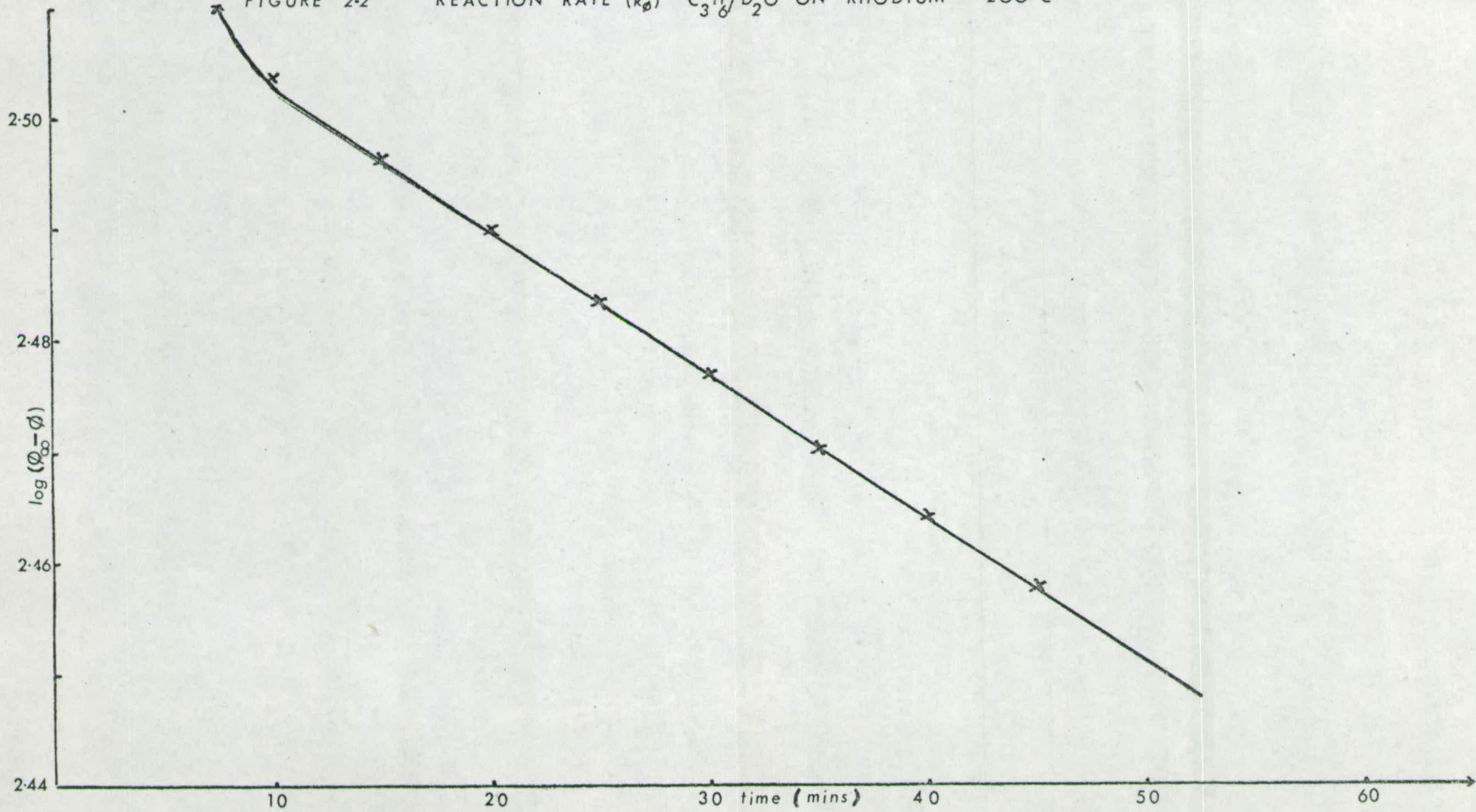


FIGURE 2-2 REACTION RATE (k_ϕ) C_3H_8/D_2O ON RHODIUM $200^\circ C$



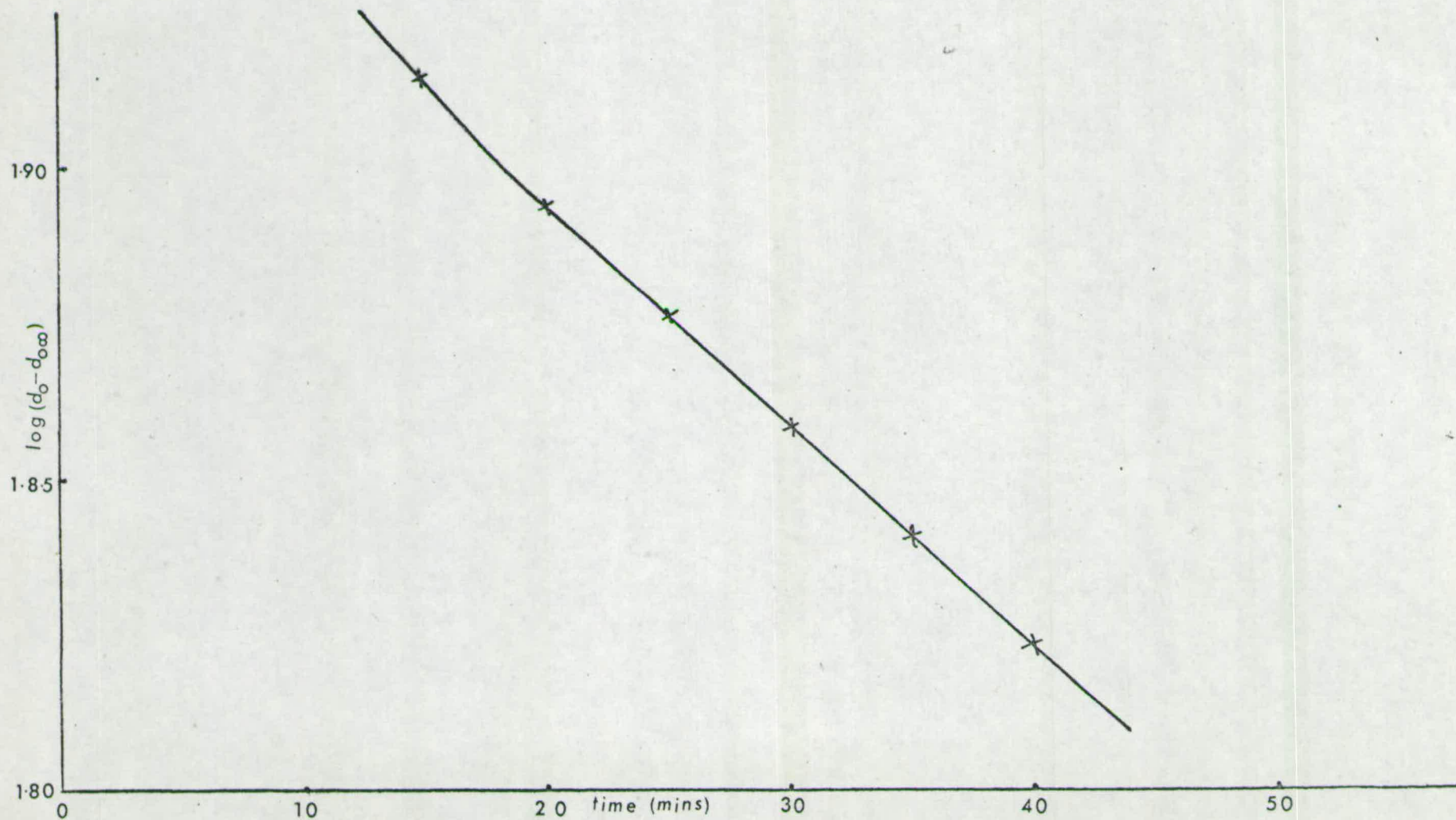


FIGURE 23 REACTION RATE (k_0) C_3H_6/D_2O EXCHANGE ON RHODIUM $200^{\circ}C$

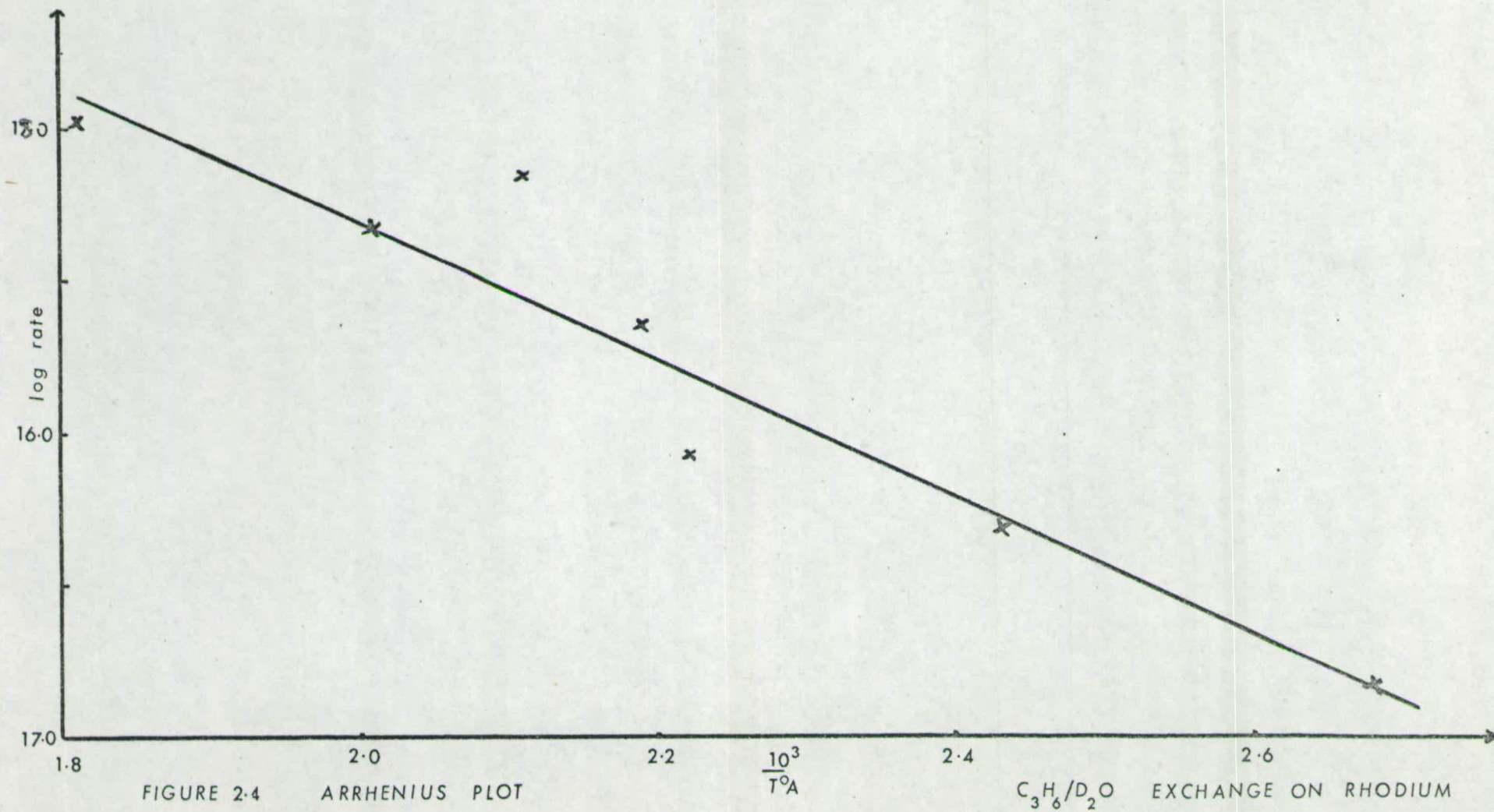


Table 2.2

A Comparison of the Distributions of Isotopic Propylene
with Distributions Calculated from a Binomial Expansion.

Catalyst	Temperature °C	ϕ^x	d_0	d_1	d_2	d_3	d_4	d_5	d_6
Pd	164	330	0.0	1.9	23.1	33.8	25.4	12.5	3.5
Calculated Distribution		330	0.8	6.1	18.7	30.3	27.5	13.3	2.7
Rh	200	200	6.0	28.0	37.9	19.5	7.5	2.0	0.1
Calculated Distribution		200	8.8	26.4	33.0	21.9	8.2	1.6	0.1

^xThe value of ϕ indicates the extent of the exchange reaction. The mean number of deuterium atoms in the molecules is $\phi/100$.

Table 2.3Propylene/D₂O Exchange on Rhodium Films.

<u>Expt. No.</u>	<u>Temp. °C.</u>	<u>Film Wt. (mg)</u>	<u>$r_o \times 10^{16}$</u>	<u>'M' value</u>
3A	224	5.8	4.71	1.13
3B	280	5.8	10.4	1.13
6A	100	4.5	0.15	1.16
6B	178	4.5	0.86	1.12
8	184	11.3	2.2	1.05
9A	138	3.7	0.48	1.26
9B	200	3.7	6.94	1.44

r_o is expressed as $\text{mol sec}^{-1} \text{m}^{-2}$.

Surface Area assumed to be $8.8 \times 10^{-2} \text{ m}^2$ per 10 mg
film weight (72)

derived.

Initial reaction rates for exchange over a palladium catalyst are shown in Table 2.4 where they are compared with results similarly obtained for the same reaction by Patterson⁽³⁹⁾. Derived from these results is the Arrhenius plot exhibited in Figure 2.5 from which the Arrhenius parameters for this equation are found to be

$$r_0 = 10^{20.9} e^{-22.0/RT}$$

where r_0 is the absolute rate in $\text{mol sec}^{-1} \text{m}^{-2}$ and the activation energy is expressed in kJ mole^{-1} .

2.5 $\text{C}_3\text{H}_6/\text{D}_2\text{O}$ Exchange on Platinum.

The exchange reaction over a platinum catalyst was studied at temperatures between 0°C and 330°C and differed markedly from the exchange over rhodium and palladium. On addition of a propylene/heavy water mixture to a freshly thrown platinum film the rate of reaction decreased with time as shown by the curved rate plot in (Figure 2.6). If the film is pretreated by exposure to propylene or a propylene/heavy water mixture the exchange reaction proceeds at a steady rate but at a higher temperature (Figure 2.7). Pretreatment with heavy water does not affect the reaction and a curved rate plot is again obtained.

The experimental data are listed in Table 2.5 and both initial and final values of reaction rates are given where the rate is not constant. An Arrhenius Plot, Figure 2.8, depicts the decrease in rate during reaction with untreated films and a line is drawn through two points corresponding to reaction after pretreatment of the catalyst with propylene at 20°C but has no particular significance. Reaction after/

Table 2.4

Expt. No.	Temp. °C.	Apparent		'M'
		Film Area, m ²	$k_0 \times 10^{17}$, mol sec ⁻¹ m ⁻²	
2	0	1.5×10^{-2}	0.65	1.18
4	18	1.5×10^{-2}	1.82	1.08
3	18.5	1.5×10^{-2}	2.36	1.13
1	19	1.5×10^{-2}	0.67	1.16
3	60	1.5×10^{-2}	2.83	1.12
1	62	1.5×10^{-2}	0.85	1.18
4	124	1.5×10^{-2}	11.6	0.99
5	132	1.5×10^{-2}	13.5	1.03
Patterson	6		0.73	0.99
Patterson	16		0.82	1.03
Patterson	51		3.48	1.13
Patterson	55		2.88	1.16

Surface area of palladium film taken to be the geometric area of the metal on the reaction vessel⁽⁷⁷⁾.

Table 2.5Propylene/D₂O Exchange on Platinum Films.

<u>Experiment</u>	<u>Temp. °C</u>	<u>Rate k_1</u> (D atoms per 100 molecules per minute per 10 mg Film)		<u>M</u>	<u>Time of Studying Reaction (mins.)</u>
		<u>Initial</u>	<u>Final</u>		
1A	0	3.10	0.276	1.9	30
	90	5.08	1.25	2.0	30
2A	22	9.5	1.55		130
	100	6.0	0.26	1.6	160
3A	0	1.40	0.114		30
	98	5:21	0.054	1.4	160
5A	20	2.65	0.105		180
	150	3.80	0.034	1.6	260
6A	60	11.0	0.718		250
	130	2.46	0.026	1.5	400
8A	20	1.85	0.073	1.7	150
8B	222	6.25			150
9C	225	19.3		2.1	35
9C	245	31.9			40
10C'	300	2.25		1.6	130
10C	332	3.31		2.0	100
11D	20	3.20	0.81		80

A No Pretreatment

B Pretreatment with Propylene/D₂O, 150 mins at 20°C.

C Pretreatment with Propylene 20 mins at 20°C.

C' Pretreatment with Propylene 20 mins at 295°C.

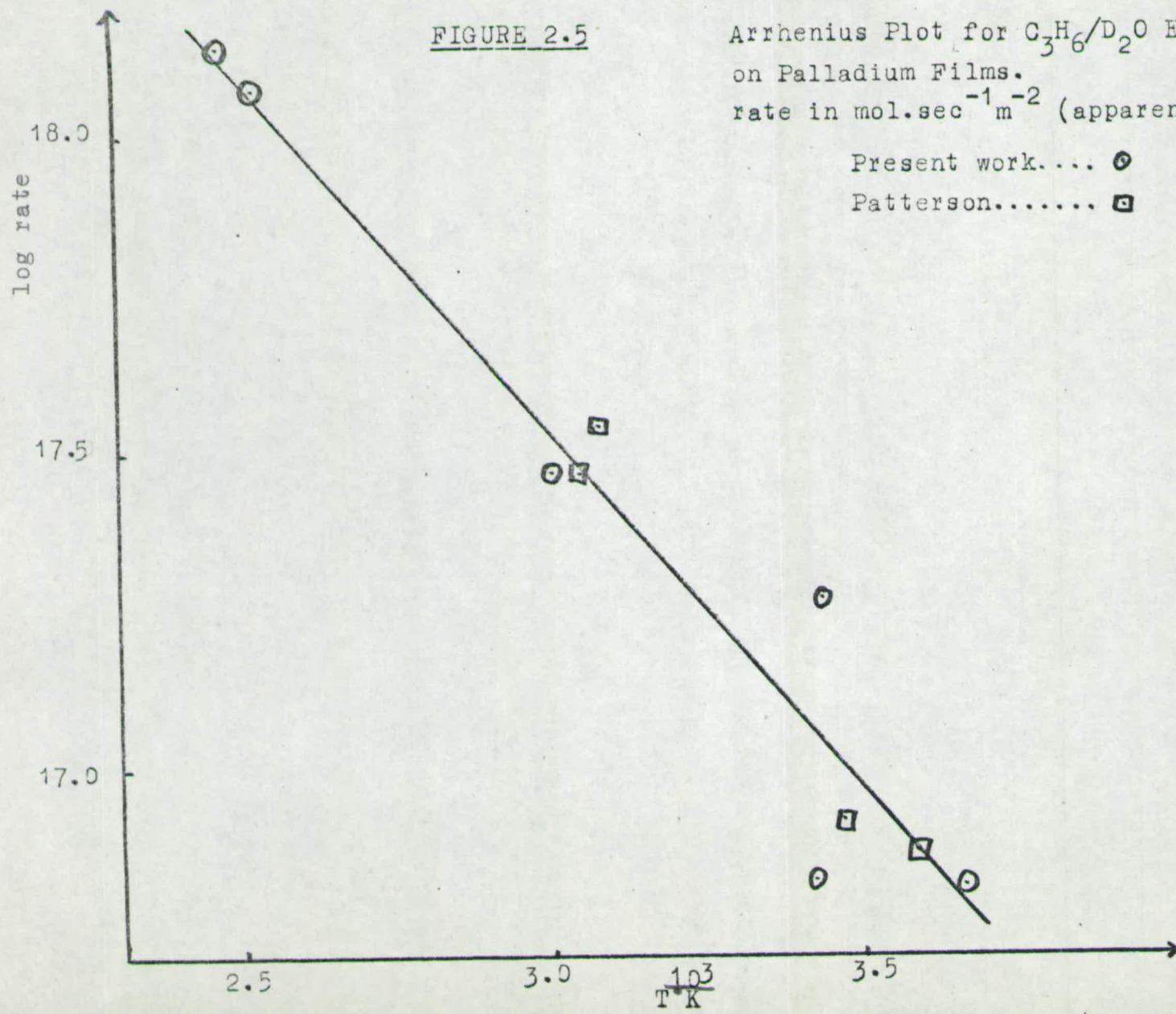
D Pretreatment with D₂O 20 mins at 20°C.

FIGURE 2.5

Arrhenius Plot for C_3H_6/D_2O Exchange
on Palladium Films.
rate in $\text{mol} \cdot \text{sec}^{-1} \cdot \text{m}^{-2}$ (apparent area)

Present work.... \circ

Patterson..... \square



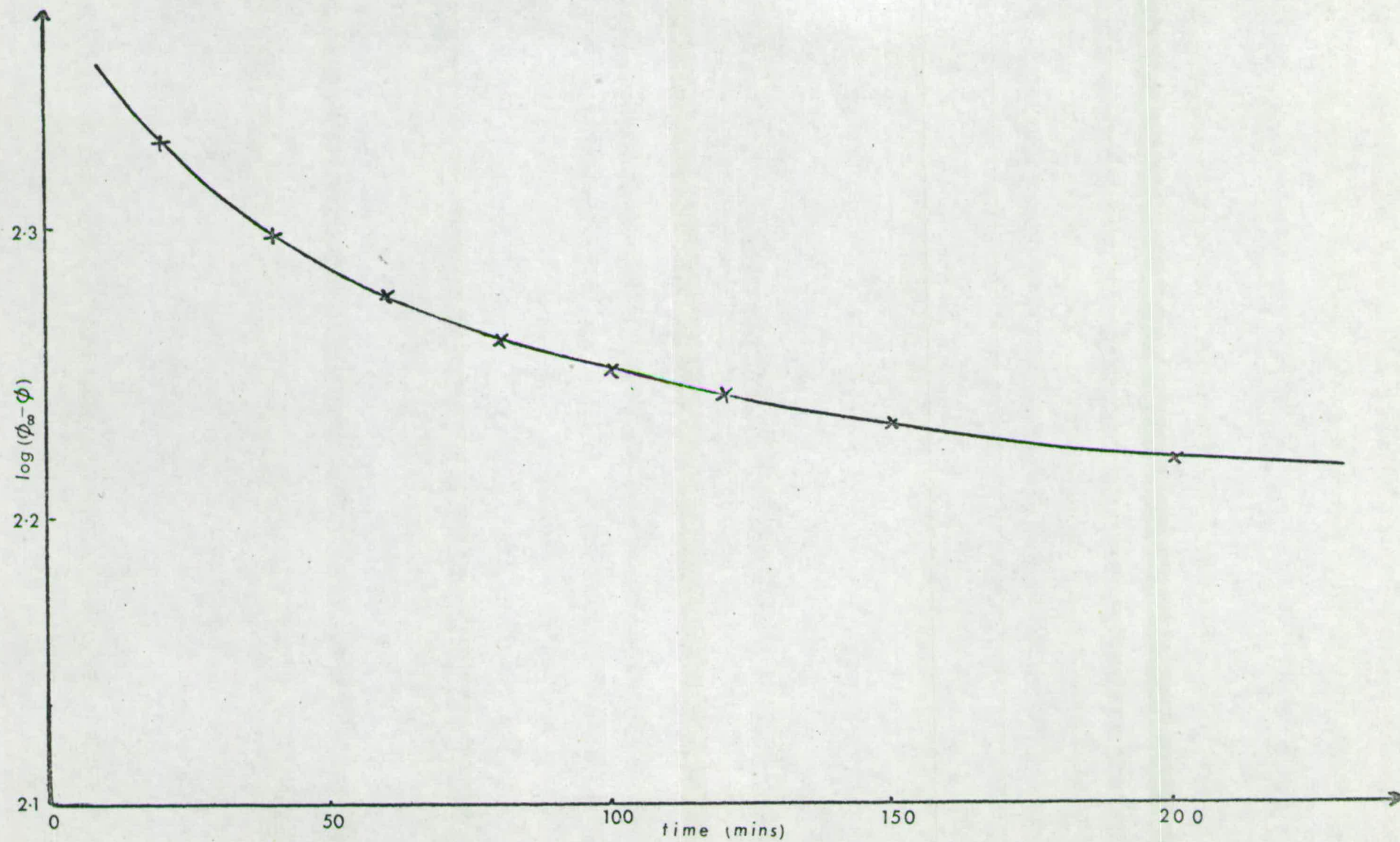


FIGURE 2.6 REACTION RATE (k_ϕ) C_3H_6/D_2O ON UNTREATED PLATINUM FILM $60^\circ C$

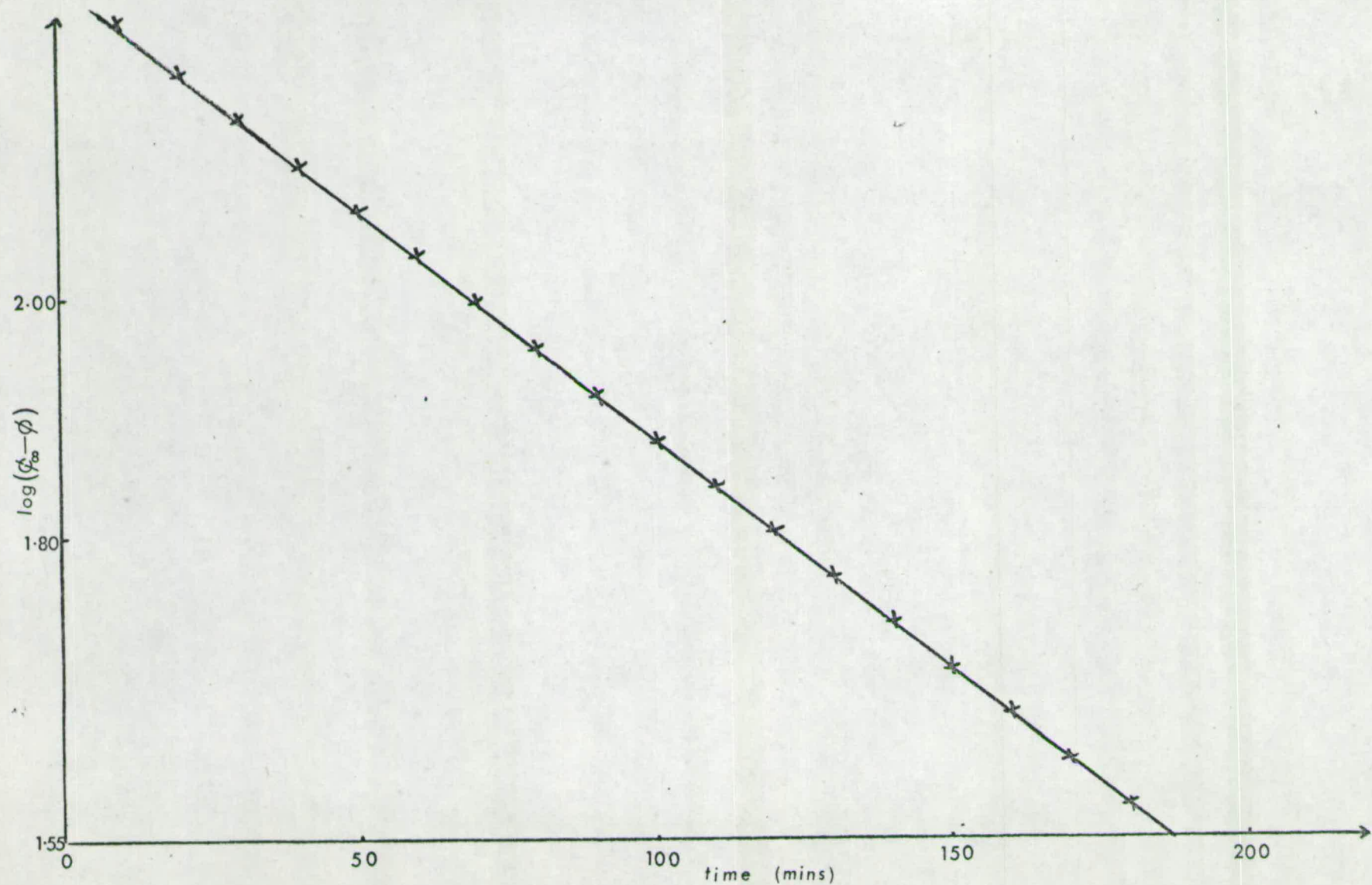
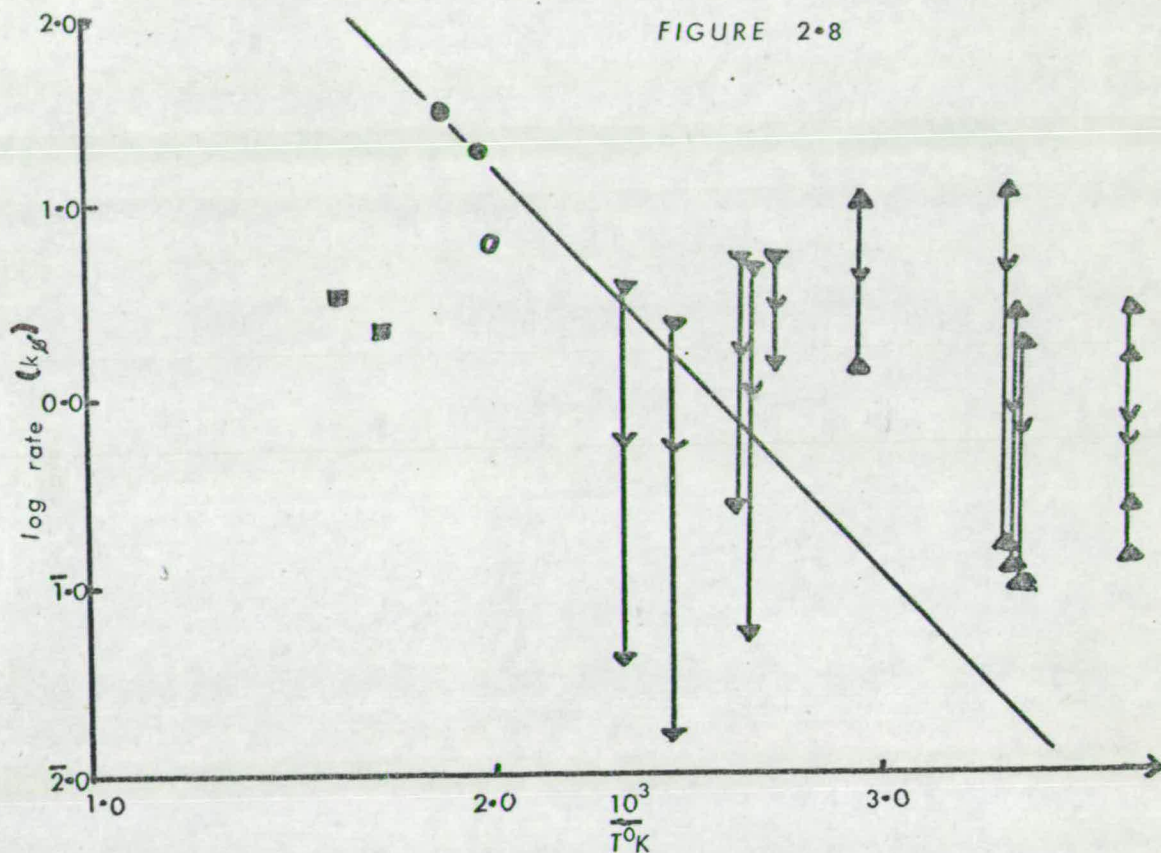


FIGURE 2.7 REACTION RATE $[k_{\phi}]$ C_3H_6/D_2O ON PRETREATED PLATINUM FILM $222^{\circ}C$



Arrhenius plot for the exchange of propylene and D_2O on platinum films.

- ▲ Exchange with no pretreatment;
- ▼ Exchange after temperature increase of previously reacting mixture;
- Exchange after pretreatment with propylene at $20^{\circ}C$ for 20 minutes;
- Exchange after pretreatment with propylene at $295^{\circ}C$ for 20 minutes;
- Exchange after pretreatment with propylene/ D_2O at $20^{\circ}C$ for 150 minutes.

after pretreatment with propylene at 295°C is much slower than the corresponding reaction after pretreatment at 20°C. The rates which have decreased to values below the dashed line represent rates measured after longer times of reaction than those above. The Arrhenius parameters of the line are included for completeness and correspond to the equation.

$$r_0 = 10^{21.2} e^{-46.0/RT}$$

where r_0 is the absolute rate in $\text{mol sec}^{-1} \text{m}^{-2}$ and the activation energy is expressed in kJ mole^{-1} .

Table 2.5 shows the 'M' values for this reaction are around 2 indicating that multiple exchange is occurring. This is borne out by the distribution of isomers, Figure 2.9, which clearly shows the formation of all six possible deuterated species in the initial stages of the reaction. The product distribution in the early stages of the reaction is similar over both untreated and pretreated films but differs from the binomial expansion as expected in the presence of multiple exchange, Table 2.6.

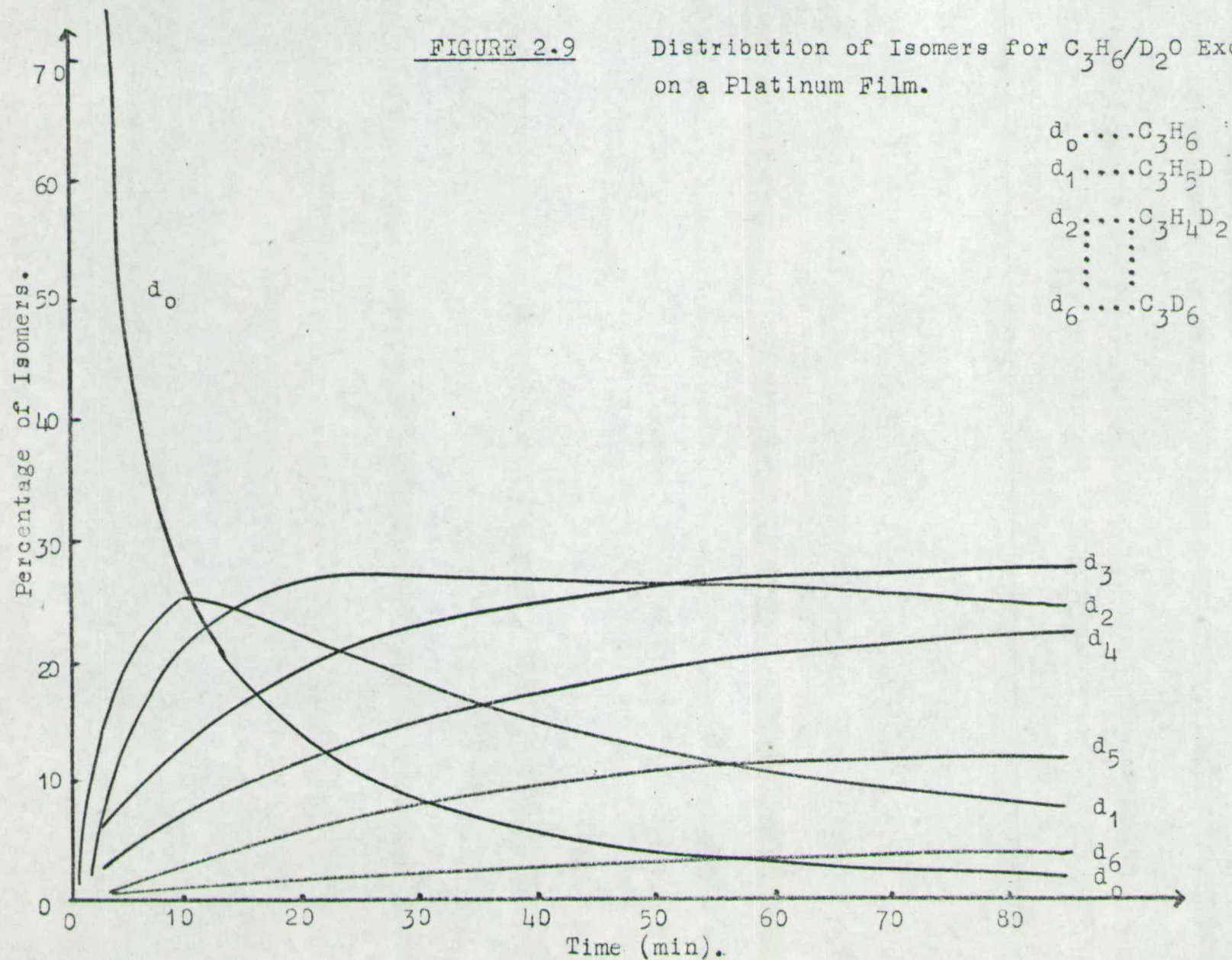
Table 2.6

Distribution of Products for Propylene/Heavy Water
Exchange over Platinum.

<u>Catalyst</u>	<u>Distributions</u>						
	<u>d₀</u>	<u>d₁</u>	<u>d₂</u>	<u>d₃</u>	<u>d₄</u>	<u>d₅</u>	<u>d₆</u>
Untreated Pt film	52.0	25.0	12.5	5.0	4.0	1.0	0.5
Pretreated Pt film	52.0	20.0	12.5	9.0	5.0	1.0	0.5
Binomial Expansion	52.0	36.0	11.0	2.0	---	---	---

FIGURE 2.9

Distribution of Isomers for C_3H_6/D_2O Exchange
on a Platinum Film.



2.6 Propylene/Heavy Water Exchange on Nickel.

This exchange has been investigated over both evaporated nickel films and nickel supported on α -alumina and exhibits a similar pattern of behaviour over both catalysts. At first sight the reaction over nickel appears similar to that over rhodium and palladium with readily measurable rates, and an 'M' value of close to unity.

There is a discrepancy in the distribution of isomers, however, as the d_2 isomer ($C_3H_4D_2$) appears more abundant than expected. This could either be caused by an excess of the d_2 species, $C_3H_4D_2$, or by the presence of light propane, C_3H_8 , both species having the same m/e value of 44 thus appearing as a single peak on the relatively insensitive M.S. 10 mass spectrometer. Analysis of the reaction products using a gas chromatograph showed the latter explanation, that light propane was formed, to be true and some further experiments were performed to investigate this reaction.

Exposure of a nickel film to propylene gas at room temperature will not give rise to the formation of any detectable quantity of propane and a temperature greater than $100^\circ C$ is required before any significant amount of propane is formed. In the presence of light water and propylene there is an immediate formation of propane at $0^\circ C$. The propane content increases to a few per cent of the total hydrocarbon content over the first 15 - 20 minutes of reaction. The percentage of propane formed varies slightly with temperature, mass spectroscopic measurements indicating $\sim 2\%$ propane at $0^\circ C$ increasing to $\sim 6\%$ at $24^\circ C$ then tailing off to $\sim 7\%$ at $58^\circ C$ with little further movement until approximately $200^\circ C$. These measurements are sensitivity corrected as the mass spectrometer is less sensitive for propane than for propylene but gas chromatography suggests that the propane content is higher/

higher ~ 15% at 24°C. In spite of the small propane content and the uncertainty of its relative abundance it is possible to extract Arrhenius parameters for this reaction and they correspond to:

$$r_o = 10^{25-1} e^{-50.0/RT}$$

where r_o is in $\text{mol sec}^{-1} \text{ m}^{-2}$ and the activation energy is in kJ mole^{-1} . As propylene hydrogenation occurs only during the first 15 minutes of exchange with D_2O it is possible to improve the accuracy of the kinetic data by eliminating the effect of propane. Once the build up of propane has ceased the rate of disappearance of the hydrocarbon will not be very different than if no propane had been formed although in the latter stages of reaction when d_o is very small the rate k_o will be more distorted. Conversely k_ϕ , depending on the deuterated isomers, will be less accurate initially when the propane contribution forms a proportionately larger section of the isomer distribution. Assuming approximately 6% propane to be formed, and knowing the fragmentation pattern of propane, the propane contributions to the various peak heights may be estimated and suitable corrections made. Revised values of d_o and ϕ may then be used to recalculate k_o and k_ϕ . Table 2.7 shows the relevant kinetic data while the Arrhenius parameters, from the plot shown in Figure 2.10 correspond to

$$\begin{aligned} r_o &= 10^{20.3} e^{-27.7/RT} && \text{on nickel film} \\ r_o &= 10^{18.8} e^{-27.4/RT} && \text{on supported nickel.} \end{aligned}$$

Where r_o is the absolute rate in $\text{mol sec}^{-1} \text{ m}^{-2}$ and the activation energy is in kJ mole^{-1} .

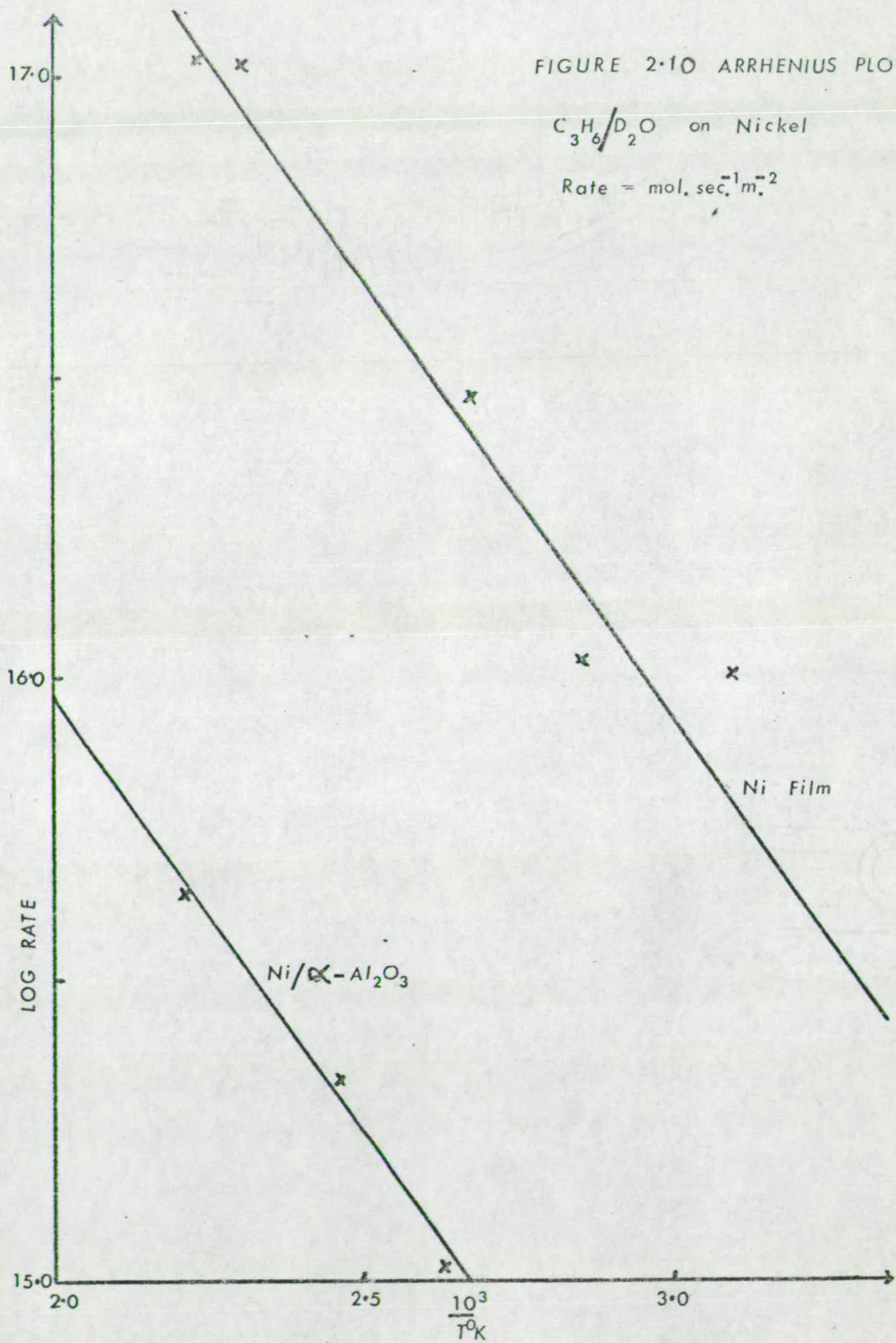


Table 2.7

Propylene/Heavy Water Exchange over Nickel.

(a) Kinetic Data

<u>Expt. No.</u>	<u>Temp. °C.</u>	<u>Film Wt. mg.</u>	<u>$k_o \times 10^{16}$</u>	<u>M</u>
Nickel film				
3	50	9.4	1.00	1.00
4	78	5.6	1.05	1.03
3	100	9.4	2.95	1.15
4	160	5.6	10.4	1.13
5	174	12.3	10.6	1.10
Nickel/ α -alumina				
2A	107	0.56	1.02×10^{-1}	1.00
1A	132	0.70	2.14×10^{-1}	0.83
2B	176	0.56	4.38×10^{-1}	1.00

k_o is in $\text{mol sec}^{-1} \text{m}^{-2}$ and it is assumed that 10 mg film weight is equivalent to $9.70 \times 10^{-2} \text{m}^{-2}$ area.

(b) Distribution of Isomers before and after correcting for propane formation.

	<u>Temp. °C</u>	<u>ϕ</u>	<u>d_0</u>	<u>d_1</u>	<u>d_2</u>	<u>d_3</u>	<u>d_4</u>	<u>d_5</u>	<u>d_6</u>
Before	160	100	36	35	23	5	2	-	-
Binomial	100	33	42	20	5	-	-	-	-
After	160	100	35	39	20	5	1	-	-

2.7 Discussion

Nickel, platinum, rhodium and palladium will all catalyse the exchange of propylene and heavy water and Table 2.8 summarises the relevant Arrhenius parameters which are displayed graphically in Figure 2.11.

The exchange over rhodium and palladium is straightforward with all six hydrogen atoms exchanging in a simple or stepwise manner, palladium being the more active metal. Over nickel similar results are obtained but with the additional complication of the formation of propane. The lower rate of reaction on a supported nickel catalyst relative to the rate on a nickel film may be due to sintering of the supported nickel while being reduced at 500°C . The formation of propane must be due to self hydrogenation of propylene as only light propane is formed in the presence of heavy water. This self-hydrogenation will only occur at temperatures below 100°C if water is present although the hydrogen atoms from the water are not incorporated into the hydrocarbon. A possible explanation for this is that water molecules, being strongly adsorbed on nickel, could dislodge any weakly held saturated hydrocarbons formed during the early/

FIGURE 2.11

Arrhenius Plot for C_3H_6/D_2O
Exchange on Metals.

rate in $\text{mol} \cdot \text{sec}^{-1} \cdot \text{m}^{-2}$.

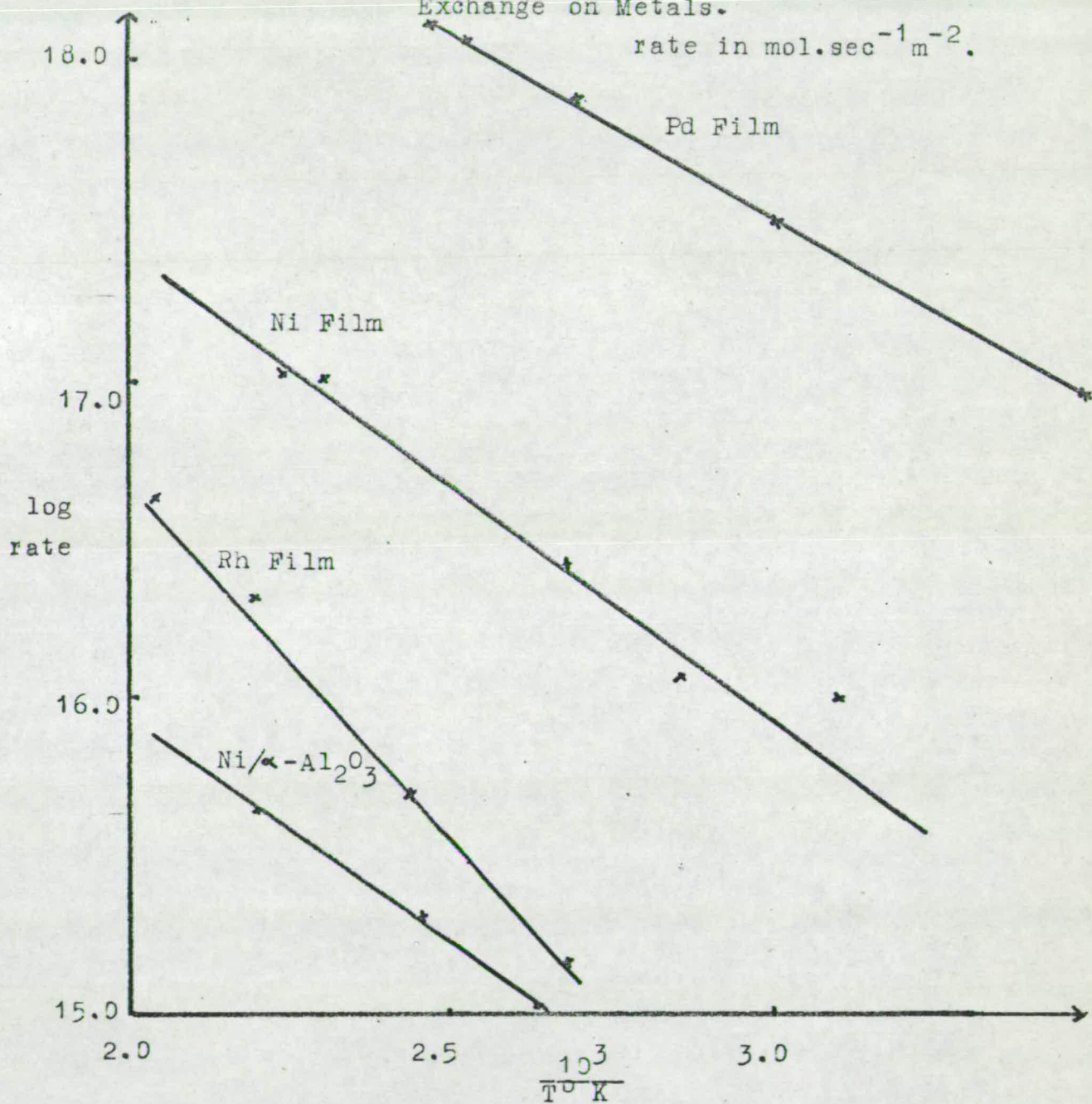


Table 2.8

Arrhenius Parameters for Propylene/Heavy Water
Exchange on Metals.

<u>Catalyst</u>	<u>E_A (kJ mole⁻¹)</u>	<u>$\log_{10} A$ (A in mol sec⁻¹ m⁻²)</u>	<u>Temp. Range (°C)</u>
Rhodium	41.8	21.1	100-280
Palladium	22.0	20.9	0-124
Platinum ^x	46.0	21.2	0-330
Nickel	27.7	20.3	50-195
Supported Nickel	27.4	18.8	107-176

^xThe parameters chosen for platinum correspond to reaction after pretreatment of the metal with propylene for 10 minutes at room temperature.

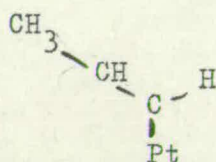
early stages of the reaction by the self-hydrogenation of propylene. Once the water has dispersed the hydrocarbons no more self-hydrogenation is likely to occur. Where no water is present propane will only be dislodged at higher temperatures.

Reaction on platinum, which differs from that on other metals, exhibits multiple exchange and a decrease in reaction rate with time probably due to the strong adsorption of propylene. As the presence of water does not hinder this adsorption of propylene the water cannot itself be strongly adsorbed in agreement with the earlier works on the H_2/D_2O exchange on platinum films described in Part II, Chapter I. After pretreatment with propylene at room temperature a steady reaction rate is obtained. If the mixture is then pumped out and a second mixture admitted the rate is lower suggesting that the water is preferentially removed and the remaining propylene further poisons the platinum. Under conditions where a steady rate was observed the water and propylene must reach an equilibrium on the surface.

The tendency for the exchange reactions to slow down and the similarity of the distributions of deuterated species for both pretreated and untreated films suggests that the sites for reaction are of the same type and are progressively poisoned by strongly adsorbed propylene residues. The presence of multiple exchange on platinum is indicative of at least two types of adsorbed propylene species on the surface.

To explain the differences in the behaviour of propylene and water over the various metal catalysts it is generally agreed⁽⁵⁸⁾ that different forms of chemisorbed propylene exist on different metals. The main problem is whether propylene is associatively or dissociatively chemisorbed on the catalyst. Both chemisorbed/

chemisorbed states are possible, the half-hydrogenated state, C_3H_7 , being formed in the course of the hydrogenation reaction of propylene to propane, and the possibility of a dissociative intermediate, C_3H_5 , being justified by the occurrence of a self-exchange reaction of $C_2D CH CH_2$ into $CH_3 CD CH_2$ or $CH_3 CH CHD$ at $30^\circ C$ on all four metals^(59,3). The existence of a dissociative state has been proposed on platinum by Barkas⁽⁹⁰⁾ and Burwell⁽⁹¹⁾, however an explanation of the propylene/heavy water exchange on platinum requires that both associative and dissociative mechanisms are involved, and multiple exchange occurs⁽⁵⁹⁾, the dissociative intermediate involved being mainly the trans-propenyl species:



On palladium all six hydrogens have been found equally exchangeable undergoing simple or stepwise exchange and a π -allyl type intermediate $CH_2 \cdots CH \cdots CH_2$ has been postulated by Hirota⁽⁵⁸⁾. This will not explain the exchange of the central hydrogen atom and an associative species and/or a trans-propenyl species may also exist on the surface, the cis-propenyl species being ruled out for steric reasons.

On nickel the associative intermediate $CH_3 - \underset{*}{CH} - \underset{*}{CH}_2$,

either π -bonded or σ -bonded to the metal has been proposed as the main chemisorbed species⁽⁵⁹⁾ with the possibility of a dissociative intermediate shown both by the self-exchange reaction and the self-hydrogenation reaction.

CHAPTER 3

The Chemical Reaction between Propylene and Light Water
and between Propane and Light Water over Nickel and
Rhodium Catalysts.

3.1 Introduction

The experiments described in the previous chapter demonstrated the need for a deeper investigation into the behaviour of a propylene/water mixture especially over a nickel catalyst. One approach to the problem is to study the chemical reaction of this mixture at higher temperatures and this has the added advantage of unifying the academic approach of this thesis with the more practical problems incurred in the industrial steam reforming process.

3.2 Experimental.

Experiments were performed at temperatures greater than 300°C using a 3:1 mixture of light water and propylene or propane. Use of heavy water would have made analysis of reaction products by mass spectrometry extremely difficult. A description of the experimental method of analysis is provided in Part I Chapter 2.8 allowing for the semi-quantitative identification of H₂, CH₄, C₂H₄, C₂H₆, C₃H₆, C₃H₈, and possible traces of gas phase oxygenated species and higher hydrocarbons. The reaction products are plotted in terms of C₃ species along with a plot of the carbon loss, also in terms of 'C₃' obtained by difference of the total carbon in the gaseous phase at any time and the initial carbon content. For the reaction

$$\text{C}_3\text{H}_6 + \text{H}_2\text{O} \rightarrow \text{C}_3\text{H}_8 + \text{CH}_4 + \text{CO}_2$$

the carbon loss at time τ would/

would be:

$$'C_3' \text{ loss} = P_{C_3H_6}^O - \left[P_{C_3H_6} + P_{C_3H_8} + \frac{1}{3} P_{CO_2} + \frac{1}{3} P_{CH_4} \right]$$

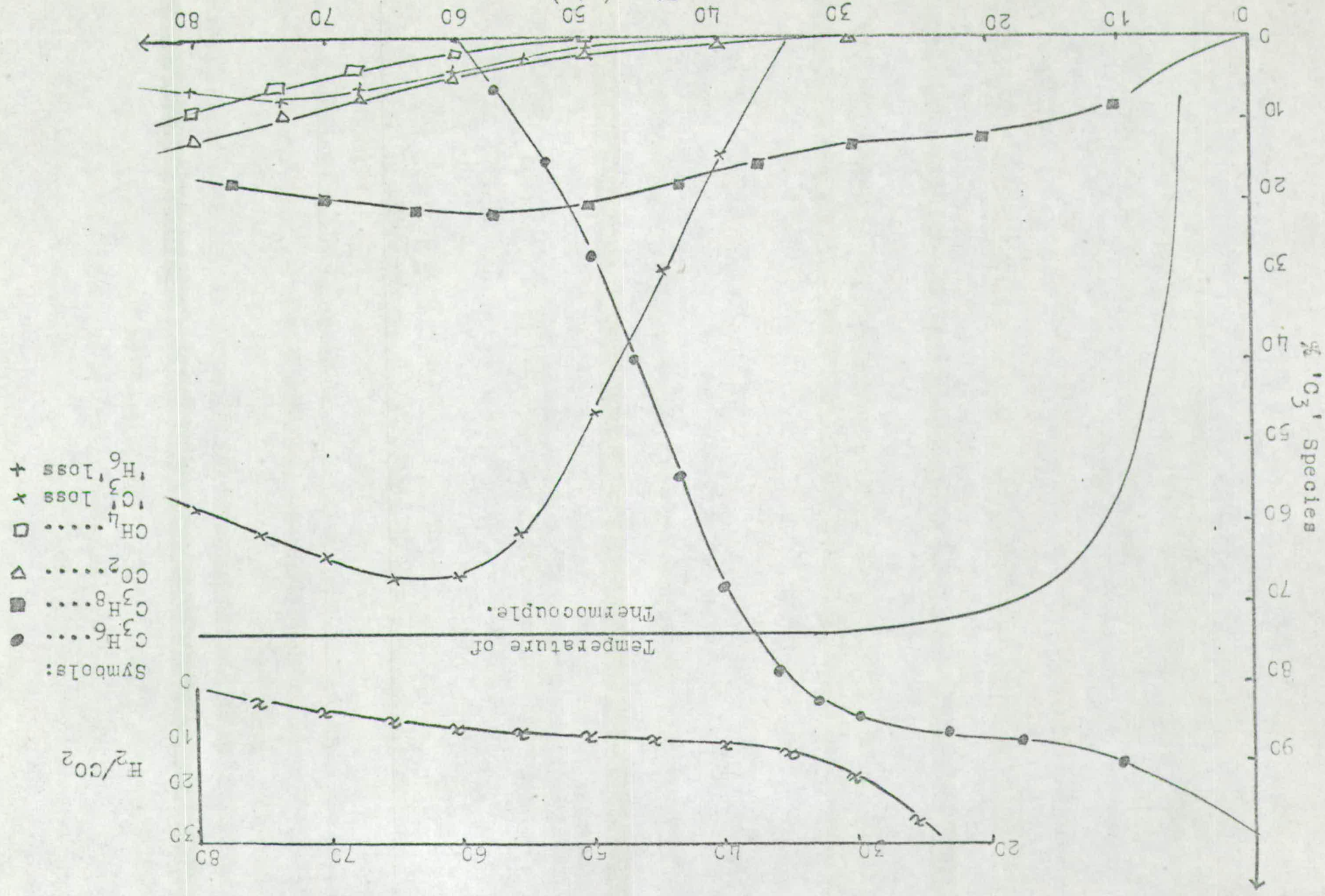
where P is the pressure of gas in the reaction vessel. Hydrogen loss may also be determined though this is complicated by the inability of the mass spectrometer to measure the water content of the system. For the purposes of calculation it has been assumed that for every CO molecule formed from hydrocarbon and water, two hydrogen atoms are liberated to the gas phase. Similarly every CO₂ molecule formed liberates four hydrogen atoms, and these must be subtracted from the sum of the other hydrogens present in the gas phase to give a measure of the total hydrogen content of the gas phase. Hydrogen loss is measured in a manner analogous to carbon loss in terms of 'H₆' species for reactant C₃H₆ and 'H₈' species for reactant C₃H₈.

3.3 The Propylene/Steam and Propane/Steam Reactions Over Nickel.

The propylene/water reaction over a nickel film catalyst may be summarised diagrammatically by plotting the various carbon containing molecules in terms of 'C₃' species against time; and separately relating the hydrogen and carbon dioxide contents by plotting the ratio H₂/CO₂ against time. Figure 3.1 shows how the reaction proceeds on a nickel film as the temperature is slowly raised through 23°C to a constant 370°C. At first there is initial self-hydrogenation of propylene to propane followed by an unreactive period and finally reaction with rapid disappearance of propylene. This is accompanied by a large loss of carbon and a smaller loss of hydrogen from the gas phase as hydrogen, carbon dioxide, and methane appear. The carbon loss reaches a maximum as the olefin content is reduced to zero, this/

FIGURE 3.1

C_3H_6/H_2O on Nickel Film at $370^\circ C.$



this being followed by a slow recovery of carbon and hydrogen to the gas phase. Inspection of the carbon balance and hydrogen balance after 17 hours showed most of the carbon and hydrogen to have returned to the gas phase. The dry gas composition at this point is compared with calculated equilibrium values in Table 3.1.

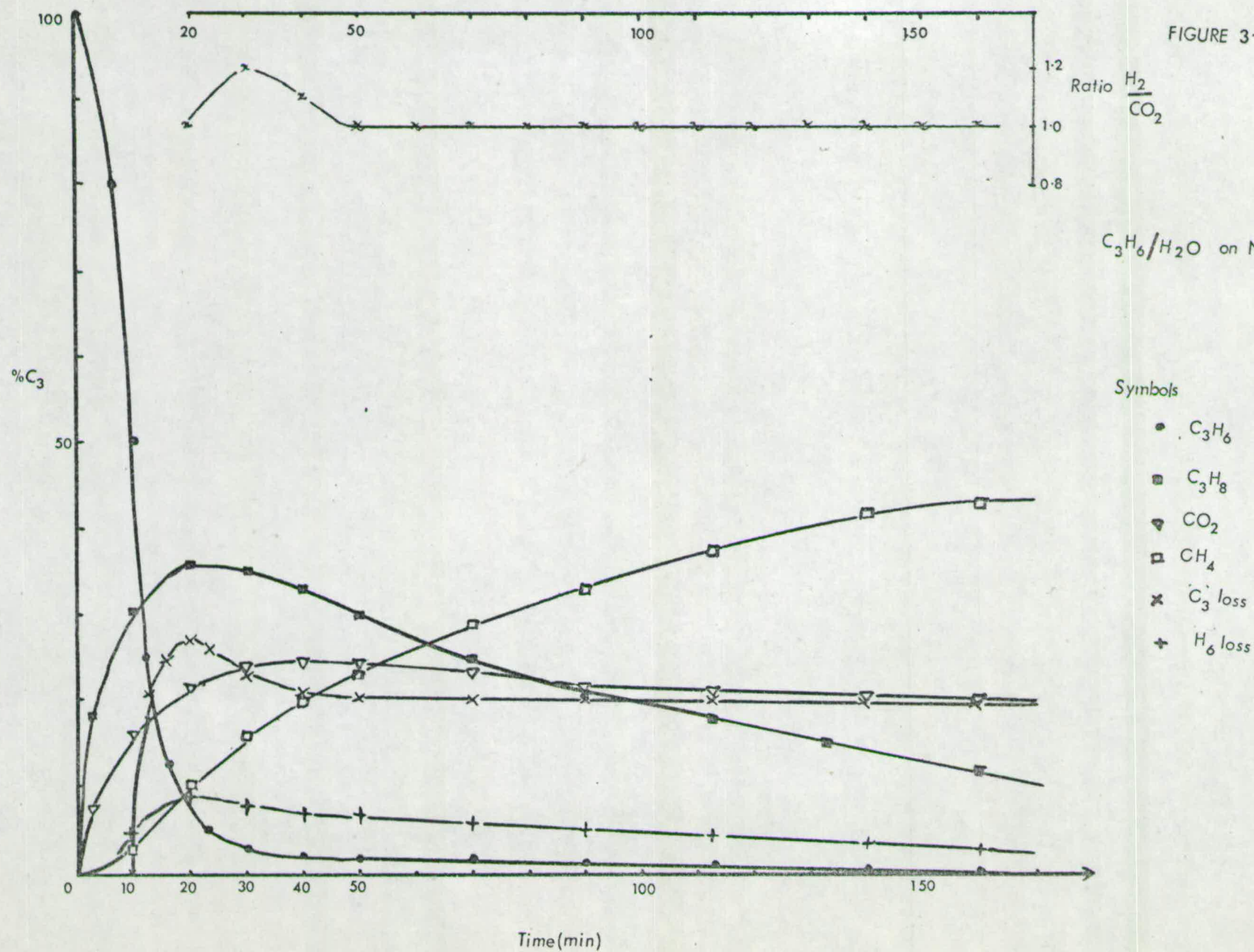
The same reaction carried out over a catalyst of nickel supported on α -alumina at 396°C (Figure 3.2), is qualitatively similar but has a smaller carbon loss, the ratio of hydrogen loss to carbon loss being roughly constant at $\text{H} : \text{C} \quad 1 : 1$. The dry gas composition shown in Table 3.1 does not include carbon monoxide which is not detectable after 200 minutes.

Since both reactions described above involve propane formation and subsequent slow disappearance as the reaction proceeds it seems reasonable to expect that use of propane as a feed might give a reaction similar to that using propylene. This is indeed the case, the propane/water reaction over nickel giving a pattern of reaction qualitatively similar to that with propylene after disappearance of the olefin and attainment of the propane maximum. Figure 3.3 demonstrates the course of this reaction over a nickel film at 395°C and Figure 3.4 shows the same reaction over a nickel/ α -alumina supported catalyst. In both cases there is production of CO_2 , H_2 , and CH_4 accompanied by ' C_3 ' and ' H_8 ' loss.

Table 3.1/

FIGURE 3.2

C_3H_6/H_2O on Nickel/ Al_2O_3 396°C



C_3H_8/D_2O Exchange on Nickel Film at $395^\circ C$

Symbols:
 C_3H_8 \blacksquare
 CO_2 \triangle
 CH_4 \square
 C_3 loss \times

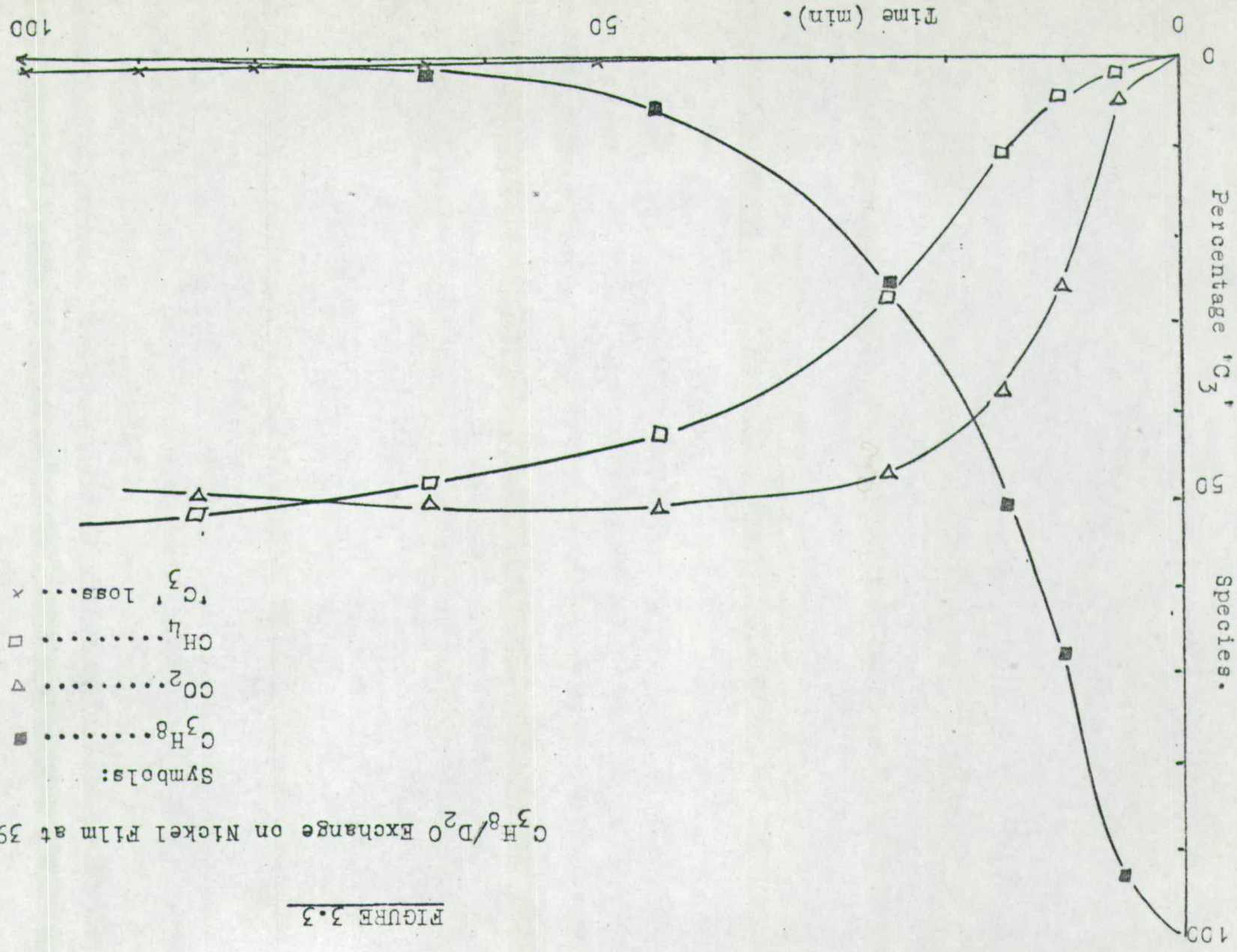


FIGURE 3.3

FIGURE 3.4

RATIO $\frac{H_2}{CO_2}$

C_3H_8/H_2O on NiKxSi/Al₂

336°C

Symbols

- C_3H_8
- ▽ CO_2
- CH_4
- X C_3 loss
- + H_6 loss

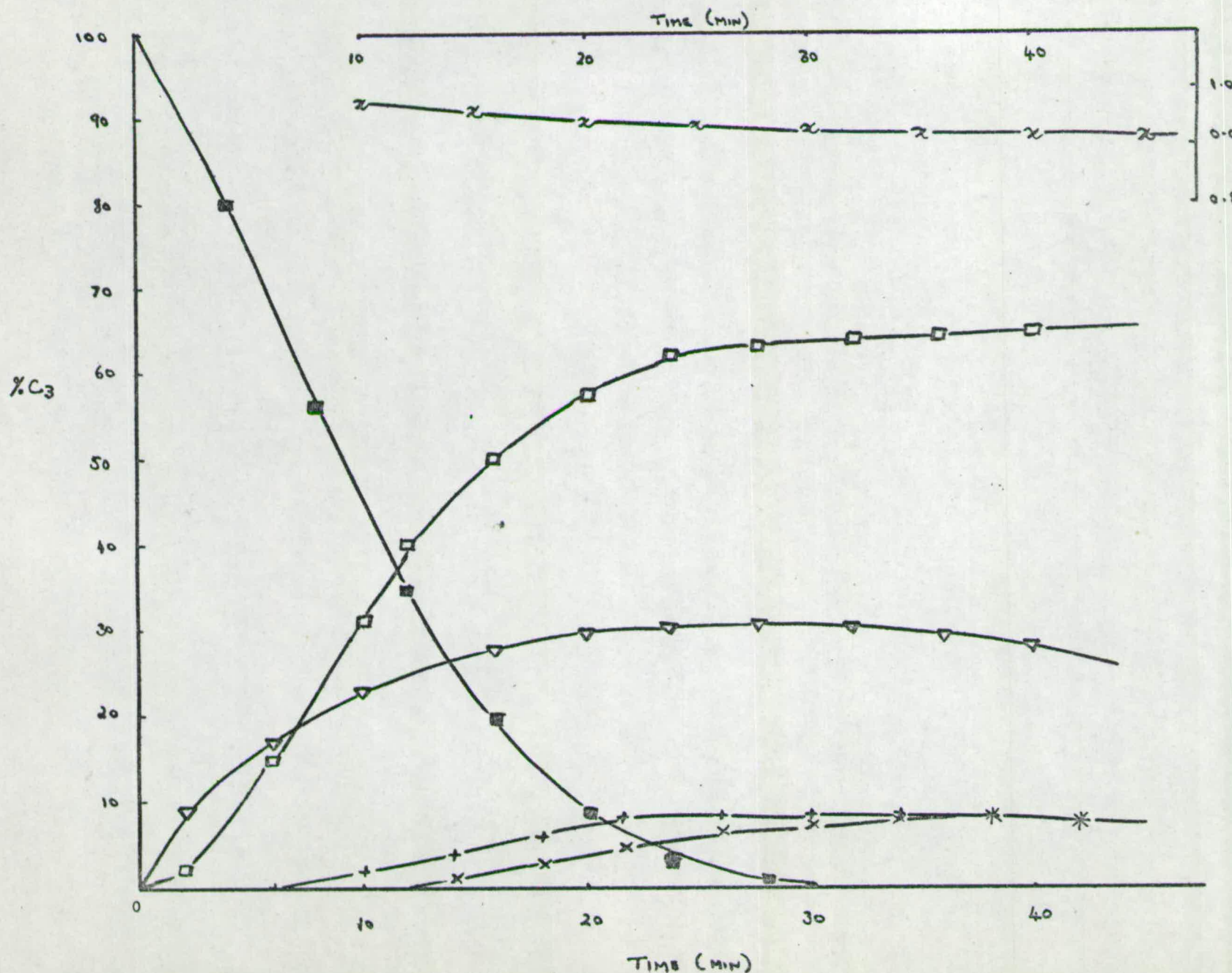


Table 3.1

Comparison of % Dry Gas Product Distribution with the
Calculated Equilibrium Values.

<u>Reaction Mixture</u>	<u>Catalyst</u>	<u>Temp. °C</u>	<u>% Dry Gas</u>			
			<u>CO</u>	<u>CO₂</u>	<u>CH₄</u>	<u>H₂</u>
C_3H_6/H_2O	Ni film	370 <u>expt.</u>	11.8	17.7	35.0	35.5
		<u>calc.</u>	3	22	42	34
C_3H_6/H_2O	Ni/ α - Al_2O_3	396 <u>expt.</u>	0	25	52	23
		<u>calc.</u>	4	22	36	38

Table 3.2 summarises these reactions in terms of reaction products, carbon loss, and hydrogen loss. Higher ' C_3 ' losses are found with a propylene/water feed and there is a consequently higher 'H' loss/'C' loss ratio.

The Arrhenius plot, Figure 3.5, correlates the hydrocarbon/water reactions in terms of the rate of disappearance of hydrocarbon. Over a nickel film propylene will disappear approximately ten times faster than propane irrespective of whether the propane was formed from propylene or was introduced as a reactant. Over a Ni/ α - Al_2O_3 catalyst propylene disappears at the same rate as on films. With propane on supported catalysts and evaporated films different results are obtained. On films propane disappears at the same rate as it does when formed from propylene while on supported catalysts propane introduced as a reactant disappears at the same rate as propylene but propane formed from propylene disappears much more slowly than the corresponding reaction in nickel films. The upper

FIGURE 3.5

Arrhenius Plot, $\log(\text{rate of disappearance of hydrocarbon})$ vs $10^3/T^\circ\text{K}$.
 (rate in $\% \text{ min}^{-1} \cdot 1000\text{cm}^{-2}$)

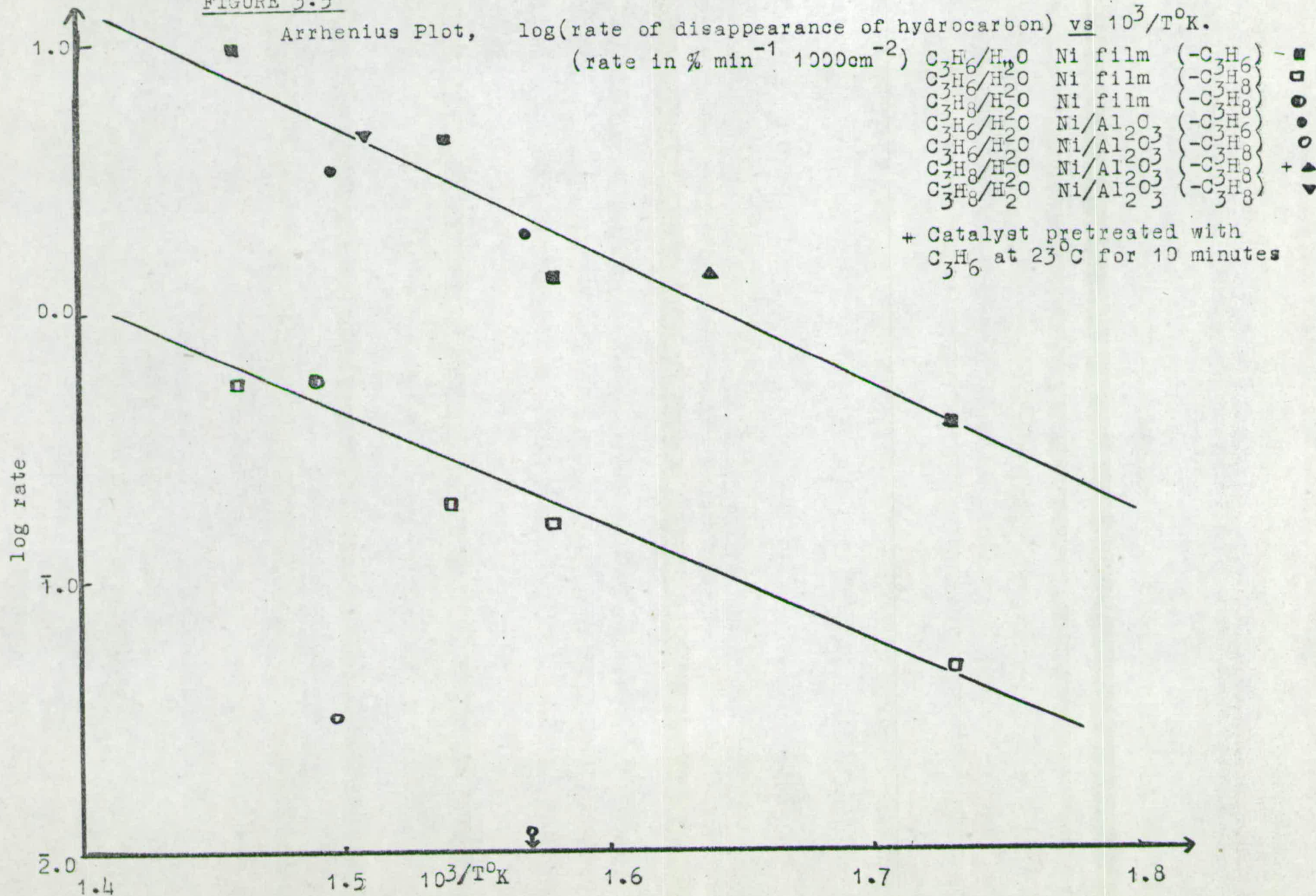


Table 3.2

Summary of Results of Hydrocarbon/Heavy Water Exchange
on Nickel Catalyst.

<u>Reaction Mixture</u>	<u>Catalyst</u>	C_3H_8	CH_4	CO_2	CO	H_2	'C ₃ ' loss	$\frac{'H' \text{ loss}}{'C' \text{ loss}}$
C_3H_6/H_2O	Ni film	✓	✓	✓	v. small		~60%	$\frac{1}{1}$
C_3H_6/H_2O	Ni/ α - Al_2O_3	✓	✓	✓	v.small		~25%	$\frac{1}{1}$
C_3H_8/H_2O	Ni film	-	✓	✓	v.small		v. small	$\frac{2}{1}$
C_3H_8/H_2O	Ni/ α - Al_2O_3	-	✓	✓	v.small		~10	$\frac{2}{1}$

92 kJ mole⁻¹ and the lower line one of 80 kJ mole⁻¹. In spite of the semi-quantitative nature of these calculations the points on the Arrhenius plot show good agreement.

Although no carbon monoxide has been detected in the early stages of reaction this does not preclude the possibility that it may be formed then rapidly react by the water gas shift reaction or methanation reaction forming hydrogen, carbon dioxide, methane, or water. Both these reactions are thermodynamically possible (cf- Appendix IV) and the strong adsorption of carbon monoxide on nickel would assist by holding the chemisorbed CO to the surface long enough for it to react with another molecule.

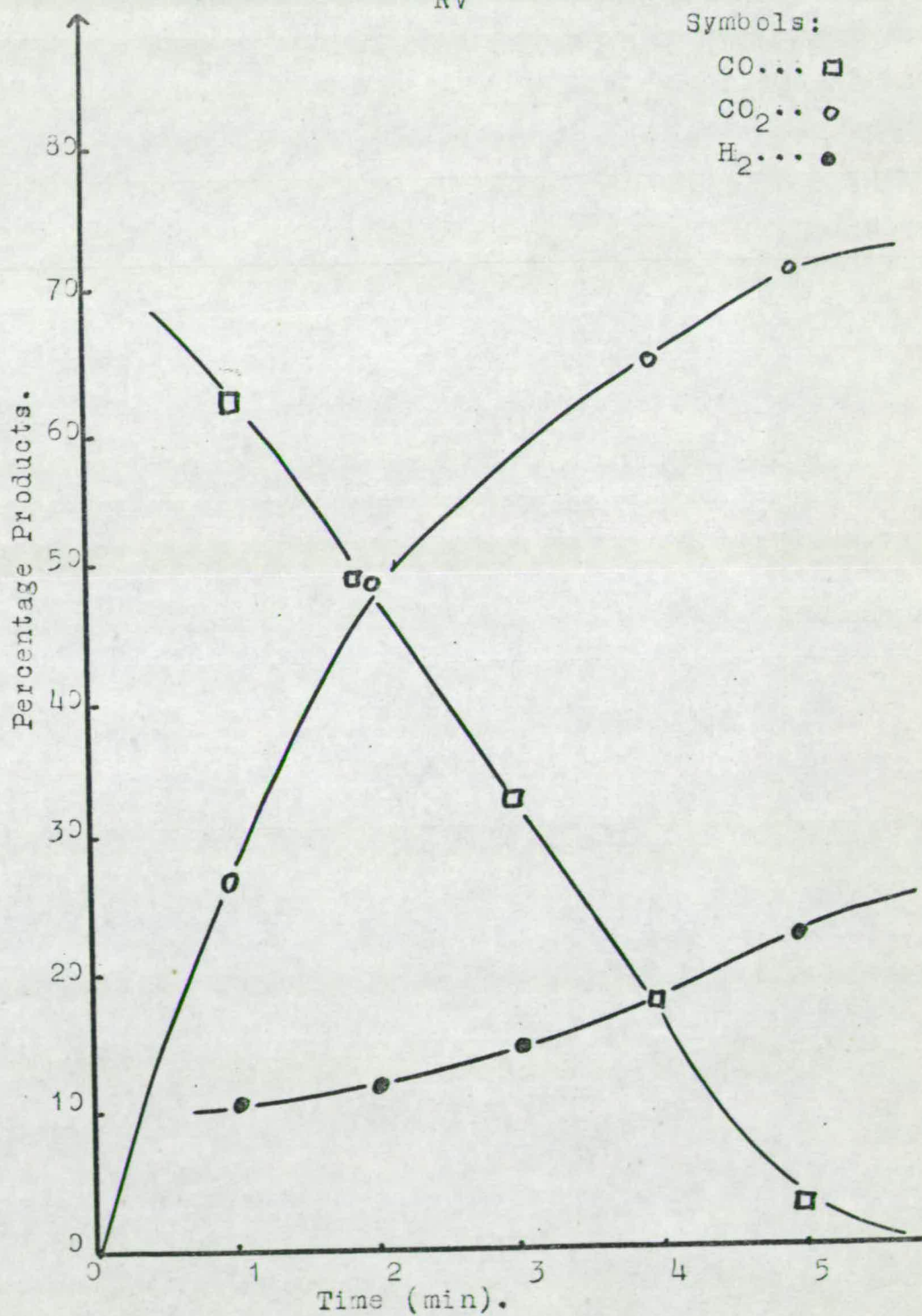
To determine the feasibility of those reactions test experiments were performed on nickel films. The water gas shift reaction, $\text{CO} + \text{H}_2\text{O} \rightleftharpoons \text{CO}_2 + \text{H}_2$, was complete at 300°C within 4 - 5 minutes. This is an exothermic reaction ($\Delta H = -41.13$ kJ) and is reversible. The equilibrium is independent of pressure and the table of equilibrium constants given in Appendix IV demonstrates the increase of the equilibrium carbon monoxide concentration with temperature. Figure 3.6 demonstrates the dry gas product distribution for this reaction at a temperature of 300°C with a reactant mixture of carbon monoxide and light water. The reaction proceeds rapidly over the first 3 - 4 minutes and as it moves towards equilibrium a small quantity of methane is formed, probably from the methanation reaction between the reactant CO and product H₂. The final equilibrium is well over to the CO₂ side of the water gas shift reaction as expected from the thermodynamic data (Appendix IV). The product distribution, approaching equilibrium, including a value for H₂O calculated by difference, is:

CO = 1% CO₂ = 53% CH₄ = 3% H₂ = 12% H₂O = 31%

Figure/

FIGURE 3.6

Dry Gas Product Composition for the
CO/H₂O Reaction on Nickel Film at 300°C.
(1:1 mixture, $P_{RV} = 130 \text{ Nm}^{-2}$)



Methanation is a more complex reaction as it incorporates the water gas shift;

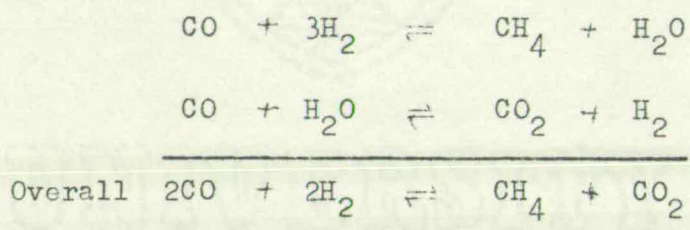


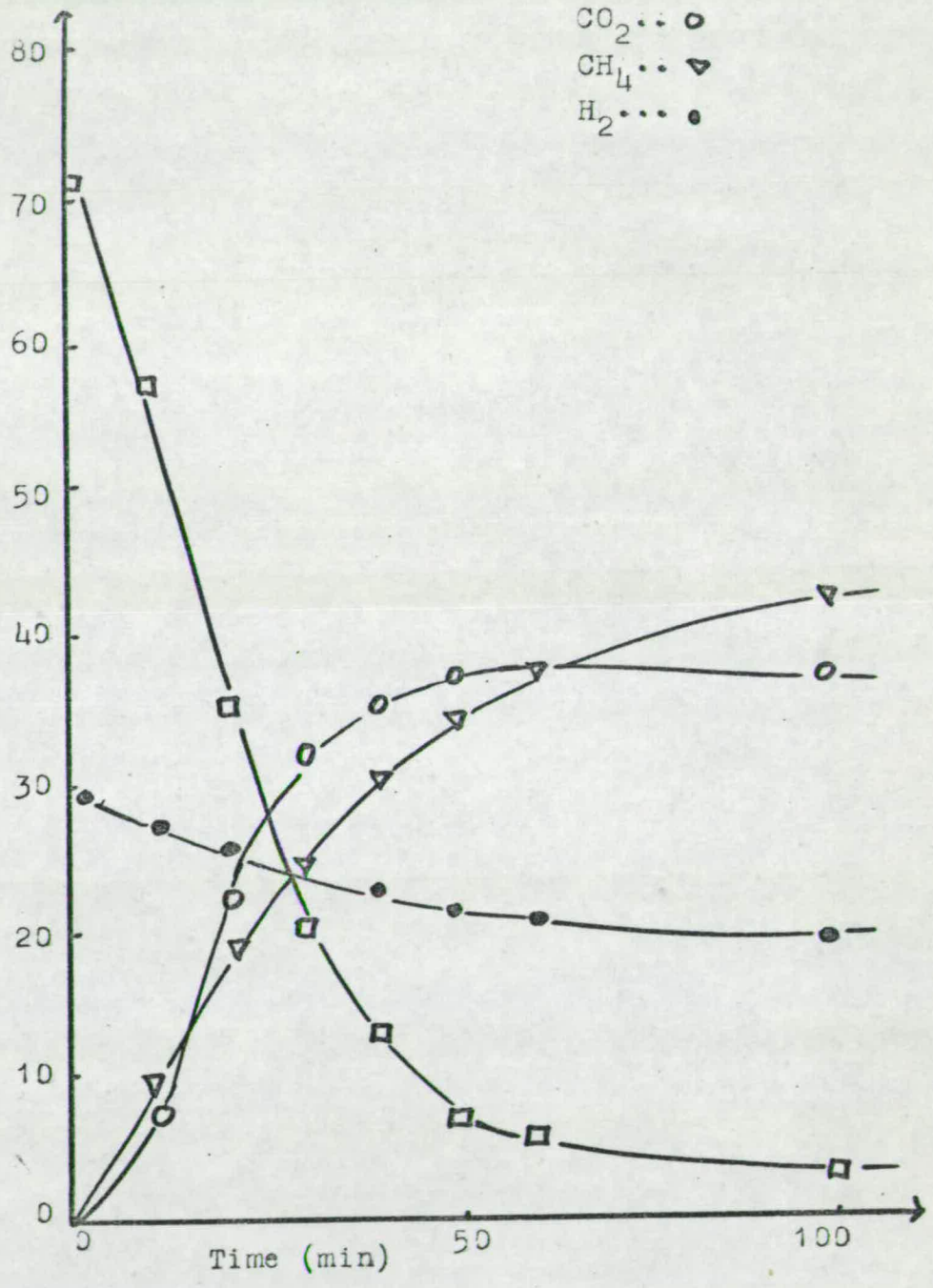
Figure 3.7 shows the product distribution for this reaction at 340°C. The production of CO₂ early in the reaction suggests that the water gas shift reaction, using the H₂O product and CO reactant, is proceeding rapidly, and the bulk of the reaction is complete after ~ 50 minutes. The relatively slow rate of disappearance of hydrogen is probably due to the simultaneous production of H₂ in the secondary water gas shift reaction.

FIGURE 3.7

Dry Gas Composition for the
Reaction CO/H_2 on a Nickel Film
at 340°C . ($\text{CO}/\text{H}_2=1/3$, $P_{\text{RV}}=170 \text{ Nm}^{-2}$)

Symbols:

- $\text{CO} \dots \square$
- $\text{CO}_2 \dots \circ$
- $\text{CH}_4 \dots \nabla$
- $\text{H}_2 \dots \bullet$



3.4 The Propylene/Steam and Propane/Steam Reactions over Rhodium.

The experimental technique and analysis of the mass spectral data correspond to those described for the same reactions over nickel. The figures shown in this section are likewise drawn in terms of ' C_3 ' species for all the carbon containing molecules and for the carbon loss.

Propylene and water will react readily together over a rhodium film at temperatures in excess of 290°C , Figure 3.8. Initially propylene vanishes and propane is formed and disappears in turn. The reaction now differs from that over nickel with the appearance of carbon monoxide and hydrogen as major products, they in turn giving way to carbon dioxide and methane formation. With the propane maximum there is a loss of carbon and hydrogen from the system. Again there is no trace of any C_2 species, higher hydrocarbons, or oxygenated species in the gas phase. The propylene/steam reaction over a supported rhodium catalyst, (Figure 3.9), behaves in a similar manner and both exhibit a ratio of hydrogen loss to carbon loss of between 1 and 2. Table 3.3 compares the percentage dry gas product distributions with the calculated equilibrium values for the propylene/water reaction over rhodium.

Table 3.3/

FIGURE 3.8

C_3H_6/H_2O Reaction on a Rhodium Film at $390^\circ C$.

ratio 'H'loss/'C'loss $\approx 1/1$

'H₂'/'CO $\approx 2/1$

Symbols:

C_3H_6 ●
 C_3H_8 ■
 CO ○
 CO_2 ▼
 CH_4 □
 ' C_3 'loss ×

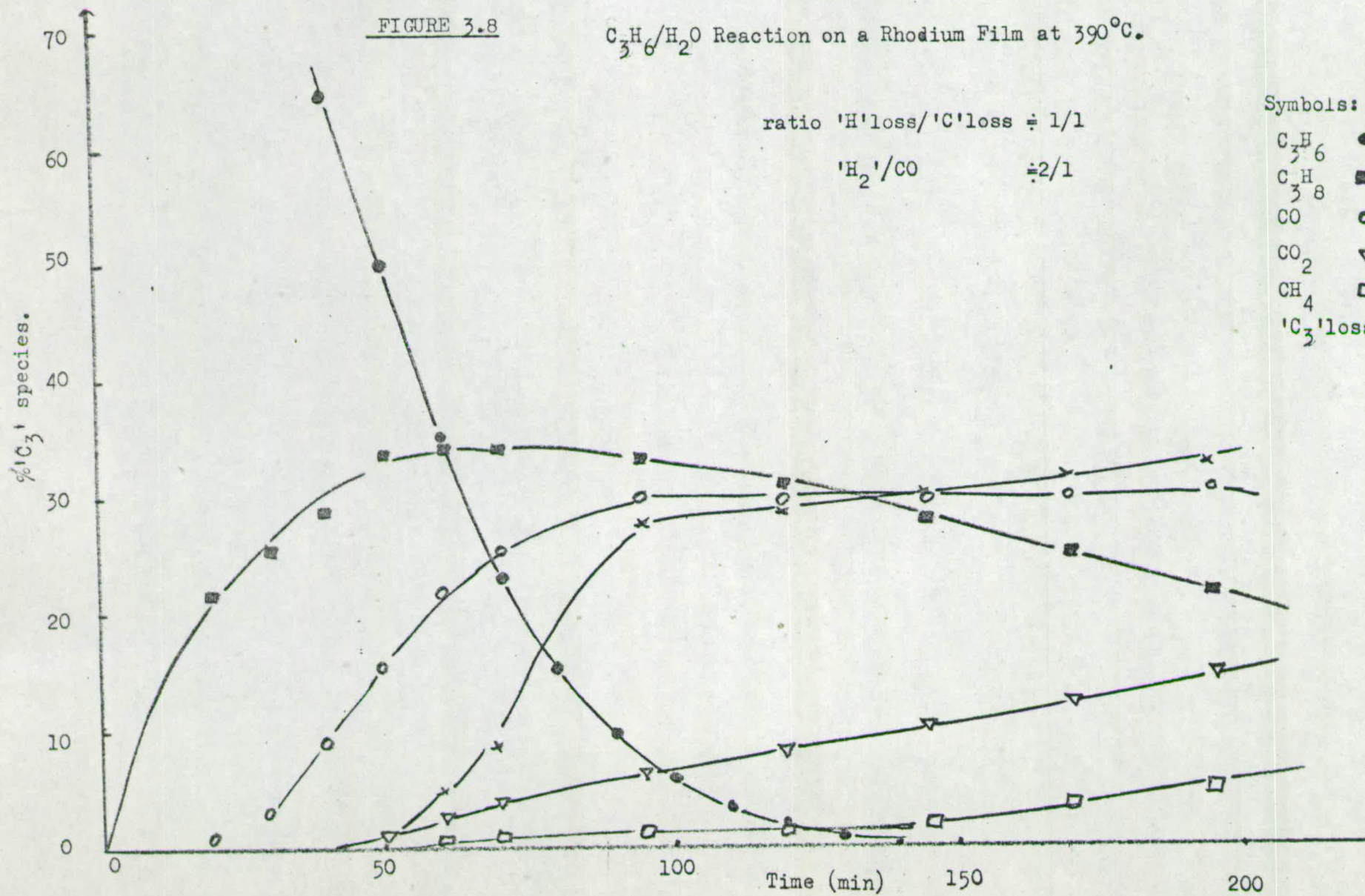


FIGURE 3.9

C_3H_6/H_2O Reaction on Rhodium/ Al_2O_3 at $294^\circ C$.

ratio $H_2/CO = 1.5/1$

Symbols:

C_3H_6●
 C_3H_8■
 CO○
 CO_2▼
 CH_4□
 $'C_3'$ loss...x

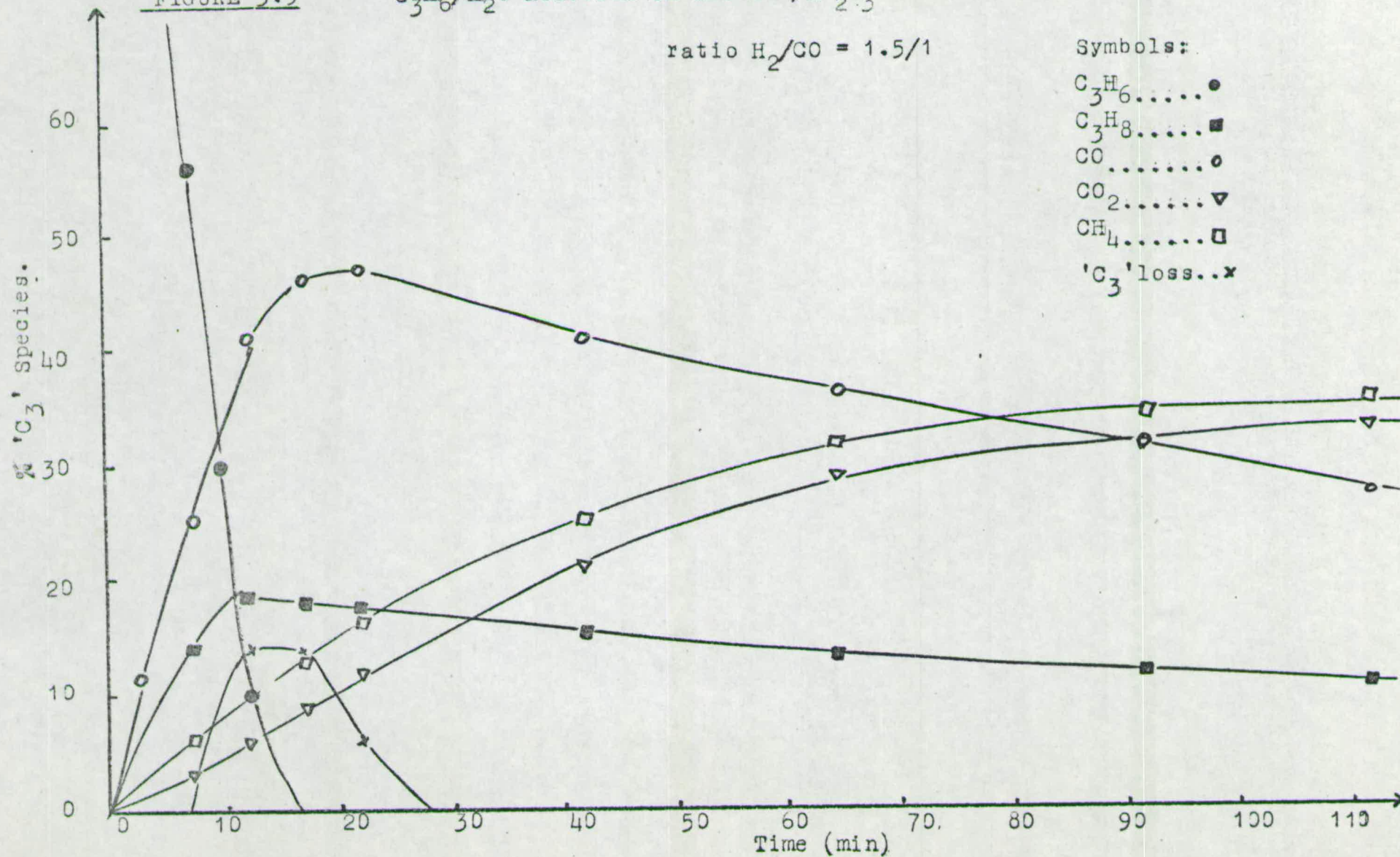


Table 3.3

Comparison of % Dry Gas Product Distribution with the
Calculated Equilibrium Values.

<u>Reaction Mixture</u>	<u>Catalyst</u>	<u>Temp. °C</u>	<u>% Dry Gas</u>				
			<u>CO</u>	<u>CO₂</u>	<u>CH₄</u>	<u>H₂</u>	
C ₃ H ₆ /H ₂ O	Rh film	390	<u>expt.</u>	32	21	17	30
			<u>calc.</u>	4	22	38	37
C ₃ H ₆ /H ₂ O	Rh/ α -Al ₂ O ₃	392	<u>expt.</u>	19	13	39	29
			<u>calc.</u>	4	22	38	37

Table 3.4 summarises these reactions over rhodium catalysts in terms of reaction products, carbon loss, and hydrogen loss.

Where propane and water are used as a feed the reaction proceeds in a manner analogous to that with propylene after the olefin supply is exhausted and the propane content reaches a maximum. Again the reaction is qualitatively similar over both rhodium films, (Figure 3.19), and supported rhodium catalysts, (Figure 3.11), with very little of the carbon loss being regained by the gas phase.

Neither the water gas shift reaction nor the methanation reaction are as fast over rhodium as they are over nickel and Figure 3.12 illustrates the dry gas composition for the water gas shift reaction over rhodium at 340°C. The reaction is markedly slower than over nickel and also demonstrates methanation occurring as a secondary reaction. From a combination of the water gas shift reaction and the methanation reaction shown below, the rate of appearance of CH₄ and CO₂ would be expected to equal the rate of disappearance of CO and H₂:

CO/

FIGURE 3.10

C_3H_8/H_2O Reaction on a Rhodium Film at $404^\circ C$.

~80%

ratio $H_2/CO \approx 2/1$

Symbols:

C_3H_8 ■
 CO ○
 CO_2 ▼
 CH_4 □
 C_3 loss ✕

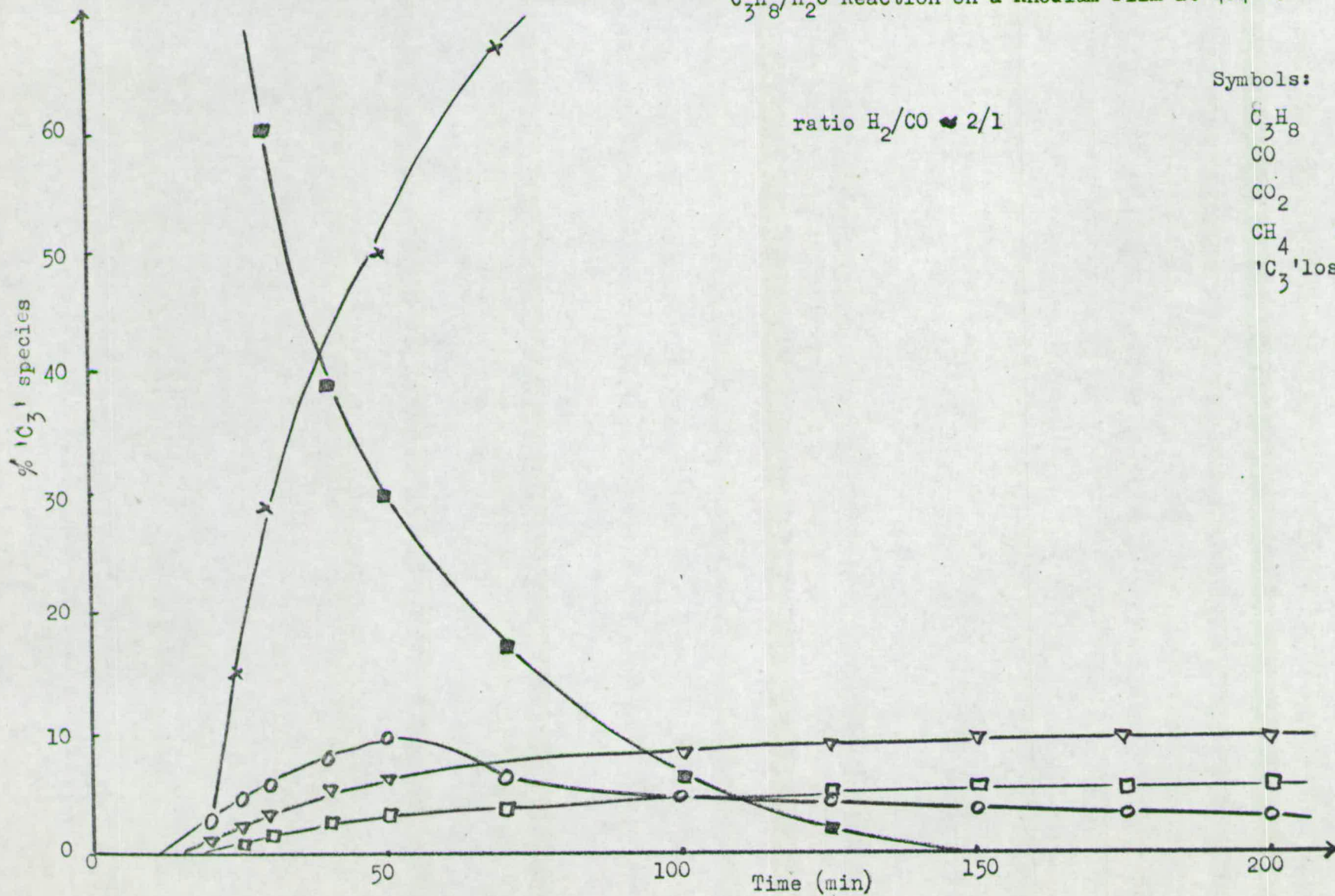


FIGURE 3.11

C_3H_8/H_2O Reaction on Rh/Al_2O_3 at $390^\circ C$.

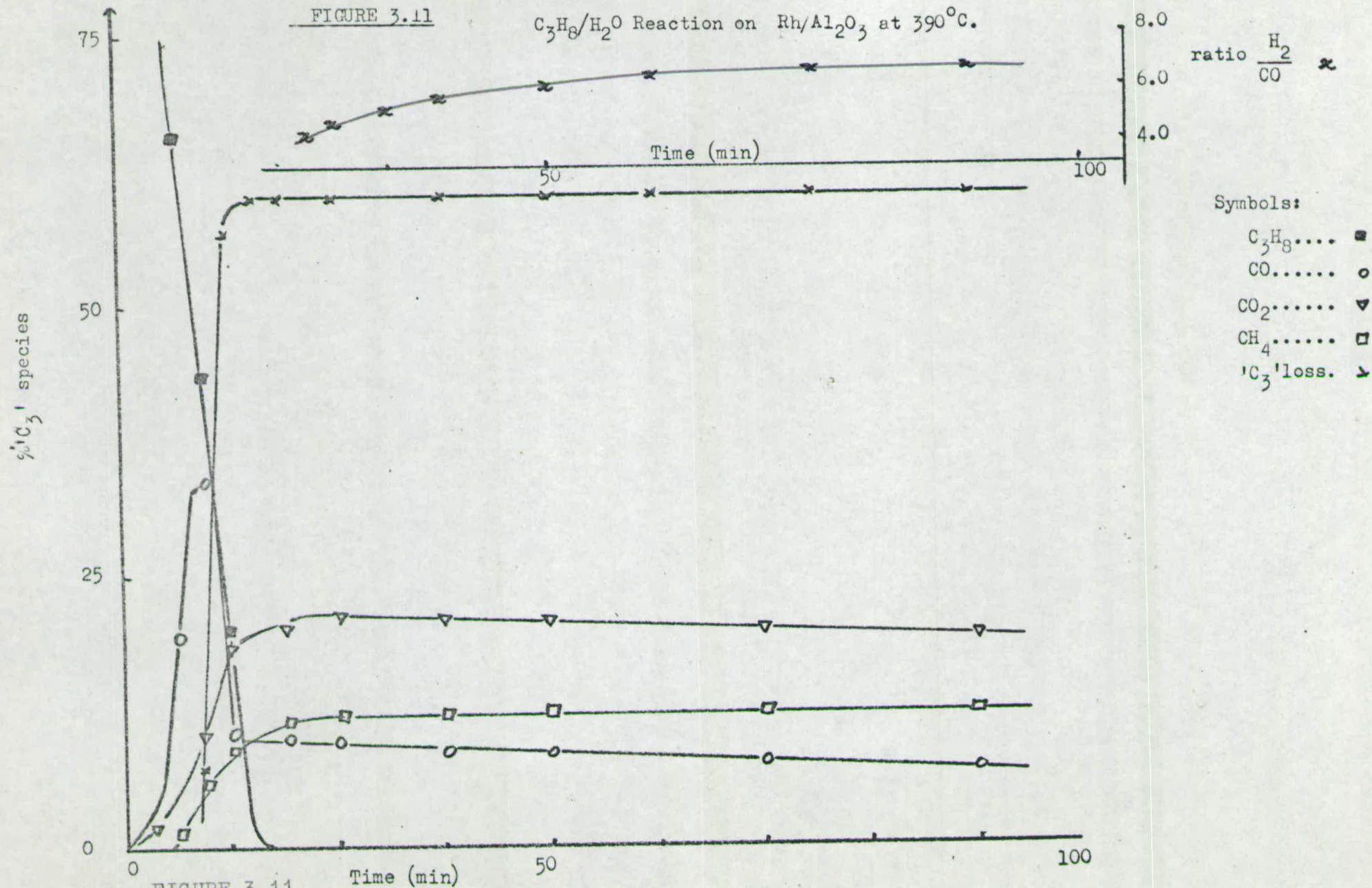


FIGURE 3.11

CO/H₂O on a Rhodium Film at 340°C. (1:1 mixture, 2)
 $P_{RV} = 120 \text{ Nm}^2$

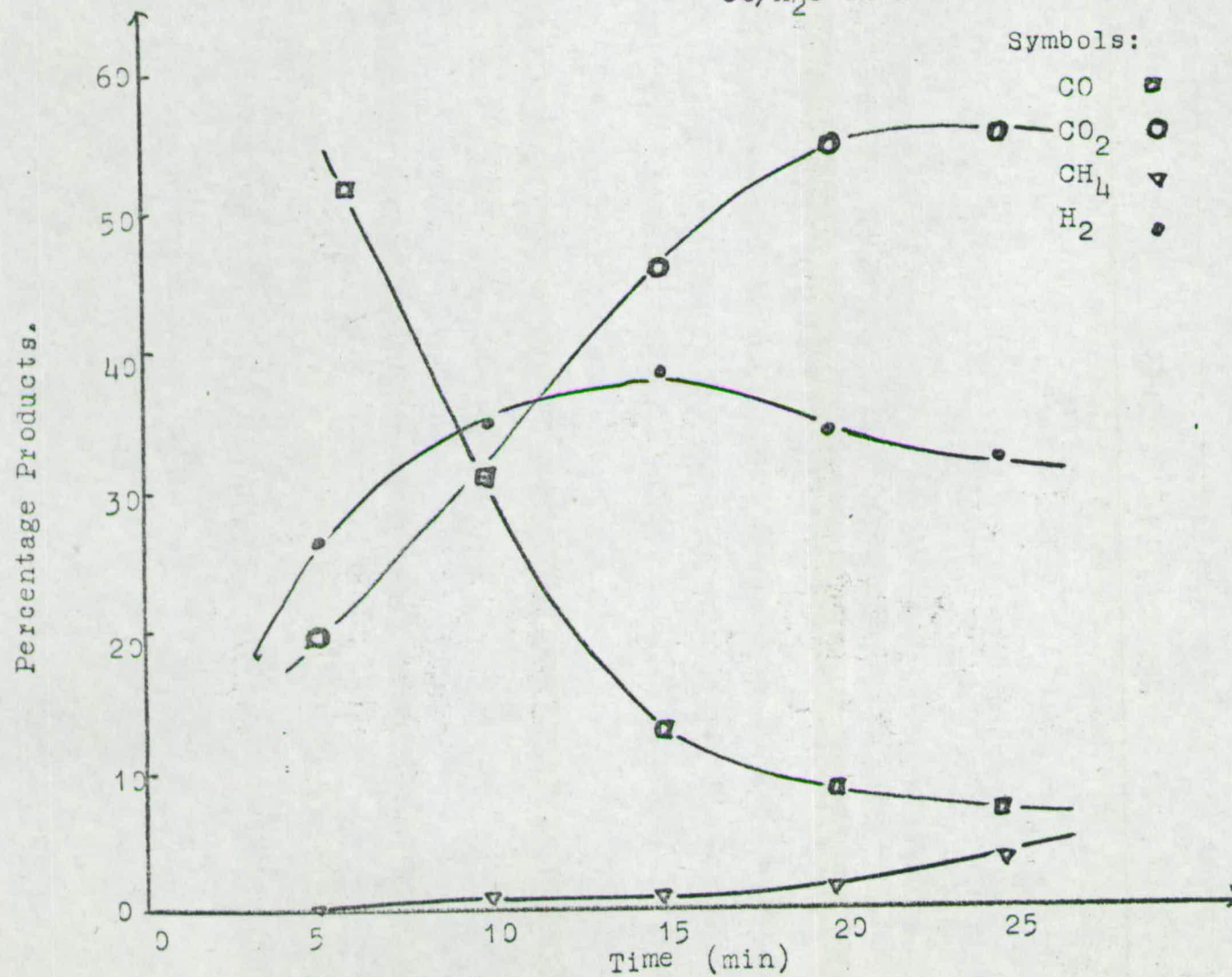
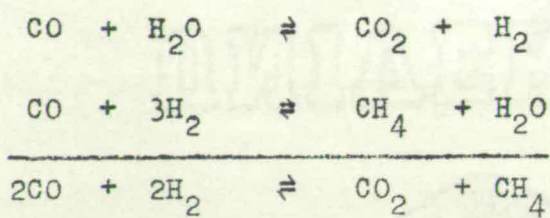


FIGURE 3.12



This is verified by measurements of the relevant rates over rhodium for the products of the $\text{C}_3\text{H}_6/\text{H}_2\text{O}$ reaction over a rhodium/ γ - Al_2O_3 catalyst at 392°C . Figure 3.13 shows the appearance and disappearance of the molecules concerned and the approximate rates are tabulated below:

<u>Molecule</u>	CO	CO ₂	CH ₄	H ₂
<u>Rate</u> (% min ⁻¹)	-0.18	0.16	0.30	-0.27

These rates balance out suggesting that the above equations are representative of the latter part of the hydrocarbon/steam reaction over rhodium.

Products of reaction $C_3H_6 // H_2O$ on Rhodium- Al_2O_3 at $392^\circ C$.

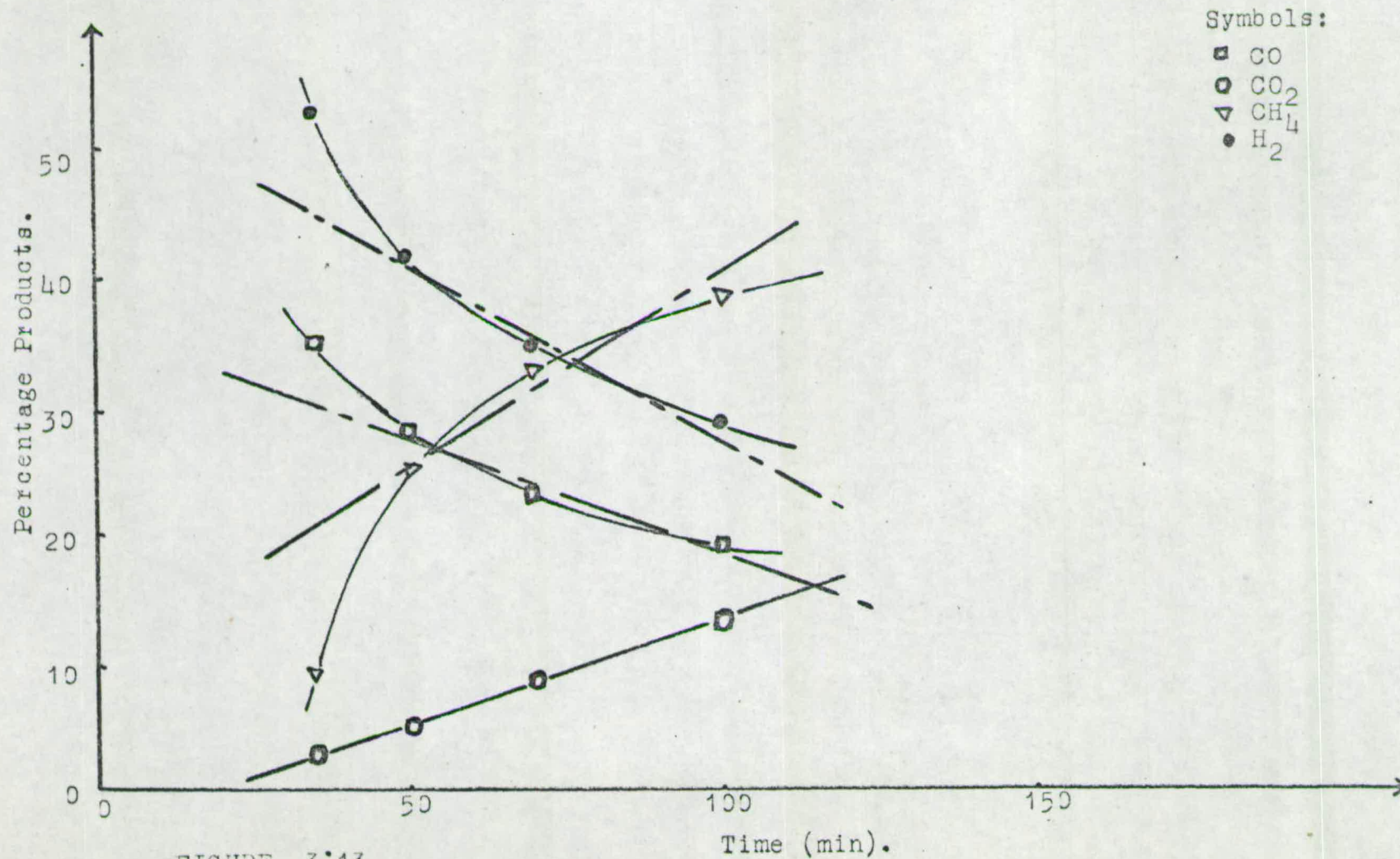


FIGURE 3.13

Table 3.4

Summary of Results for the Hydrocarbon/Heavy Water
Exchange on Rhodium Catalysts.

<u>Reaction Mixture</u>	<u>Catalyst</u>	<u>C₃H₈</u>	<u>CH₄</u>	<u>CO₂</u>	<u>CO</u>	<u>H₂</u>	<u>'C₃' loss</u>	<u>'H' loss 'C' loss</u>
C ₃ H ₆ /H ₂ O	Rh film	✓	✓	✓	//	//	~ 40%	1/1
C ₃ H ₆ /H ₂ O	Rh/ α -Al ₂ O ₃	✓	✓	✓	//	//	~ 15%	2/1
C ₃ H ₈ /H ₂ O	Rh film	----	✓	✓	//	//	~ 80%	2/1
C ₃ H ₈ /H ₂ O	Rh/ α -Al ₂ O ₃	----	✓	✓	//	//	~ 60%	2/1

An attempt to derive an Arrhenius plot as with reaction over nickel proved unsuccessful partly due to the difficulty in obtaining accurate rhodium film weights and the intrinsic semi-quantitative nature of the analysis.

3.5 Discussion

(a) Reaction over nickel.

The chemical reaction between propylene and water and between propane and water at temperatures between 300 and 420°C results in qualitatively similar product distributions with breakdown of the C_3 molecules to single carbon species and hydrogen. Methane, carbon dioxide, and hydrogen are the only molecules to appear in the gas phase during the early stages of reaction with carbon monoxide showing up as the reaction approaches equilibrium. The activation energy for the disappearance of the hydrocarbon feed correspond closely to that found by Phillips et al⁽⁶⁵⁾ for the analogous reactions with hexane/water and heptane/water systems over nickel on alumina catalysts. These workers also found that the reactions involving steam and $C_5 \rightarrow C_8$ hydrocarbons again resulted in single carbon molecules and hydrogen as products, similar results being obtained with n-butane by Bhatta and Dixon⁽⁶⁶⁾.

As the experimental techniques used here involve relatively long contact times it is difficult to assess the initial behaviour of the reactants and it is not possible to comment on the surface species directly. However some general points may be made.

Schnell⁽⁶⁴⁾ has shown that steam reforming of naphtha over a nickel catalyst proceeds via the olefin produced/

produced by the catalytic cracking of a paraffin to an olefin and methane. The production of propane from a propylene feed is therefore unexpected and must occur as a side reaction, the propane later breaking down to an olefin. Dehydrogenation is not likely to play a significant part in this reaction as nickel will preferentially crack hydrocarbons.

There are three main possibilities for the reaction mechanism.

- (i) Initial decomposition of the hydrocarbon to carbon and hydrogen followed by reaction of the hydrocarbon with steam but this reaction is too slow to support such a mechanism^(92, 93).
- (ii) Stepwise breakdown of the hydrocarbons and direct reaction of steam with the hydrocarbon fragments on the catalyst surface.
- (iii) Direct reaction of hydrocarbons and steam giving oxygenated intermediates possibly on the catalyst surface. It is improbable that any oxygenated intermediates appear in the gas phase in any significant quantities as mass spectrometric evidence of them would be expected.

Although no C_2 species were found in this work these have been noted by Schnell at very short contact times (5×10^{-4} seconds) but rapidly react without ever reaching a significant concentration in the gas phase. The thermodynamic data in Table 3.5 emphasises this point, demonstrating the preference for cracking rather than dehydrogenation exhibited by the C_3 hydrocarbon while the further breakdown of the C_2 species to methane is even more favoured. The values are given at $600^\circ K$ but the general arguments hold good up to $1100^\circ K$.

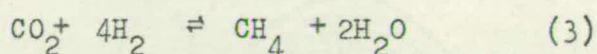
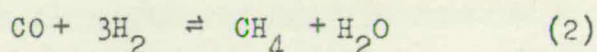
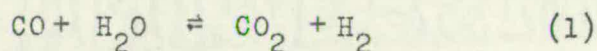
Table 3.5/

Table 3.5

ΔG Values for Dehydrogenation and Cracking of Olefins
at 600°K.

<u>Reaction</u>	<u>ΔG kJ mole⁻¹</u>
$C_3H_8 = C_3H_6 + H_2$	59
$C_2H_6 = C_2H_4 + H_2$	60
$C_3H_8 = C_3H_4 + CH_4$	-19
$C_3H_8 + H_2 = C_2H_6 + CH_4$	-75
$C_3H_6 + H_2 = C_2H_4 + CH_4$	-88
$C_3H_6 + 2H_2 = C_2H_6 + CH_4$	-102
$C_2H_6 = H_2 + 2CH_4$	-73
$C_2H_4 = 2H_2 + 2CH_4$	-133

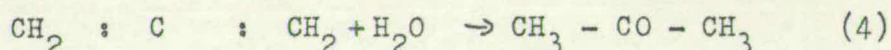
It is not possible to decide whether carbon monoxide or carbon dioxide appear separately or together (94, 95) although Phillips et al (96.) suggest that hydrogen and carbon monoxide are the primary products. There is general agreement that the equilibration reactions between H_2 , CO , CO_2 , CH_4 , and H_2O shown below lead to the final product distributions (97, 98).



All three equilibria lie well over to the right in the temperature range 300 - 420°C used in this work. Reactions (1) and (2) both occur rapidly at 300°C over nickel which could, in part, account for the non-appearance of carbon monoxide in the early stages of the hydrocarbon/

hydrocarbon/steam reaction, the carbon monoxide reacting with hydrogen or water before the gas phase concentration was sufficient for mass spectrometric analysis.

Although it has not been possible to comment on the surface intermediates from an experimental viewpoint, it is possible to suggest some thermodynamically plausible intermediates which may exist on the surface, using Dowden's "virtual mechanistic" approach⁽⁹⁹⁾. The reaction of steam and olefins may lead to the formation of surface complexes resembling alcohols, aldehydes, acids, and ketenes via the thermodynamically viable gas-phase reactions shown below.



The intermediates are unstable and would decompose rapidly. Steam cracking is more favoured by thermodynamics than hydration.

A major problem in the steam reforming process is the formation of strongly adsorbed carbon species on the catalyst surface. Again it has not proved possible to distinguish those species on the surface but some general conclusions may be drawn. It is improbable that nickel carbide formation plays a major role in removing carbon from the gas-phase as it does not account for the parallel loss of hydrogen and further, the residue cannot easily be removed by treatment with hydrogen. More probably strongly adsorbed surface residues formed from the polymerisation of dehydrogenated unsaturated intermediates appear. The polymerisation of olefins is catalysed by nickel and by the acid sites on a support, infra-red studies having provided evidence for both monomeric/

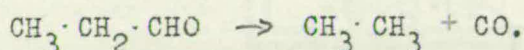
monomeric and polymeric surface structures on the metal (16, 100, 101). The difficulty involved in removing surface residues either with hydrogen or with steam together with the empirical structure of $(CH_{1-2})_n$ suggested by the ratios of carbon loss to hydrogen loss, augment the case for polymeric residues.

(b) Reaction over rhodium.

The behaviour of propylene/steam and of propane/steam mixtures over rhodium and rhodium supported on α -alumina catalysts is analogous to their behaviour over nickel. Qualitatively similar patterns of products occur over both rhodium films and supported rhodium with propane being formed as a major product from propylene then giving way to single carbon species and hydrogen. The major difference that is exhibited by reaction over propylene is the formation of carbon monoxide as a primary product followed by reaction with steam and hydrogen by a combination of the water gas shift and methanation reactions (1) and (2) giving:



This equation fits the experimental evidence that the rate of disappearance of CO and H_2 equals the rate of appearance of CH_4 and CO_2 . A possible surface intermediate for the formation of carbon monoxide could be an aldehydic species which could crack to a hydrocarbon and carbon monoxide, e.g.:

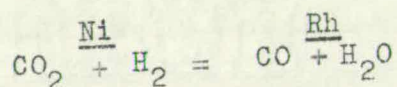


While carbon dioxide is adsorbed on nickel it is not adsorbed on rhodium indicating little carbon dioxide formation in the initial stages of reaction over rhodium and reinforcing the argument that it is formed as part of a secondary reaction.

Over rhodium, as over nickel, carbon and hydrogen are/

are both lost from the gas phase in the ratio C : H₁₋₂ as strongly held surface residues. This again suggests that polymerisation of fragmented hydrocarbons may be occurring on the surface.

It has been fairly well established that paraffins are demethanated over nickel catalysts⁽⁶⁴⁾. Rhodium differs in that it is a much more active dehydrogenation catalyst, and a correspondingly good hydration catalyst otherwise olefins and carbon would be the only products, and this offers an alternative reaction pathway to nickel, with paraffins dehydrogenating to olefins which may then react with steam. However this cannot be substantiated by the present work. A comparison of results over nickel and rhodium suggests that a rather naive picture is of rhodium catalysing the hydrocarbon/steam reaction to the carbon monoxide side of the water gas shift reaction and nickel tending to the carbon dioxide side, followed by equilibration of H₂, CO, CO₂, CH₄ and H₂O.



There is some evidence that with an α -alumina supported catalyst hydroxyl groups are formed on the support and migrate to the metal where they react with the hydrocarbon^(66, 102) but reaction also occurs on the plain metal.

CONCLUSION

The exchange reactions between hydrogen and heavy water and between propylene and heavy water over nickel, platinum, palladium, and rhodium, are relevant to an investigation of catalytic steam reforming as they provide an insight into the behaviour of water and a reactive hydrocarbon in this reaction. All four metals will catalyse the steam reforming process to some extent but although rhodium is a more active catalyst than nickel only nickel is an economically viable proposition for an industrial process.

The relative activities exhibited by the metals for the $\text{H}_2/\text{D}_2\text{O}$ exchange reaction, $\text{Pt} > \text{Rh} > \text{Pd} > \text{Ni}$, differs from their activities for the $\text{C}_3\text{H}_6/\text{D}_2\text{O}$ exchange reaction where platinum is initially the most reactive catalyst but poisoning reduces its rate drastically to become least active. This leaves palladium as the most active metal followed by nickel then rhodium. An added complication with reaction over nickel is the self-hydrogenation of some propylene to propane in the presence of water which occurs at 0°C . Boosting the temperature to around 300°C causes a slight rise in the propane content and rapid decrease of the parent olefin followed by a slower decrease in propane content. At the same time carbon oxides, methane, and hydrogen are formed and there is a loss of carbon and hydrogen from the gas phase. Although it has not been possible to identify any surface species directly the probable mechanism involves demethylation of the hydrocarbon feed on the catalyst surface followed by reaction of the fragments with water forming oxygenated intermediates which lead to carbon oxides and hydrogen. Finally there is an equilibration reaction between CO , CO_2 , CH_4 , H_2 and H_2O .

The/

The use of a rhodium catalyst for the C_3H_6/H_2O reaction at temperatures in excess of $290^\circ C$ also leads to the formation of propane initially. However no trace of propane was detected in the course of the C_3H_6/D_2O exchange reaction up to $280^\circ C$ and consequently it is not known whether the propane is formed by the self-hydrogenation of propylene as in the case of nickel, or by incorporation of hydrogen from water. To decide which is the case it would be necessary to stop the reaction of propylene and heavy water after a few minutes of reaction at $300^\circ C$ and analyse the mixture using a gas chromatograph to identify the propane. Rhodium will dehydrogenate a hydrocarbon rather than demethanate it as over nickel and oxygenated intermediates are probably formed breaking down to hydrogen and carbon monoxide mainly and finally equilibrium is again approached between CO , CO_2 , CH_4 , H_2 and H_2O .

Both nickel and rhodium catalyse reactions with propane and water as reactants resulting in an analogous pattern of behaviour to their respective reactions with a propylene/water feedstock after attainment of the propane maximum. The use of alumina supported metals results in qualitatively similar product distributions as the plain metal catalysts. To prepare a catalyst with a metal surface area of approximately 1 m^2 per gram of catalyst it was necessary to use 5% nickel on alumina but only 0.8% rhodium on alumina. No traces of any C_2 species are noted in the gas phase during reaction over either metal but this does not preclude the existence of such species as transient intermediates.

The next logical step from the work described in this thesis would be the identification of the surface intermediates involved in the reforming reaction. This might be accomplished by outgassing the reaction vessel, removing/

removing the metal film in an inert atmosphere, and
subjecting the metal and surface residues to chemical
analysis. The use of E.S.R. and infra-red methods⁽¹⁰²⁾
should give a more comprehensive analysis of the
surface species present.

Appendix I

Computer Program for Analysis of a C_2H_4/D_2O mixture.

```

%BEGIN
%INTEGER I,J,K,L,R,S,Q,A,N,B,M
%ARRAY P(-20:20)
%ARRAY F(1:6)
%REAL Z,T,H,C,D,E,G,TOTAL,PHI,X
READ (I)
%COMMENT I SETS OF DATA
7: READ(N)
%COMMENT NO. OF HYDROGENS TO BE CONSIDERED
READ (M)
%COMMENT NO. OF FRAGMENTS TO BE CONSIDERED
READ (X)
%COMMENT SINGLE ISOTOPE CORRECTION
%CYCLE B=1,1,6
READ (F(B))
%REPEAT
%CYCLE J=1,1,I
1: READ (Z)
->1 %UNLESS Z=-1
READ (T)
%COMMENT T IS TIME
%CYCLE A=-M,1,N
READ (P(A))
%IF P(A)=-2 %THEN ->6
%IF P(A)=-3 %THEN ->7
%STOP %IF P(A)=-4
%REPEAT
%COMMENT P(-M:N) ARE RAW PEAK HEIGHTS
READ (Z)
->2 %IF Z=-2
6: %CAPTION ~ FAULTY SET OF DATA
PRINT (J,3,0)
->1
%COMMENT CORRECTIONS FOR S.I.C., D.I.C., AND NAT. D. FOLLOW
2: %CYCLE K=-M,1,N-1
H=X +(N-!K!)*0.0002
P(K+1)=P(K+1)-H*P(K)
%IF K>(N-2) %THEN ->3
P(K+2)=P(K+2)-H*((H-0.011)/2)*P(K)
3: %REPEAT
%COMMENT CORR. FOR FRAG. CONS. LOSS OF UP TO 6 MASS UNITS ONLY
%CYCLE L=N,-1,0
%IF P(L)<0 %THEN ->10
%COMMENT -1
P(L-1)=P(L-1)-(F(1)*((N-L)/N)*P(L))
%COMMENT -2
P(L-2)=P(L-2)-((F(1)*(L/N)*P(L))+(F(2)*((N-L)
* ((N-1)-L)/(N*(N-1))*P(L)))
% C

```



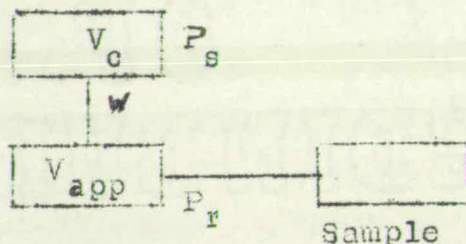
```

%COMMENT -3
  C=P(L)*(F(2)*(2*L/N*(N-L)/(N-1)))
  D=P(L)*(F(3)*((N-L)/N*((N-1)-L)/(N-1)*((N-2)-L)/(N-2)))
P(L-3)=P(L-3)-(C+D)
%COMMENT -4
  C=P(L)*(F(2)*(L/N*(L-1)/(N-1)))
  D=P(L)*(F(3)*3*(L/N*(N-L)/(N-1)*((N-1)-L)/(N-2)))
  E=P(L)*(F(4)*((N-L)/N*((N-1)-L)/(N-1)*((N-2)-L)/(N-2)*
    ((N-3)-L)/(N-3)))
P(L-4)=P(L-4)-(C+D+E)
%COMMENT -5
  C=P(L)*(F(3)*3*(L/N*(L-1)/(N-1)*(N-L)/(N-2)))
  D=P(L)*(F(4)*4*(L/N*(N-L)/(N-1)*((N-1)-L)/(N-2)*((N-2)-L)/(N-3)))
P(L-5)=P(L-5)-(C+D+E)
%COMMENT -6
  C=P(L)*(F(3)*(L/N*(L-1)/(N-1)*(L-2)/(N-2)))
  D=P(L)*(F(4)*6*(L/N*(L-1)/(N-1)*(N-L)/(N-2)*((N-1)-L)/(N-3)))
P(L-6)=P(L-6)-(C+D+E+G)
10: %REPEAT
%COMMENT CALCULATION OF PERCENT, PHI AND PRINT INSTRUCTIONS
NEWLINES (2)
TOTAL=0
%CYCLE S=0,1,N
%IF P(S)<0 %THEN ->5
TOTAL=TOTAL+P(S)
5: %REPEAT
%CAPTION CORRECTED PEAK HEIGHTS
NEWLINES (1)
%CYCLE R=-M,1,N
%CAPTION D; PRINT (R,1,0)
%CAPTION =; PRINT (P(R),1,2)
%REPEAT
%CAPTION ~ TOTAL PEAK HEIGHT NEGLECTING D-1 TO D-M =
PRINT (TOTAL,1,2)
%CAPTION ~ PERCENTAGE OF ISOTOPIC SPECIES
NEWLINES (1)
%CYCLE R=0,1,N
%CAPTION D; PRINT (R,1,0)
%CAPTION =; PRINT (P(R)*100/TOTAL,1,2)
%REPEAT
PHI=0
%CYCLE Q=1,1,N
%IF P(Q)<0 %THEN ->44
PHI=PHI+Q*P(Q)*100/TOTAL
44: %REPEAT
%CAPTION ~ PHI =; PRINT (PHI,1,2)
%CAPTION ~ TIME =; PRINT (T,1,2)
99: %REPEAT
%END %OF %PROGRAM

```

Appendix II

Calculation of Results for Surface Area Measurements.



Calibrated Volume	$= V_c$
Volume beyond tap W	$= V_{app}$
Volume of gas adsorbed on sample	$= V_{ads}$

When no sample is present we have

Quantity of gas in $V_c = P_{s1} V_c$ for 1st increment

$$P_{s1} V_c = P_{r1} V_{app} + P_{r1} V_c \quad \text{where}$$

$P_{r1} V_c$ is the quantity left in V_c

$$P_{r1} V_{app} = P_{s1} V_c - P_{r1} V_c$$

$$\text{Also } P_{s2} V_c = P_{r2} V_{app} + P_{r2} V_c - P_{r1} V_{app} \quad \begin{array}{l} \text{i.e. remains} \\ \text{after 1st} \\ \text{increment} \end{array}$$

$$P_{r2} V_{app} = P_{s2} V_c + P_{s1} V_c - P_{r1} V_c - P_{r2} V_c$$

$$\text{i.e. } P V_{app} = P_s V_c - P_r V_c \quad \text{for a blank run (1)}$$

With a sample present

$$P_{s1} V_c = P_{r1} V_{app} + P_{r1} V_c + P_{r1} V_{ads1}$$

$$P_{s2} V_c = P_{r2} V_{app} + P_{r2} V_c + P_{r2} V_{ads2} - P_{r1} V_{app}$$

$$\text{i.e. } \sum P V_{ads} = \sum P_s V_c - \sum P_r V_c - P V_{app} \quad (2)$$

$$\text{and } \sum P V_{total} = \sum P_s V_c - \sum P_r V_c \quad \text{where } \sum P V_{total} = \sum P V_{ads} - \text{Blank}$$

A/

A graph of $\sum PV_{app}$ vs P_R will give a straight line gradient V_{app} for a blank. From the adsorption run we have P_s, P_R , and V_c thus we can get $\sum PV_{total}$,

or by, (2). The value of PV_{app} on 'Blank Value' may be read off the blank graph for any P_R to get (PV) sample.

Correcting all to N.T.P. $PV_{sample}/760$ will be V_{ads} in mls at N.T.P.

Correction for Temperature

$$V_c \times \frac{\text{temp (N.T.)}}{\text{temp (R.T.)}} = V_{NT}$$

Therefore we may calculate $k_{N.T.} = V_c \times \frac{T_o}{T_R}$ for both calibrated volumes.

$P_{s1} V_c$ at N.T. is $P_{s N.T.} k_{N.T.}$ at the temperature of addition of the increment, i.e. $P_{s N.T.} k_{N.T.} = P_{s1}^l V_c$ and $P_{R1} k_{N.T.} = P_R^l V_c$

Thermomolecular Flow Calculations

At temperatures very different from room temperature

$P_N = R \times P_R$ where R is obtained from a T.M.F. graph.

Area Measurement

$$\sum = \frac{V_m}{22,400} \times N \times \sigma_g \times 10^{-2}$$

Where \sum = surface area in $m^2 g^{-1}$

V_m = Volume of gas adsorbed to monolayer in mls.

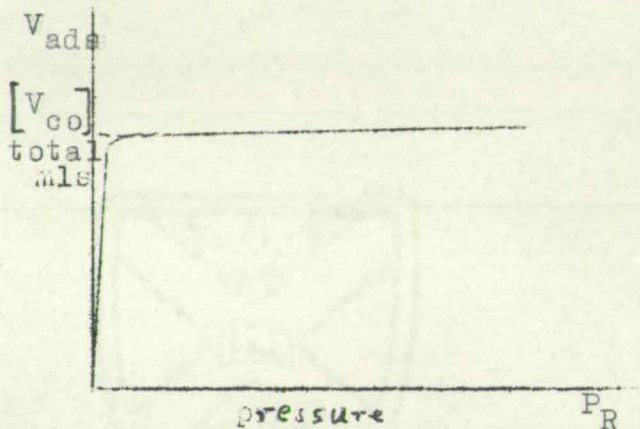
N = Avogadro's Number -

σ_g = cross-sectional area of gas in square angstroms per molecule.

A/

A plot of V_{ads} vs P_R , shown below, gives a point $\left[\frac{V_{co}}{V_{total}} \right]$ equivalent to monolayer coverage.

$$\begin{aligned} V_{co} &= \frac{x}{760} \text{ ml NTP} \\ &= g \text{ ml NTP} \\ &= \frac{g}{z} \text{ ml g}^{-1} \text{ where } z \text{ catalyst weight.} \end{aligned}$$



The above calculations give a measure of surface area on a metal. CO is not strongly adsorbed on alumina and krypton adsorption may be employed to give a total surface area using the B.E.T. equation.

$$\text{Thus } \frac{V_{kr}}{V_{co}} = a \text{ and } \sigma_{co} \text{ (The CO site area)} = a \times 19.6 \text{ \AA}^2$$

Calculation/

Calculation of Results on Supported Nickel.

Let a = surface area of nickel in m^2

and b = " " " support " "

For krypton adsorption; surface area $V_{mls} \cdot K_r \times 5.17$

$$V_{Kr} = \frac{\text{surface area}}{5.17}$$

$$\text{By definition } V_{Kr} \quad a = \frac{a}{5.17} \quad V_{Kr} \quad b = \frac{b}{5.17}$$

$$V_{Kr} \text{ total} = \frac{a+b}{5.17} \quad (1)$$

$$\text{Also } [V_{co}]_{\text{total}} = \frac{a}{3.34} (3.34 \quad 12.4A^{o^2} \times 0.269 \text{ converting to } m^2 g^{-1})$$

$$\text{For Support } \frac{V_{Kr}}{V_{co}} = 1340 \text{ and for nickel } \frac{V_{Kr}}{V_{co}} = 0.643$$

$$\text{For Support } [V_{co}]_{\text{supp}} = 3.34 = \frac{b}{1340/0.643} = \frac{b}{2080}$$

i.e. effectively the support only adsorbs $(\frac{1}{2080})^{th}$ of CO w.r.t. nickel.

$$V_{co} \text{ total} = \frac{\text{Effective area for CO}}{3.34} = \frac{a + \frac{b}{2080}}{3.34} \quad (2)$$

From (1) and (2) we get a and b .

Appendix II (cont.)

ICI Program for calculation of V_{ads} and P_R for surface area measurements.

```

ADSORB;
"BEGIN" "REAL" VB,FS,FF,VC,HS,HF,TS,TF,PS,PF,SPVT,SPVS;
      "INTEGER" M;
      "INTEGER" "ARRAY" NAME[1:100];
      "SWITCH" L:= START, GAS;

      "READ" VB,FS,FF;

START: "PRINT" 'L2';
      M:=1;
      INSTRING (NAME,M);
      M:=1;
      OUTSTRING (NAME,M);
      "PRINT" 'L2' PRESSURE      MLS.ADSORBED      PS';
      SPVT:=0;

GAS:   "READ" VC;
      "IF" VC<0 "THEN" "GO TO" START;
      "READ" HS,HF,TS,TF;
      PS:= 273/(TS+273)/(1/(HS*HS*FS) - 1/HS);
      PF:= HF*HF*FF*273/(TF + 273);
      SPVT:= SPVT + PS*VC - PF*VC;
      SPVS:= SPVT - PF*VB;
      "PRINT" SCALED(3),PF*(TF+273)/273,SAME LINE,
              'S7',SCALED(3),SPVS/760,'S4',SCALED(3),
              PS*(273+TS)/273;
      "GO TO" GAS;

"END";

```


Appendix III

Calculation of the binomial distribution for any exchange reaction to obtain the expected random distribution.

The binomial expansion is $(x+y)^n$ where
 n number of exchangeable 'hydrogens' in the hydro-
 carbon

$$x = \frac{H}{H+D} = 1 - \frac{\phi}{100n}$$

$$y = \frac{D}{H+D} = \frac{\phi}{100n}$$

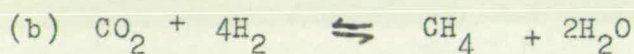
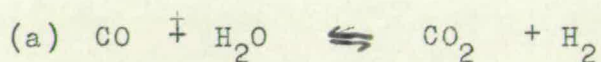
We have $(x+y)^n = \frac{x^n}{(d_0)} + \frac{nx^{n-1}y}{(d_1)} + \frac{n(n-1)}{2!} \frac{x^{n-2}y^2}{(d_2)} + \dots + \frac{y^n}{(d_n)}$

For propylene the equations are

$$\begin{aligned} d_0 &= 100 \times 1 \times x^6 y^0 \\ d_1 &= 100 \times 6 \times x^5 y^1 \\ d_2 &= 100 \times 15 \times x^4 y^2 \\ d_3 &= 100 \times 20 \times x^3 y^3 \\ d_4 &= 100 \times 15 \times x^2 y^4 \\ d_5 &= 100 \times 6 \times x^1 y^5 \\ d_6 &= 100 \times 1 \times x^0 y^6 \end{aligned}$$

Appendix IV.

Gas Phase Equilibrium Constants for Reactions.



Temp. °C	$K_a = \frac{p_{\text{CO}_2} p_{\text{H}_2}}{p_{\text{CO}} p_{\text{H}_2\text{O}}}$	$K_b = \frac{p_{\text{CH}_4} p_{\text{H}_2\text{O}}^2}{p_{\text{CO}_2} p_{\text{H}_2}^4}$	$K_c = \frac{p_{\text{CO}} p_{\text{H}_2}^3}{p_{\text{CH}_4} p_{\text{H}_2\text{O}}}$
200	2.279×10^2	9.509×10^8	4.614×10^{-12}
250	8.651×10^1	1.377×10^7	8.397×10^{-10}
300	3.922×10^1	3.998×10^5	6.378×10^{-8}
350	2.034×10^1	1.980×10^4	2.483×10^{-6}
400	1.170×10^1	1.491×10^3	5.732×10^{-5}
450	7.311	1.570×10^2	8.714×10^{-4}
500	4.878	2.171×10^1	9.442×10^{-3}
550	3.434	3.761	7.741×10^{-2}
600	2.527	7.868×10^{-1}	5.029×10^{-1}
650	1.923	1.930×10^{-1}	2.686
700	1.519	5.424×10^{-2}	1.214×10^1
750	1.228	1.714×10^{-2}	4.753×10^1
800	1.015	5.995×10^{-3}	1.644×10^2
850	8.552×10^{-1}	2.292×10^{-3}	5.101×10^2
900	7.328×10^{-1}	9.478×10^{-4}	1.440×10^3

References.

- (1) Kirchhoff, G.R., Schweigger's Journal, 4, 108 (1812).
- (2) de Saussure, N.T., Journ. de. Phys., 84, 225 (1817).
- (3) Davy, H., Phil. Trans., 77, (1817).
- (4) Döbereiner, J., Schweigger's Journal, 34, 91 (1822),
38, 321 (1823).
- (5) Berzelius, J., Jahresber. Chem., 15, 237 (1836).
- (6) Ostwald, W., Physik. Zhur., 3, 313 (1902).
- (7) Faraday, M., Phil. Trans., 114, 55 (1834).
- (8) Mitscherlich, E., Liebigs Ann., 44, 186 (1842).
- (9) Langmuir, I., Phys. Rev., 6, 79 (1915); J. Amer.
Chem. S ., 37, 1139 (1915).
- (10) Scholten, J.J.F., and Zvietering, P., Actes. Congr.
Intern. Catalyse, 2, Paris (1960), 2, 389 (Ed.
Technip, Paris, (1961)).
- (11) Brunauer, S., Emmett, P.H., and Teller, E., J. Amer.
Chem. Soc., 60, 309 (1938).
- (12) Barrett, E.P., Joyner, L.G., and Halenda, P.P., J.
Amer. Chem. Soc., 73, 373 (1951).
- (13) Joyner, L.G., Barrett, E.P., and Skold, R., J. Amer.
Chem. Soc., 73, 3155 (1951).
- (14) Trapnell, B.M.W., "Chemisorption" (Butterworth,
London), (1955).
- (15) Dowden, D.A., J. Chem. Soc., 242 (1950).
- (16) Eischens, R.P., and Pliskin, W.A., Adv. Catalysis
10, 1 (1958).
- (17) Langmuir, I., Trans. Faraday Soc., 17, 621 (1922).
- (18) Dowden, D.A., 'Catalyst Handbook', Wolfe, London
(1970).
- (19) Kemball, C., Proc. Chem. Soc., 264 (1960).
- (20) Pease, R.N., J. Amer. Chem. Soc., 45, 1196, 2235,
2296 (1923).
- (21)/

References Contd:

- (21) Prichard, C.R., and Hinshelwood, C.N., J. Chem. Soc., 127, 806 (1925).
- (22) Taylor, H.S., Proc. Roy. Soc., A, 108, 105 (1925)
- (23) Tamaru, K., Boudart, M., and Taylor, H.S., J. Phys. Chem., 59, 801 (1955).
- (24) Tamaru, K., and Boudart, M., Adv. Catalysis, 9, 699 (1957).
- (25) Spratt, D.A., Spec. Publ. Chem. Soc. (London) No.10, p. 53 (1957).
- (26) Nielsen, A., "An Investigation on Promoted Iron Catalysts for the Synthesis of Ammonia", (Gjellerups, Copenhagen), (1950).
- (27) McGeer, J.P., and Taylor, H.S., J. Amer. Chem. Soc., 73, 2743 (1951).
- (28) Burk, R.E., J. Phys. Chem., 30, 1134 (1926).
- (29) Balandin, A., 2. Phys. Chem., B2, 299; B3, 167 (1929).
- (30) Palmer, W.G., and Constable, F.H., Proc. Roy. Soc. A 107, 225, 270 (1925).
- (31) Sherman, A., and Eyring, H., J. Am. Chem. Soc., 54, 2661 (1932).
- (32) Twigg, G.H., and Rideal, E.K., Trans. Faraday Soc. 36, 533 (1940).
- (33) Beeck, O., Smith, A.E., and Wheeler, A., Proc. Roy. Soc. A 177, 62 (1940).
- (34) Beeck, O., Rev. Mod. Phys., 17, 61 (1945).
- (35) Beeck, O., Disc. Faraday Soc., 8, 118 (1950).
- (36) Schlier, R.E., and Farnsworth, H.E., Phys. Rev., 78, 316 (1950).
- (37) Cunningham, R.F., and Gwathmey, A.T., Adv. Catalysis, 9, 25 (1957).
- (38) Gomer, R., Adv. Catalysis, 7, 93 (1955).
- (39) Trapnell, B.M.W., "Chemisorption", Butterworth, London (1955).
- (40)/

References Contd:

- (40) Trapnell, B.M.W., Proc. Roy. Soc. A 218, 566 (1953).
- (41) Krishenbaum, I., Physical Properties and Analysis of Heavy Water, McGraw-Hill, New York (1951).
- (42) Couper, A., and Eley, D.D., Disc. Faraday Soc., 8, 172 (1950).
- (43) Daglish, A.G., and Eley, D.D., Proc. 2nd Inter. Cong. Catalysis, (Ed. Technip, Paris), p. 1615 (1961).
- (44) Schwab, G.M., Disc. Faraday Soc., 8, 166 (1950).
- (45) Schwab, G.M., Z. Electrochem, 53, 274 (1949).
- (46) Schwab, G.M., and Holz, G., Z Anorg. Chem., 252, 205 (1944).
- (47) Dowden, D.A., and Reynolds, P.W., Disc. Faraday Soc., 3, 184 (1950).
- (48) Reynolds, P.W., J. Chem. Soc., 265 (1950).
- (49) Boudart, M., J. Amer. Chem. Soc., 72, 1040 (1950).
- (50) Mann, R.S., and Lien, T.R., J. Catalysis, 15, No. 1 1 (1969).
- (51) Kemball, C., Proc. Roy. Soc. A 214, 413 (1952).
- (52) Rooney, J.J., Gault, F.G., and Kemball, C., Proc. Roy. Soc., 407 (1960).
- (53) Balandin, A.A., Doklady Akad. Nauk., S.S.S.R., 97, 667 (1954).
- (54) Balandin, A.A., Izvest. Akad. Nauk., S.S.S.R., 4, 624 (1955).
- (55) Balandin, A.A., and Tolstopiatova, A.A., Proc. 3rd Inter. Cong. Catalysis (North Holland, Amsterdam), p. 533 (1965).
- (56) Fahrenfort, J., van Reijen, L.L., and Sachtler, W.M.H., "The Mechanism of Heterogeneous Catalysis", (Elsevier), p. 23, (1960).
- (57) Schuit, G.C.A., van Reijen, L.L., and Sachtler, W.M.H., Proc. 2nd Inter. Cong. Catalysis (Ed. Technip, Paris), p. 893, (1961).
- (58) Hirota, K., and Hironaka, Y., Bull. Chem. Soc. Japan, 39, 2638 (1966).
- (59)/

References Contd:

- (59) Ueda, T., Hara, J., Hirota, K., Teratani, S., and Yoshida, N., Z. Phys. Chem. Neue. Folge, Bd. 64, S. 64-70 (1969).
- (60) Horiuti, J., and Polanyi, M., Trans. Faraday Soc., 30, 1164 (1934).
- (61) Garnett, J.L., and Sollich, W.A., Advan. in Catalysis 16, 95 (1966).
- (62) Calf, G.E., Garnett, J.L., and Pickles, V.A., Australian J. Chem. 21, 961 (1968).
- (63) Calf, G.E., and Garnett, J.L., Australian J. Chem. 21, 1221 (1968).
- (64) Schnell, C.R., J. Chem. Soc. (B) 158 (1970).
- (65) Phillips, T.R., Yarwood, T.A., Mulhall, J., and Turner, G.E., J. Catal. 17, 28 (1970).
- (66) Bhatta, K.S.M., and Dixon, G.M., I. E.C. Prod. Res. and Dev. 8, 324 (1969).
- (67) Bousquet, J.L., and Teichner, S.J. Bull. Soc. Chim. (France), 2963 (1969).
- (68) Nier, A.D., Rev. Sci. Instrum., 18, 398 (1947).
- (69) Halsted, R.E., and Nier, A.D., Rev. Sci. Instrum., 21, 1019 (1950).
- (70) Kemball, C., Proc. Roy. Soc. A 207, 539 (1951).
- (71) Barnard, G.P., "Modern Mass Spectrometry", 112, The Institute of Physics, London .
- (72) Kemball, C., Proc. Roy. Soc., A 214, 413 (1952).
- (73) Matsen, F.A., and Franklin, J.L., J. Amer. Chem. Soc., 72, 3334 (1950).
- (74) Kemball, C., Adv. Catalysis XI 223 (1959).
- (75) Harper, R.J., Siegel, S., and Kemball, C., J. Catalysis, 6, 72 (1966).
- (76) Kemball, C., Proc. Roy. Soc. A 207, 539 (1951).
- (77) Gault, F.G., and Kemball, C., Trans. Faraday Soc. 57, 1781 (1961).
- (78) Pines, H. and Haag, W.O., J. Amer. Chem. Soc., 82, 2471 (1960).
- (79)/

References Contd:

- (79) Peri, J.B., J. Phys. Chem., 69, 220 (1965).
- (80) Gregg, S.J., and Sing, K.S.W., "Adsorption Surface Area and Porosity", Academic Press (1967).
- (81) Lanyon, M.A.H., and Trapnell, B.M.W., Proc. Roy. Soc., A 227, 387 (1955).
- (82) Yates, J.T., and Garland, C.W., J. Phys. Chem., 65, 617 (1961).
- (83) Olariu, A.L., and Marginean, P., Revue Romaine de Physique, 13, 832 (1968).
- (84) Garnett, J.L., and Sollich, W.A., Adv. Catalysis, 16, 95 (1966).
- (85) Eley, D.D., Adv. Catalysis, 1, 185 (1948).
- (86) Hanner, Z.K., Acta. Chem. Scand., 10, 655 (1956).
- (87) Bond, G.C., "Catalysis by Metals", Academic Press, London (1962).
- (88) Anderson, J.R., and Kemball, C., Trans. Faraday Soc. No. 391, 51, 366 (1955).
- (89) Patterson, W.R., Ph.D. Thesis, (Queen's University, Belfast). (1963).
- (90) Farkas, A., and Farkas, L., J. Amer. Chem. Soc. 60, 22 (1938).
- (91) Burwell, R.L., Chem. Revs. 57, 895 (1957).
- (92) Gordon, A.S., Ind. Eng. Chem. 44, 1857 (1952).
- (93) Redpath, C.R., and Williams, B.M. Unpublished Work (1963).
- (94) Akers, W.W., and Camp, D.P., Amer. Inst. Chem. Engineers J., 1, 771 (1955).
- (95) Bodrow, N.M., Apelbaum, L.O., and Temkin, M.I., Kinetics and Catalysis (USSR), 5, 614 (1964).
- (96) Phillips, T.R., Yarwood, T.A., Mulhall, J., and Turner, G.E., J. Catalysis 17, 28 (1970).
- (97) Yarze, J.C. and Loc erbie, T.E., 137th Meeting of the A.C.S. Div. Gas and Fuel Chemistry, Ohio (1960).
- (98) Rodgers, M.C.F., and Crooks, W.M., J. Appl. Chem. 16, 133 (1966).
- (99)/

References Contd:

- (99) Dowden, D.A., Chem. Eng. Progr. Symp., 63, 90 (1967).
- (100) Little, L.H., Sheppard, N., and Yates, D.J.C., Proc. Roy. Soc. A 259, 242 (1960).
- (101) Pickering, H.L., and Eckstrom, H.C., J. Phys. Chem. 63, 512 (1959).
- (102) Eley, D.D., Morgan, D.M., and Rochester, O.H., Trans. Faraday Soc. 64, 2168 (1968).
- (103) Eischen, R.P., and Pliskin, W.A., Proc. 2nd Inter. Congr. Catalysis (Ed. Technip, Paris) (1961).